Received: 4 January 2022 | Revised: 19 July 2024 | Accepted: 15 November 2024

DOI: 10.1112/plms.70022

RESEARCH ARTICLE

Proceedings of the London Mathematical Society

Conformal invariance of double random currents I: Identification of the limit

Hugo Duminil-Copin[1,2] | **Marcin Lis**[3] | **Wei Qian**[4,5]

[1]Institut des Hautes Études Scientifiques, Bures-sur-Yvette, France

[2]Université de Genève, Geneva, Switzerland

[3]Technische Universität Wien, Vienna, Austria

[4]City University of Hong Kong, Kowloon, Hong Kong

[5]CNRS and Laboratoire de Mathématiques d'Orsay, Université Paris-Saclay, Orsay, France

Correspondence
Marcin Lis, Technische Universität Wien.
Email: marcin.lis@tuwien.ac.at

Funding information
NCCR SwissMap; European Research Council, Grant/Award Number: 57296

Abstract

This is the first of two papers devoted to the proof of conformal invariance of the critical double random current model on the square lattice. More precisely, we show the convergence of loop ensembles obtained by taking the cluster boundaries in the sum of two independent currents with free and wired boundary conditions. The strategy is first to prove convergence of the associated height function to the continuum Gaussian free field, and then to characterise the scaling limit of the loop ensembles as certain local sets of this Gaussian free field. In this paper, we identify uniquely the possible subsequential limits of the loop ensembles. Combined with Duminil-Copin et al., this completes the proof of conformal invariance.

MSC 2020
82B20 (primary)

1 | INTRODUCTION

1.1 | Motivation and overview

The rigourous understanding of conformal field theory (CFT) and conformally invariant random objects via the developments of the Schramm–Loewner evolution (SLE) and its relations to the Gaussian free field (GFF) has progressed greatly in the last 25 years. It is fair to say that once a discrete lattice model is proved to be conformally invariant in the scaling limit, most of what

mathematical physicists are interested in can be exactly computed using the powerful tools in the continuum.

A large class of discrete lattice models are conjectured to have interfaces that converge in the scaling limit to SLE_κ-type curves for $\kappa \in (0, 8]$. Unfortunately, such convergence results are only proved for a handful of models, including the loop-erased random walk [57] and the uniform spanning tree [40] (corresponding to $\kappa = 2$ and 8), the Ising model [15] and its FK representation [65] (corresponding to $\kappa = 3$ and $16/3$) and Bernoulli site percolation on the triangular lattice [64] (corresponding to $\kappa = 6$). Known proofs involve a combination of exact integrability[†] enabling the computation of certain discrete observables, and of discrete complex analysis to imply the convergence in the scaling limit to holomorphic/harmonic functions satisfying certain boundary value problems that are naturally conformally covariant.

To upgrade the result from conformal covariance of these 'witness' observables to the convergence of interfaces in the system, one needs an additional ingredient. In some cases, when properties of the discrete models are sufficiently nice (typically tightness of the family of interfaces, mixing-type properties, etc.), a clever martingale argument introduced by Oded Schramm enables to prove convergence of interfaces to SLEs and CLEs. This last step involves the *spatial Markov properties* of the discrete model in a crucial fashion. We refer to the proofs of conformal invariance of interfaces in Bernoulli site percolation, the Ising model, the FK Ising model or the harmonic explorer for examples. Unfortunately, the discrete properties of the model are sometimes not sufficiently nice to implement this martingale argument and there are still many remaining examples for which the scaling limit of the interfaces cannot be easily deduced from the conformal invariance of certain observables — most notably for the case of the double dimer model, for which an important breakthrough was performed by Kenyon in [37], followed by a series of impressive papers [8, 18].

In this paper, we prove convergence of the nested inner and outer boundaries of clusters in the critical double random current (DRC) model with free boundary conditions, as well as in its dual model with wired boundary conditions, to level loops of a GFF. In particular, the outer boundaries of clusters in the critical DRC model with free boundary conditions converge to CLE_4. The random current model has proved to be a very powerful tool to understand the Ising model. Its applications range from correlation inequalities [29], exponential decay in the off-critical regime [1, 23, 26], classification of Gibbs states [54], continuity of the phase transition [3], and so on. Even in two dimensions, where a number of other tools are available, new developments have been made possible via the use of this representation [4, 21, 45]. In particular, as mentioned at the end of this Section 1.2, the scaling limit of the DRC gives access to the scaling limit of spin correlations in the Ising model. For a more exhaustive account of random currents, we refer the reader to [20].

Convergence to SLE_4-type curves were previously proved for the harmonic explorer [61], zero contour lines of the discrete GFF [58] (also in the cable-graph representation [5]), the zero contour lines of the Ginzburg–Landau $\nabla\phi$ interface model [46, 47] and cluster boundaries of a random walk loop-soup with the critical intensity [10, 44].

As mentioned above, our proof does not follow the martingale strategy. Instead, it relies on a coupling between the DRC and a naturally associated height function, and can be decomposed into three main steps (see the next sections for more details).

(i) Proving the joint tightness of the family of interfaces in the DRC model and the height function, as well as certain properties of the joint coupling.

[†] Only approximately for site percolation on the triangular lattice.

(ii) Proving convergence of the height function to the GFF.
(iii) In the continuum, identifying the scaling limit of the interfaces using properties of the GFF and its local sets.

Each of the three previous steps involves quite different branches of probability. The first one extensively uses percolation-type arguments for dependent percolation models. The second one concerns a height function studied already by Dubédat [17] and Boutilier and de Tilière [9]. However, unlike in [9, 17], it harvests a link between a percolation model (the DRC) and dimers. Moreover, it uses techniques introduced by Kenyon to prove convergence of the dimer height function, but with a new twist as the proof relies heavily on fermionic observables introduced by Chelkak and Smirnov to prove conformal invariance of the Ising model, as well as a delicate result on the DRC model (see Section 2) helping identifying the boundary conditions. Finally, the last step relies on properties of the local sets of the GFF introduced by Schramm and Sheffield [59], and in particular on the two-valued local sets introduced by Aru, Sepúlveda and Werner [7]. This step crucially uses the spatial Markov properties of the interfaces and the associated height function deduced from step (ii), but also establishes a certain spatial Markov property of the outer boundaries of the clusters in the continuum limit (which turn out to be CLE_4 of the limiting GFF) which is unknown in the discrete.

Part (i) of the proof is postponed to the second paper [22]. In this paper, we focus on (ii) and (iii).

In the reminder of this introduction, we state the results of the convergence of the interfaces in the DRC models with free and wired boundary conditions (Section 1.2) and the convergence of the height function associated with the DRCs (Section 1.3). In reality, the DRCs with free and wired boundary conditions can be coupled on the primal and dual graphs and be associated with the same height function, so that these three objects converge jointly. In particular, we have more precise descriptions on their joint limit, but we postpone these further results to Section 6 for simplicity.

Notation

Throughout the article, we work with planar graphs embedded in the plane. We will consider *Jordan domains* $D \subsetneq \mathbb{C}$, that is, simply connected domains whose boundary ∂D is a Jordan curve. In certain situations, we will impose a regularity condition on ∂D, namely that it is a C^1 curve.

Below, we will speak of convergence of random variables taking values in families of loops contained in D, and distributions (generalised functions). While the latter is classical and has a well defined associated topology, we provide some details on the former. To this end, let $\mathfrak{C} = \mathfrak{C}(D)$ be the collection of locally finite families $\mathcal{F}$ of non-self-crossing loops contained in D that do not intersect each other. Inspired by [2], we define a metric on $\mathfrak{C}$,

$$\mathbf{d}(\mathcal{F}, \mathcal{F}') \leqslant \varepsilon \iff \begin{array}{c} \exists f : \mathcal{F}_\varepsilon \to \mathcal{F}' \text{ one-to-one s.t. } \forall \gamma \in \mathcal{F}_\varepsilon, d(\gamma, f(\gamma)) \leqslant \varepsilon \\ \text{and similarly when exchanging } \mathcal{F}' \text{ and } \mathcal{F} \end{array}, \tag{1.1}$$

where $\mathcal{F}_\varepsilon$ is the collection of loops in $\mathcal{F}$ with a diameter larger than ε, and for two loops γ_1 and γ_2, we set

$$d(\gamma_1, \gamma_2) := \inf \sup_{t \in \mathbb{S}^1} |\gamma_1(t) - \gamma_2(t)|, \tag{1.2}$$

with the infimum running over all continuous bijective parametrisations of the loops γ_1 and γ_2 by $\mathbb{S}^1$.

We will say that simply connected graphs $D^\delta \subset \delta\mathbb{Z}^2$ *approximate* D if $d(\partial D^\delta, \partial D) \to 0$ as $\delta \to 0$, where d is as in (1.2).

1.2 | Convergence of interfaces in double random currents

Consider a finite graph $G = (V, E)$ with vertex set V and edge set E. A *current* $\mathbf{n}$ on G is a function defined on the undirected edges $\{v, v'\} \in E$ and taking values in the natural numbers. The current set of *sources* is defined as the set

$$\partial\mathbf{n} := \left\{ v \in V : \sum_{v' \in V : v' \sim v} \mathbf{n}_{\{v,v'\}} \text{ is odd} \right\}, \tag{1.3}$$

where $v' \sim v$ means that $\{v, v'\} \in E$.

Let Ω^B be the set of currents with the set of sources equal to B. When $B = \emptyset$, we speak of a *sourceless* current. We associate to a current $\mathbf{n}$ the *weight*

$$\mathrm{w}_{G,\beta}(\mathbf{n}) := \prod_{\{v,v'\} \in E} \frac{(\beta J_{\{v,v'\}})^{\mathbf{n}_{\{v,v'\}}}}{\mathbf{n}_{\{v,v'\}}!}, \tag{1.4}$$

which comes from the associated Ising model on G [29] (which also has coupling constants J and inverse temperature β). For now, we focus on the critical parameters on the square lattice

$$\beta = \beta_c = \frac{1}{2}\ln(\sqrt{2}+1),$$

and $J_{\{v,v'\}} = 1$ for every $\{v, v'\}$ which is an edge of G, and 0 otherwise, and drop them from the notation. General models will be considered in Section 3.

We introduce the probability measure on currents with sources $B \subseteq V$ given by

$$\mathbf{P}_G^B(\mathbf{n}) := \frac{\mathrm{w}_G(\mathbf{n})}{Z_G^B}, \qquad \text{for every } \mathbf{n} \in \Omega^B, \tag{1.5}$$

where Z_G^B is the partition function. The random variable $\mathbf{n}$ is called a *random current configuration on* G with free boundary conditions and source-set B.

We define $\mathbf{P}_{G,H}^{A,B}$ to be the law of $(\mathbf{n}_1, \mathbf{n}_2)$, where $\mathbf{n}_1$ and $\mathbf{n}_2$ are two independent currents with respective laws $\mathbf{P}_G^A$ and $\mathbf{P}_H^B$. The *DRC* (model) is the law of $\mathbf{n}_1 + \mathbf{n}_2$ under $\mathbf{P}_{G,H}^{A,B}$. We call a *cluster* of any current $\mathbf{n}$ a connected component of the graph with vertex set V and edge set $E(\mathbf{n}) := \{e \in E : \mathbf{n}_e > 0\}$. To a given cluster $\mathcal{C}$, we associate a loop configuration made up of the dual edges e^* where $e = \{v, v'\}$ is such that $v \in \mathcal{C}$ and $v' \notin \mathcal{C}$. Note that this loop configuration is made up of loops on the dual graph corresponding to the different connected components of $\mathbb{Z}^2 \setminus \mathcal{C}$. The loop corresponding to the unbounded component is called the *outer boundary* of the cluster, and the loops corresponding to the boundaries of the bounded ones (sometimes referred to as *holes*) are called the *inner boundaries*. We define the *(nested) boundaries interface configuration* $\eta(\mathbf{n})$ to be the collection of outer and inner boundaries of the clusters in $\mathbf{n}$. We note that the inner and outer

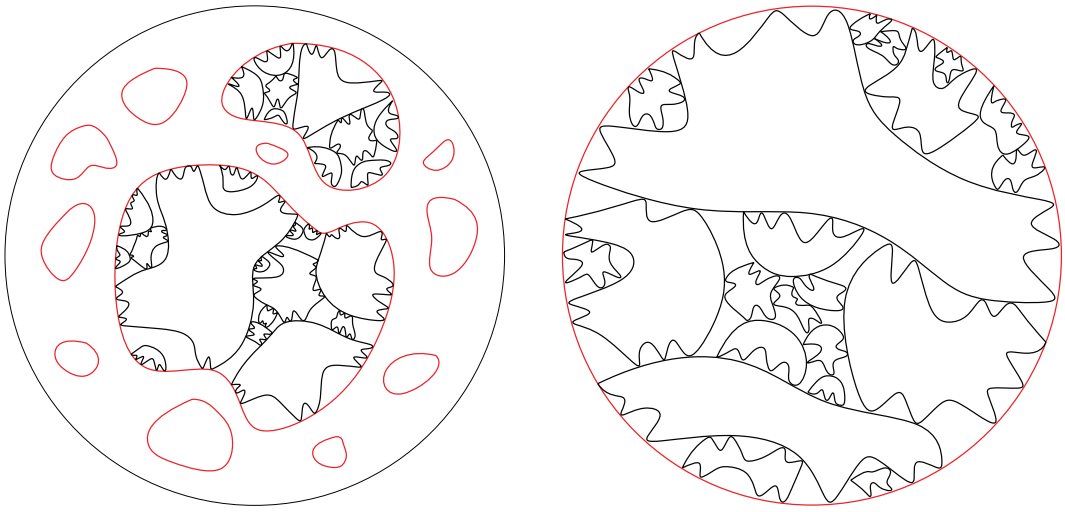

FIGURE 1.1 Left: We depict the outermost clusters in a double random current with free boundary conditions. The outer boundaries of these clusters are in red (they form a CLE_4). The inner boundaries of the clusters are in black. Right: We depict the unique outermost cluster in a double random current with wired boundary conditions. The inner boundaries of this cluster are in black. For both: In each domain encircled by an inner boundary loop, one has (the scaling limit of) an independent double random current with free boundary conditions. This allows us to iteratively sample the nested interfaces.

boundaries of different clusters may share edges (but they do not cross). We will often refer to the elements of $\eta(\mathbf{n})$ as the interfaces of $\mathbf{n}$.

As before, we fix a simply connected Jordan domain $D \subsetneq \mathbb{C}$ and consider the DRC on D^δ. To state the following theorem, we will need the notion of two-valued sets $\mathbb{A}_{-a,b}$ introduced in [7], which is the unique thin local set of the GFF in D with boundary values $-a$ and b. In this work, we use $\mathcal{L}_{-a,b}$ to denote the collection of outer boundaries (which are SLE_4-type simple loops and level loops of the GFF) of the connected components of $D \setminus \mathbb{A}_{-a,b}$. We refer to Section 5 for more details on two-valued sets and related objects. We define

$$\lambda = \sqrt{\pi/8}.$$

Theorem 1.1 (Convergence of DRC clusters with free boundary conditions). *Let D be a Jordan domain, and let D^δ approximate D. Moreover, let η^δ be the nested boundaries interface configuration of the critical DRC on D^δ with free boundary conditions. Then, as $\delta \to 0$, η^δ converges in distribution to a limit whose law is invariant under all conformal automorphisms of D. More precisely, we have that (see Figure 1.1 Left)*

- *The outer boundaries of the outermost clusters converge to a CLE_4 in D.*
- *If the outer boundary of a cluster converges to γ, then the inner boundaries of this cluster converge to $\mathcal{L}_{-2\lambda,(2\sqrt{2}-2)\lambda}$ in the domain encircled by γ.*

This picture repeats iteratively in each hole of every cluster. In particular,

- *If a loop in the inner boundary of a cluster converges to γ, then the outer boundaries of the outermost clusters enclosed by γ converge to a CLE_4 in the domain encircled by γ.*

We will also work with the *random current model with wired boundary conditions* on G. For the purpose of the statement below, we define it explicitly for the critical model on the square lattice without referring to the dual model. Later, in Section 3.1, a version for a general planar graph will be stated. Let $G \subset \mathbb{Z}^2$ be a simply connected subgraph of $\mathbb{Z}^2$ that is a union of square faces (in particular does not have vertices of degree one). Let ∂G be the set of vertices of G that lie on the unbounded face of G and are of degree 2 or 3. We define G^+ to be the graph with vertex set $V^+ := V \cup \{\mathfrak{g}\}$ where $\mathfrak{g}$ is an additional vertex that lies in the unbounded face of G, and $E^+ := E \cup \{\{v, \mathfrak{g}\} : v \in \partial G\}$, where vertices of degree two contribute two edges. This condition comes from the fact that G is a weak dual graph of some subgraph of the dual square lattice, and in this case, G^+ is the full dual graph. The coupling constants on the new edges are the same as on all other edges, and are critical. Accordingly, we introduce the measures $\mathbf{P}^B_{G^+}$ and $\mathbf{P}^{A,B}_{G^+,H^+}$ as before.

Theorem 1.2 (Convergence of DRC clusters with wired boundary conditions). *Let D be a Jordan domain, and let D^δ approximate D. Moreover, let η^δ be the nested boundaries interface configuration of the critical DRC on D^δ with wired boundary conditions. Then, as $\delta \to 0$, η^δ converges in distribution to a limit whose law is invariant under all conformal automorphisms of D. More precisely, we have that (see Figure 1.1 Right)*

- *The inner boundaries of the unique outermost cluster converge to $\mathcal{L}_{-\sqrt{2}\lambda,\sqrt{2}\lambda}$ in D.*
- *If the inner boundary of a cluster converges to γ, then the outer boundaries of the outermost clusters enclosed by γ converge to a CLE_4 in the domain encircled by γ.*
- *If the outer boundary of a cluster converges to γ, then the inner boundaries of this cluster converge to $\mathcal{L}_{-2\lambda,(2\sqrt{2}-2)\lambda}$ in the domain encircled by γ.*

Remark 1.3. The values of a and b in $\mathcal{L}_{-a,b}$ that we obtain in our results are combinations of $\sqrt{2}\lambda$ and 2λ. The mechanism for the generation of each of these gaps in the scaling limit is very different, and this realisation is one of the main (and possibly surprising) insights of this work. The appearance of multiplies of $\sqrt{2}\lambda$ is directly related to the value of the multiplicative constant in front the GFF that arises as the scaling limit of the associated height function (see Section 1.3 and Theorem 1.4 therein). This is the same constant as the one in the scaling limit of height functions in the dimer model [35]. Moreover, the inner boundaries of clusters possess a Markov property already at the discrete level as can be easily seen from the definition of the DRC. This means that the gap $\sqrt{2}\lambda$ is in some sense present already in the discrete. On the other hand, 2λ is the height gap between the two sides of a level line in the GFF [58], which only emerges in the continuum. We have identified it using properties of two-valued sets [6, 7] (see Section 5) and properties of the scaling limit of the model (in particular, how the interfaces intersect in the continuum, which we derive in our companion paper [22]). Also, the outer boundaries do not have any apparent Markov property at the discrete level, and hence, one can think of the value 2λ as an *emergent* or *effective* gap.

Theorems 1.1 and 1.2 have the following applications.

- The Hausdorff dimension of a DRC cluster in the scaling limit (for both free and wired boundary conditions) is $7/4$ [56].
- (Difference in log conformal radii) The difference of log conformal radii between two successive loops that encircle the origin in the scaling limit of DRC interfaces is equal to $T_1 + T_2$, where

T_1 is the first time that a standard Brownian motion exits $[-\pi, (\sqrt{2}-1)\pi]$ and T_2 is the first time that a standard Brownian motion exits $[-\pi, \pi]$ (see [7, Proposition 20]).

- (Number of clusters) Let $N(\varepsilon)$ be the number of DRC clusters in the unit disk surrounding the origin such that their outer boundaries have a conformal radius w.r.t. the origin at least ε. We will show in Lemma 6.11 that almost surely,

$$N(\varepsilon)/\log(\varepsilon^{-1}) \underset{\varepsilon\to 0}{\longrightarrow} \frac{1}{\sqrt{2}\pi^2}.$$

- (Scaling limit of the magnetisation in domains) With a little bit of additional work, one may derive from our results the conformal invariance of the n-point spin–spin correlations of the critical Ising model already obtained in [14] as these correlations are expressed in terms of connectivity properties of $\mathbf{n}_1^\delta + \mathbf{n}_2^\delta$. The additional technicalities would consist in relating the point-to-point connectivity in $\mathbf{n}_1^\delta + \mathbf{n}_2^\delta$ to the probabilities that the ε-neighbourhoods of the points are connected. Such reasonings have been implemented repeatedly when proving conformal invariance, and we omit the details here as it would lengthen the paper even more. Even though the result is already known, we still wished to mention this corollary as our paper uses only the convergence of certain fermionic observables to obtain convergence of the nesting field height function to the GFF. Unlike the spinor observables used in [14], these are local functions of the Kadanoff–Ceva fermions. The convergence of such fermionic observables has been obtained for the critical Ashkin–Teller model (which is a combination of two interacting Ising models) in [28] via renormalisation arguments using the crucial fact that the observables are local. Notoriously, the spin–spin correlations are not of this kind, which makes renormalisation arguments much more difficult to implement. We believe that the strategy of this paper may be of use to extend the universality results from [28] to non-local Grassmann observables.

Finally, we remark that Theorems 1.1 and 1.2 are simplified versions of more detailed results (see Theorems 6.4 and 6.2) that we will prove in Section 6. We do not include all details in the introduction in order to facilitate the reading, but let us make some comments on the additional properties that we can obtain:

- The proofs of Theorems 1.1 and 1.2 rely on the coupling of the models with a height function that we will present in the next subsection. In fact, the primal and dual DRCs can be coupled together with the same height function (see Theorem 3.1). Consequently, the limiting interfaces of the primal and dual models are also coupled with the same GFF, so that we fully understand the nesting and intersecting behaviour of their limiting interfaces.
- Theorems 1.1 and 1.2 state the convergence of the boundaries of DRC clusters. To identify the cluster of a current, one only needs to know the edges where the current is strictly positive. However, apart from the shape of the clusters, we also have an additional information on whether the current is even and positive or odd on each edge. A hole of a DRC cluster is called odd if the flux of the cluster around this hole is an odd number, and otherwise it is called even. Here, the flux is the total current flowing across any dual path that connects any face in the hole to the boundary of the graph. In the discrete, given the shape of the clusters, there is additional randomness to determine the parity of the holes. However, in the continuum limit, as we will show in Theorem 6.4, the parity of each hole in a DRC cluster with free b.c. is a *deterministic function* of the shape of the cluster.

1.3 | Convergence of the nesting field of the double random current to the Gaussian free field

As mentioned above, a central piece in our strategy is a new convergence result dealing with the so-called nesting field of the DRC introduced by two of the authors in [21]. Let $G = (V, E)$ be a generic planar graph. For a current $\mathbf{n}$, let

- $\mathbf{n}_{\text{odd}}$ be the set of edges with an odd value in $\mathbf{n}$ (called the *odd part* of $\mathbf{n}$),
- $\mathbf{n}_{\text{even}}$ be the set of edges with an even and strictly positive value of $\mathbf{n}$ (called the *even part* of $\mathbf{n}$).

We clearly have $\mathbf{n}_{\text{odd}} \cup \mathbf{n}_{\text{even}} = E(\mathbf{n})$, and hope that no confusion will arise from the fact that the zero values are not included in the even part of a current. In what follows we will often identify a current $\mathbf{n}$ with the pair $(\mathbf{n}_{\text{odd}}, \mathbf{n}_{\text{even}})$ as it carries all the relevant information for our considerations.

A non-trivial connected component of the graph $(V, \mathbf{n}_{\text{odd}})$ will be called a *contour*. In particular, each contour C is contained in a unique cluster of $\mathbf{n}$, and each cluster $\mathscr{C}$ is associated to a contour configuration $\mathscr{C} \cap \mathbf{n}_{\text{odd}}$. Each contour configuration gives rise to a ± 1 spin configuration on the faces of G, where the external unbounded face is assigned spin $+1$, and where the spin changes whenever one crosses an edge of a contour. We call a cluster $\mathscr{C}$ *odd around a face* u if the spin configuration associated with the contour configuration $\mathscr{C} \cap \mathbf{n}_{\text{odd}}$ assigns spin -1 to u (this is the same as asking for the total flux of the current in the cluster to be odd across any dual path connecting u to infinity).

For a current $\mathbf{n}$, let $\mathfrak{C}(\mathbf{n})$ be the collection of all clusters of $\mathbf{n}$, and let $(\epsilon_{\mathscr{C}})_{\mathscr{C} \in \mathfrak{C}(\mathbf{n})}$ be i.i.d. random variables equal to $+1$ or -1 with probability $1/2$ indexed by $\mathfrak{C}(\mathbf{n})$. These random variables are called the *labels* of the clusters. The *nesting field with free boundary conditions* of a current $\mathbf{n}$ on G evaluated at a face u of G is defined by

$$h_G(u) := \sum_{\mathscr{C} \in \mathfrak{C}(\mathbf{n})} \mathbf{1}\{\mathscr{C} \text{ odd around } u\}\epsilon_{\mathscr{C}}. \tag{1.6}$$

Analogously, the *nesting field with wired boundary conditions* of a current $\mathbf{n}$ on G^+ evaluated at a face u of G^+ is defined by

$$h^+_{G^+}(u) := (\mathbf{1}\{\mathscr{C}_{\mathfrak{g}} \text{ odd around } u\} - 1/2)\epsilon_{\mathscr{C}_{\mathfrak{g}}} + \sum_{\mathscr{C} \neq \mathscr{C}_{\mathfrak{g}}} \mathbf{1}\{\mathscr{C} \text{ odd around } u\}\epsilon_{\mathscr{C}}, \tag{1.7}$$

where $\mathscr{C}_{\mathfrak{g}}$ is the cluster containing the external vertex $\mathfrak{g}$, and where the sum is taken over all remaining clusters of $\mathbf{n}$. Here, whether $\mathscr{C}_{\mathfrak{g}}$ is odd around a face of G or not depends on the embedding of the graph G^+. However, one can see that the distribution of $h^+_{G^+}(u)$ is independent of this embedding.

Note that due to the term corresponding to $\mathscr{C}_{\mathfrak{g}}$, the nesting field with wired boundary conditions takes half-integer values, whereas the one with free boundary conditions is integer-valued. Such definition is justified by the next result, and by the joint coupling of h_G and $h^+_{G^*}$ via a dimer model described in Section 3.2.3. We note that the global shift of $1/2$ between h_G and $h^+_{G^*}$ is the same as in the work of Boutilier and de Tilière [9].

The following is the main result of this part of the argument. We identify the function h_{D^δ} defined on the faces of D^δ with a distribution on D in the following sense: extend h_{D^δ} to all points in D by setting it to be equal to $h_{D^\delta}(u)$ at every point strictly inside the face u, and 0 on

the complement of the faces in D. Then, we view h_{D^δ} as a *distribution* (*generalised function*) by setting

$$h_{D^\delta}(f) := \int_D f(x) h_{D^\delta}(x) dx,$$

where f is a *test function*, that is, a smooth compactly supported function on D. We proceed analogously with the field $h^+_{(D^\delta)^*}$ and extend it to all points within the faces of $(D^\delta)^*$. We will say that a sequence of random generalised functions X_n *converges weakly to* a random generalised function X, if $X_n(f)$ converges in distribution to $X(f)$ for every test function f.

The *GFF* h_D with zero boundary conditions in D is a random distribution such that for every smooth function f with compact support in D, we have

$$\mathbb{E}\left[\left(\int_D f(z) h_D(z) dz\right)^2\right] = \int_D \int_D f(z_1) f(z_2) G_D(z_1, z_2) dz_1 dz_2, \tag{1.8}$$

where G_D is the Green's function on D with zero boundary conditions satisfying $\Delta G_D(x, \cdot) = -\delta_x(\cdot)$, where δ_x denotes the Dirac mass at x. This normalisation means, for example, that for the upper half plane $\mathbb{H}$, we have

$$G_{\mathbb{H}}(x, y) = \frac{1}{2\pi} \log |(x - \bar{y})/(x - y)|.$$

Given a planar graph G, we write $G^\dagger$ for its *weak dual*, that is, the planar dual graph with the vertex corresponding to the outer boundary of G removed.

Theorem 1.4 (Convergence of the nesting field). *Let D be a Jordan domain, and let D^δ approximate D. Denote by h_{D^δ} the nesting field of the critical double random current model on D^δ with free boundary conditions, and by $h^+_{(D^\delta)^\dagger}$ the nesting field of the critical DRC model on the weak dual graph $(D^\delta)^\dagger$ with wired boundary conditions. Then,*

$$\lim_{\delta \to 0} h_{D^\delta} = \lim_{\delta \to 0} h^+_{(D^\delta)^\dagger} = \frac{1}{\sqrt{\pi}} h_D,$$

where h_D is the GFF in D with zero boundary conditions, and where the convergence is in distribution in the space of generalised functions.

We want to mention that h_{D^δ} and $h^+_{(D^\delta)^\dagger}$ can be coupled together as one random height function H_{D^δ} defined on the faces of a planar graph C_{D^δ} (whose faces correspond to both the faces of D^δ and $(D^\delta)^\dagger$; see Figure 3.3) in such a way that $\lim_{\delta \to 0} H_{D^\delta} = \frac{1}{\sqrt{\pi}} h_D$, and moreover, the values of h_{D^δ} and $h^+_{(D^\delta)^\dagger}$ differ locally by an additive constant. More properties of this coupling are described in Section 3.1.

Our proof is based on the relationship between the nesting field of DRCs on a graph G and the height function of a dimer model on decorated graphs G^d and C_G established in [21]. We will first explicitly identify the inverse Kasteleyn matrix associated with these dimer models with the correlators of real-valued Kadanoff–Ceva fermions in the Ising model [32]. This is valid for

arbitrary planar weighted graphs, and can also be derived from the bozonisation identities of Dubédat [17]. For completeness of exposition, we choose to present an alternative derivation that uses arguments similar to those of [21]. Compared to [17], rather than using the connection with the six-vertex model, we employ the DRC model. We then express the real-valued observables on general graph in terms of the complex-valued observables of Smirnov [65], Chelkak and Smirnov [15] and Hongler and Smirnov [31]. This is a well-known relation that can be, for example, found in [13]. We also state the relevant scaling limit results for the critical observables on the square lattice obtained in [15, 31, 65].

All in all, we identify the scaling limit of the inverse Kasteleyn matrix on graphs C_{D^δ} as $\delta \to 0$. This is an important ingredient in the computation of the limit of the moments of the height function which is done by modifying an argument of Kenyon [34]. Another crucial and new ingredient is a class of delicate estimates on the critical random current model from [22] that allow us to do two things:

- to identify the boundary conditions of the limiting GFF to be zero boundary conditions;
- to control the behaviour of the increments of the height function between vertices at small distances.

The first item is particularly important as handling boundary conditions directly in the dimer model is notoriously difficult. Here, the identification of the limiting boundary conditions is made possible by the connection with the DRC as well as the main result of [22] stating that large clusters of the DRC with free boundary conditions do not come close to the boundary of the domain (see Theorem 2.4 below). We see this observation and its implication for the nesting field as one of the key innovation of our paper.

We stress the fact that Theorem 1.4 does not follow from the scaling limit results of Kenyon [34, 35] as the boundary conditions considered in these papers are related to Temperley's bijection between dimers and spanning trees [38, 39, 66], whereas those considered in this paper correspond to the double Ising model [9, 17, 21]. Moreover, we note that the infinite volume version of Theorem 1.4 was obtained by de Tilière [16]. Finally, it can also be shown that the hedgehog domains of Russkikh [55] are a special case of our framework, where the boundary of D^δ makes turns at each discrete step.

Organisation

The paper is organised as follows. In Section 2, we state the main results from our second paper [22]. In Section 3, we recall the relationship between different discrete models and derive a connection between the inverse Kasteleyn matrix and complex-valued fermionic observables. While some (but not all) of these results are not completely new, they are scattered around the literature, and we therefore review them here. In Section 4, we derive Theorem 1.4. Section 5 presents more preliminaries on the continuum objects. Section 6 is devoted to the identification of the scaling limit of DRCs.

2 | INPUT FROM THE SECOND PAPER OF THE SERIES

In this section, we briefly recap some inputs from [22] that are used in this paper. We refer to [22] for the proofs. We only mention the main tools from [22] that we will use and refer, later in the proof, to the precise statements of [22] when they were not mentioned in this section.

Results for the double random current model

We will need tightness results for several families of loops, notably for the outer and inner boundaries of the DRC clusters. This is done using an Aizenman–Burchard-type criterion for the DRC. Below, for a subset A of vertices, an *A-cluster* is a cluster for the current configuration restricted to A. A *domain* D is a subgraph of $\mathbb{Z}^2$ whose boundary is a self-avoiding polygon in $\mathbb{Z}^2$. Let $\Lambda_r := [-r, r]^2$ and $\mathrm{Ann}(r, R) := \Lambda_R \setminus \Lambda_{r-1}$. Call an $\mathrm{Ann}(r, R)$-cluster (i.e. an A-cluster with $A = \mathrm{Ann}(r, R)$) *crossing* if it intersects both $\partial\Lambda_r$ and $\partial\Lambda_R$. For an integer $k \geqslant 1$, let $A_{2k}(r, R)$ be the event[†] that there are k distinct $\mathrm{Ann}(r, R)$-clusters crossing $\mathrm{Ann}(r, R)$.

Theorem 2.1 (Aizenman–Burchard criterion for the DRC model). *There exist sequences $(C_k)_{k\geqslant 1}, (\lambda_k)_{k\geqslant 1}$ with λ_k tending to infinity as $k \to \infty$, such that for every domain D, every $k \geqslant 1$ and all r, R with $1 \leqslant r \leqslant R/2$,*

$$\mathbf{P}^{\emptyset,\emptyset}_{D,D}[A_{2k}(r, R)] \leqslant C_k \left(\frac{r}{R}\right)^{\lambda_k}. \tag{2.1}$$

If the domain has a C^1 boundary, the same holds for the model with wired boundary conditions but with the constants C_k and λ_k depending on D.

We will also need some *a priori* properties of possible subsequential scaling limits. These will be obtained using estimates in the discrete on certain four-arm type events. We list them now. Let

$$A_4^{\square}(r, R) := \{\text{there exist two } \Lambda_R\text{-clusters crossing } \mathrm{Ann}(r, R)\},$$

and let $A_4^{\square}(x, r, R)$ be the translate of $A_4^{\square}(r, R)$ by x.

Theorem 2.2. *There exists $C > 0$ such that for all r, R with $1 \leqslant r \leqslant R$,*

$$\mathbf{P}^{\emptyset,\emptyset}_{\mathbb{Z}^2,\mathbb{Z}^2}[A_4^{\square}(r, R)] \leqslant C(r/R)^2. \tag{2.2}$$

Furthermore, for every $\varepsilon > 0$, there exists $\eta = \eta(\varepsilon) > 0$ such that for all r, R with $1 \leqslant r \leqslant \eta R$ and every domain $\Omega \supset \Lambda_{2R}$,

$$\mathbf{P}^{\emptyset,\emptyset}_{\Omega,\Omega}[\exists x \in \Lambda_R : A_4^{\square}(x, r, R)] \leqslant \varepsilon. \tag{2.3}$$

The result is coherent with the fact that the scaling limit of the outer boundaries of large clusters in the DRC model with free boundary conditions is given by CLE_4, which is known to be made up of simple loops that do not touch each other. Interestingly, to derive the convergence to the continuum object, it will be necessary to first prove this property at the discrete level.

We turn to a second result of the same type. For a current $\mathbf{n}$, let $\mathbf{n}^*$ be the set of dual edges e^* with $\mathbf{n}_e = 0$. For a dual path $\gamma = (e_1^*, e_2^*, \dots, e_k^*)$, call the $\mathbf{n}$-flux through γ the sum of the $\mathbf{n}_{e_i}$. Call an $\mathrm{Ann}(r, R)$-*hole in* $\mathbf{n}$ a connected component of $\mathbf{n}^*$ restricted to $\mathrm{Ann}(r, R)^*$ (note that it can be seen as a collection of faces). An $\mathrm{Ann}(r, R)$-hole is said to be *crossing* $\mathrm{Ann}(r, R)$ if it intersects $\partial\Lambda_r^*$

[†] The subscript $2k$ instead of k is meant to illustrate that there are k $\mathrm{Ann}(r, R)$-clusters from inside to outside separated by k dual clusters separating them.

and $\partial\Lambda_R^*$. Consider the event

$$A_4^{\blacksquare}(r,R) := \left\{ \begin{array}{l} \text{there exist two Ann}(r,R)\text{-holes crossing Ann}(r,R) \text{ and the} \\ \text{shortest dual path between them has even } (\mathbf{n}_1+\mathbf{n}_2)\text{-flux} \end{array} \right\}.$$

Denote its translate by x by $A_4^{\blacksquare}(x,r,R)$.

Theorem 2.3. *There exists $C>0$ such that for all r,R with $1 \leqslant r \leqslant R$,*

$$\mathbf{P}^{\emptyset,\emptyset}_{\mathbb{Z}^2,\mathbb{Z}^2}[A_4^{\blacksquare}(r,R)] \leqslant C(r/R)^2. \tag{2.4}$$

Furthermore, for every $\varepsilon>0$, there exists $\eta=\eta(\varepsilon)>0$ such that for all r,R with $1 \leqslant r \leqslant \eta R$ and every domain $D \supset \Lambda_{2R}$,

$$\mathbf{P}^{\emptyset,\emptyset}_{\Omega,\Omega}[\exists x \in \Lambda_R \,:\, A_4^{\blacksquare}(x,r,R)] \leqslant \varepsilon. \tag{2.5}$$

Let us mention that the previous results are obtained using the following key statement, which is of independent interest and is also directly used in this paper. For a set D, let $\partial_r D$ be the set of vertices in D that are within a distance r from ∂D.

Theorem 2.4 (Connection probabilities close to the boundary for DRC). *There exists $c>0$ such that for all r,R with $1 \leqslant r \leqslant R$ and every domain D containing Λ_{2R} but not Λ_{3R},*

$$\frac{c}{\log(R/r)} \leqslant \mathbf{P}^{\emptyset,\emptyset}_{D,D}[\Lambda_R \overset{\mathbf{n}_1+\mathbf{n}_2}{\longleftrightarrow} \partial_r D] \leqslant \epsilon(\frac{r}{R}),$$

where $x \mapsto \epsilon(x)$ is an explicit function tending to 0 as x tends to 0.

We predict that the upper bound should be true for $\epsilon(x) := C/\log(1/x)$ but we do not need such a precise estimate here. Again, the result is coherent with the fact that the scaling limit of the outer boundary of large clusters in the DRC with free boundary conditions is given by CLE_4.

The lower bound is to be compared with recent estimates [24, 25] obtained for another dependent percolation model, namely the critical Fortuin–Kasteleyn random cluster model with cluster weight $q \in [1,4)$. There, it was proved that the crossing probability is bounded from below by a constant $c=c(q)>0$ uniformly in r/R. We expect that the behaviour of the critical random cluster model with cluster weight $q=4$ on the other hand is comparable to the behaviour presented here: large clusters do not come close to the boundary of domains when the boundary conditions are free.

3 | PRELIMINARIES ON DISCRETE MODELS

The main two goals of this section are the following. First of all, we describe a coupling between DRCs (both primal and dual) and the associated nesting fields. This is stated in Theorem 3.1, and the properties of the coupling are crucial in the proofs of our main theorems (they exactly mimic the structure of level sets in the continuum GFF discussed in Section 5). For the proof, we study

three auxiliary and related to each other discrete models: random alternating flows (introduced in [43]), and two bipartite dimer models on two different modifications G^d and C_G of the underlying graph G (introduced in [21] and [17, 27], respectively). These are described in Section 3.2. We stress the fact that the alternating flow model and the dimer model on G^d are not used outside this section, but they are a convenient tool to relate the DRC model with the dimer model on C_G. This is then used in Section 4 to show convergence of the nesting field to the GFF. The main new result on the dimer model on C_G contained in this section is the fact that the associated inverse Kasteleyn matrix is *exactly* equal to the fermionic observable of Chelkak and Smirnov [15].

3.1 | A coupling between the primal and dual double random current

Let $G = (V, E)$ be a graph as in Section 1.3. In this section, we discuss the joint coupling of the DRC on G and the DRC on the dual graph G^* together with a height function that restricts to both the nesting field of the primal and the dual random current (see Figure 3.1 for an illustration). The coupling constants for the dual model satisfy the Kramers–Wannier duality relation

$$\exp(-2\beta^* J^*_{e^*}) = \tanh(\beta J_e). \tag{3.1}$$

We note that if $J_e = J^*_{e^*} = 1$ for all e, and $\beta = \beta_c$, then $\beta^* = \beta_c$ (the critical point is self-dual). Properties of this coupling will be used in Section 6 to identify the scaling limit of the boundaries of the DRC clusters. We will provide a proof of this result at the end of Section 3.2.3 using a relation with the dimer model.

Theorem 3.1 (Master coupling). *One can couple the following objects:*

(i) *a DRC* $\mathbf{n}$ *with free boundary conditions on the primal graph* $G = (V, E)$*, together with i.i.d.* ± 1*-valued spins* $(\tau_C : C \in \mathfrak{C}(\mathbf{n}))$ *associated to each cluster of* $\mathbf{n}$*,*
(ii) *the dual DRC* $\mathbf{n}^\dagger$ *with free boundary conditions on the full dual graph* $G^* = (U, E^*)$ *(that we will refer to as the* wired boundary conditions *on the weak dual graph* $G^\dagger$*) and with the dual coupling constants, together with i.i.d.* ± 1*-valued spins* $(\tau^\dagger_C : C \in \mathfrak{C}(\mathbf{n}^\dagger))$ *associated with each cluster of* $\mathbf{n}^\dagger$*,*
(iii) *a height function* H *defined on* $V \cup U$*,*

in such a way that the following properties hold:

1. *The configurations* $\mathbf{n}$ *and* $\mathbf{n}^\dagger$ *are disjoint in the sense that* $\mathbf{n}_e > 0$ *implies* $\mathbf{n}^\dagger_{e^*} = 0$ *and* $\mathbf{n}^\dagger_{e^*} > 0$ *implies* $\mathbf{n}_e = 0$*, where* e^* *is the dual edge of* e*.*
2. *The odd part (the set of edges with odd values) of* $\mathbf{n}$ *is equal to the collection of interfaces of* $\tau^\dagger$ *(the set of primal edges separating dual clusters with* $+1$ *and* -1 *spins of* $\tau^\dagger$*), and the odd part of* $\mathbf{n}^\dagger$ *is equal to the collection of interfaces of* τ *(the set of dual edges separating primal clusters with* $+1$ *and* -1 *spins of* τ*).*
3. *For a face* $u \in U$ *and a vertex* $v \in V$ *incident on* u*, we have*

$$H(u) - H(v) = \frac{1}{2}\tau^\dagger_u \tau_v.$$

Moreover, the height function H *restricted to the faces of* G *(resp.* G^**) has the law of the nesting field of* $\mathbf{n}$ *with free boundary conditions (resp.* $\mathbf{n}^\dagger$ *with wired boundary conditions) as denoted by* h *(resp.* $h^\dagger$*).*

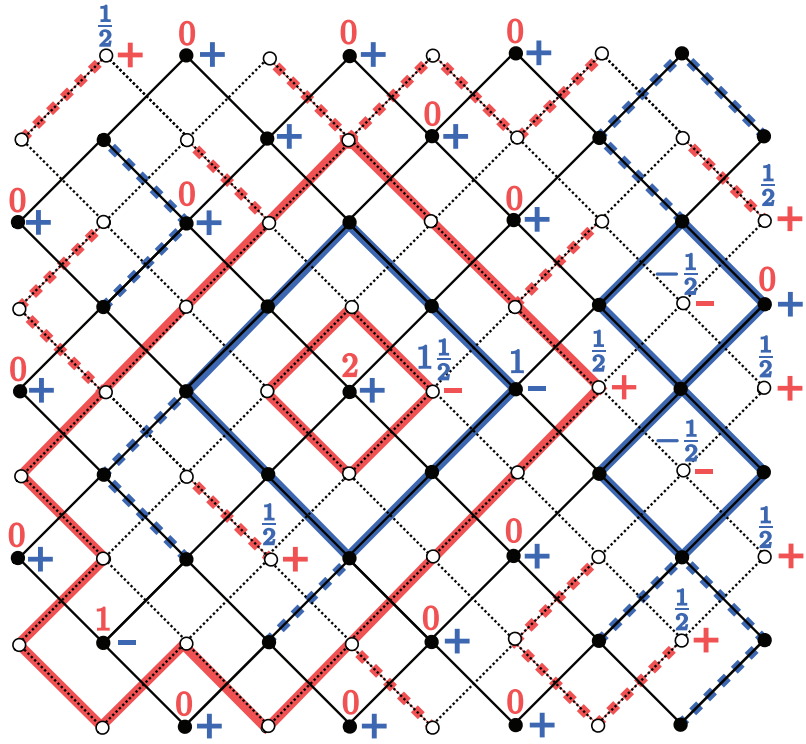

FIGURE 3.1 An illustration of the coupling from Theorem 3.1. A piece of the (rotated) primal square lattice with white vertices, and its dual square lattice with black vertices is shown. The primal and dual DRC clusters are drawn in blue and red, respectively. The odd parts of the current are marked with solid lines, whereas the non-zero even parts are marked with dashed lines. Each vertex (primal black vertex) and a face (dual white vertex) carry both a ± 1 spin (τ and $\tau^\dagger$, respectively) and the value of the height function H. The height function takes integer values in $\mathbb{Z}$ on the black vertices and in $\frac{1}{2}+\mathbb{Z}$ on the white vertices as implied by property 3 of the master coupling. Property 3 and the fact that the spins τ and $\tau^\dagger$ are constant on the primal and dual clusters, respectively, imply that the height function is also constant on both the primal and dual clusters. This is why in the figure we marked the values of the spins and height only at the rightmost vertices of the clusters (including isolated vertices).

4. *When exploring a cluster of* $\mathbf{n}$ *from the outside, inside each of its holes the dual current* $\mathbf{n}^\dagger$ *has wired boundary conditions, where each inner boundary of the hole (as defined in Section 1.2) is identified as a single dual vertex (note that a single hole can have multiple inner boundaries since the inner boundaries by definition do not cross primal edges whose both endpoints are in the cluster of* $\mathbf{n}$*). To be more precise, let* $\tilde{G}$ *be a connected component (which is not the component of the boundary) of* G *obtained after removing a cluster* C *of* $\mathbf{n}$ *and all its adjacent edges. Then,* $\mathbf{n}^\dagger$ *restricted to* $\tilde{G}^*$ *is a DRC with wired boundary conditions (here we disregard the state of* $\mathbf{n}^\dagger$ *on edges dual to a primal edge that is adjacent to* C*). By duality, the same holds with the roles of* $\mathbf{n}$ *and* $\mathbf{n}^\dagger$ *exchanged.*

We stress the fact that the interfaces of τ and $\tau^\dagger$ are disjoint in the sense of property 1 appears already in the works of Dubédat [17], and Boutilier and de Tilière [9]. However, property 1 is a stronger statement as it concerns the full DRC, and not only its odd part.

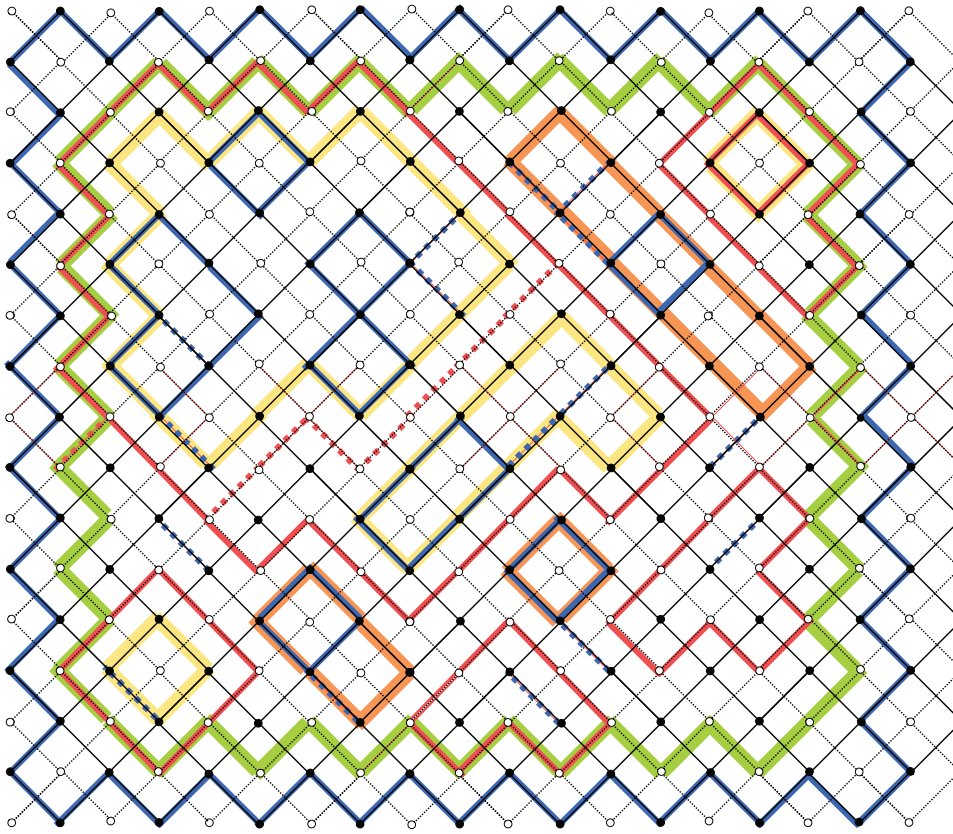

FIGURE 3.2 A configuration of primal (red) and dual (blue) double random currents $\mathbf{n}$ and $\mathbf{n}^\dagger$. The outermost blue circuit is part of a cluster of the boundary in $\mathbf{n}^\dagger$ whose remainder is not shown here. The green edges denote the inner boundary loop ℓ of this cluster (i.e. a loop in Q_0 as defined in Section 6.1). The primal vertices on this loop are identified with each other in the exploration process described in property (4) of the master coupling from Theorem 3.1. After this identification, the primal current $\mathbf{n}$ has wired boundary conditions. The clusters of the modified current $\mathbf{n}_\ell$ defined in Section 6.1 are given by the union of the green loop and the red clusters surrounded by it. Finally, $Q_1(\ell)$ is defined as the collection of loops in the inner boundary of the external most cluster (touching ℓ) of this modified current $\mathbf{n}^\ell$. These loops come in two types, the yellow loops that are part of $A_0(\ell)$ and the orange loops are in $Q_1(\ell) \setminus A_0(\ell)$. Each orange loop traces the red clusters from the outside and/or the green loop from the inside. This property is used in Lemma 6.8 to obtain pre-compactness of the orange loops given pre-compactness of the red and green loops. Inside each yellow loop of the inner boundary of the primal clusters, the procedure is repeated and now the primal clusters surrounded by each such loop have wired boundary conditions.

We note that the laws of τ and $\tau^\dagger$ are those of a XOR Ising model and the dual XOR Ising model, respectively (see Corollary 3.3 below). However, we will not use this fact in the rest of the article, and our main results do not have direct implications for the scaling limit of the interfaces in the XOR Ising model. An extension of this coupling to the Ashkin–Teller model can be found in the works [41, 42] that appeared before but were based on the current article. As mentioned, we will provide a different proof that uses the associated dimer model representation (see Section 3.2.3).

The following statement identifies the labels introduced in the definition (1.3) that correspond to the two nesting fields encoded by H.

Corollary 3.2. *In the coupling as above, each cluster C of $\mathbf{n}$ (resp. a cluster of $\mathbf{n}^\dagger$ different from the cluster of the ghost vertex $\mathfrak{g}$) can be assigned a well-defined dual spin $\tau^\dagger_C$ (resp. τ_C). This is the spin assigned to any face of G (resp. G^*) incident on C from the outside. For the cluster of $\mathfrak{g}$, we set this spin to be $+1$. With this definition, the independent labels associated to the clusters as in the definition (1.3) are given by*

$$\epsilon_C = \tau_C \tau^\dagger_C. \tag{3.2}$$

Proof. We first argue that $\tau^\dagger_C$ is well defined. By property 2, for each primal cluster C, all the dual spins at the faces adjacent to the outer boundary of C (the innermost dual circuit surrounding C) have the same value. Indeed, otherwise there would exist two consecutive dual vertices along the outer boundary of C with opposite $\tau^\dagger$ spins. However, by property 2, the corresponding primal edge would then belong to C, and hence, the two dual vertices could not be consecutive on the outer boundary of C. This justifies the definition (3.2).

We also need to argue that given $\mathbf{n}$, the spins $(\epsilon_C)_{C\in\mathfrak{C}(\mathbf{n})}$ are independent (as in the definition of the nesting field). As mentioned, we will not use this result in the rest of the article. This follows easily since given $\mathbf{n}$, $\tau^\dagger_C$ is a deterministic function of $\mathbf{n}$ (by property 2), and τ_C are independent by definition. □

Finally, for the sake of independent interest, we establish a connection with the XOR Ising model. Recall that the XOR Ising model is just the pointwise product of two i.i.d. Ising models.

Corollary 3.3. *In the master coupling described above:*

- *The spins τ_v, $v \in V$, where we define $\tau_v = \tau_C$, with C being the cluster containing v, have the law of the XOR Ising model on G with free boundary conditions, coupling constants J_e and inverse temperature β.*
- *The spins τ_u, $u \in U$, where we define $\tau^\dagger_u = \tau^\dagger_C$, with C being the dual cluster containing u, conditioned on the spin of the outer vertex $\mathfrak{g}$ being $+1$, have the law of the XOR Ising model on the dual graph G^* with $+$ boundary conditions and dual parameters as in (3.1).*

Proof. We prove the first statement as the second one follows by duality. To this end, let $\mathbb{P}_{G,\beta}$ denote the master coupling probability measure and $\mathbb{E}_{G,\beta}$ its expectation. Moreover, let $E^{\text{Ising}}_{G,\beta}$ be the expectation with respect to the Ising model on G with free boundary conditions, coupling constants J_e and inverse temperature β. For every $A \subseteq V$, since the spins τ are independent for all clusters, we have

$$\mathbb{E}_{G,\beta}\left[\prod_{v\in A}\tau_v\right] = \mathbb{P}_{G,\beta}[\mathcal{F}_A] = \mathbf{P}^{\emptyset}_{G,\beta}\otimes\mathbf{P}^{\emptyset}_{G,\beta}[\mathbf{n}_1+\mathbf{n}_2\in\mathcal{F}_A],$$

where $\mathbf{n}\in\mathcal{F}_A$ is the event that each cluster of $\mathbf{n}$ contains an even number (possibly zero) of vertices of A. Now, the classical switching lemma of Griffiths, Hurst and Sherman for DRCs [29] (see also [22]) gives that

$$\mathbf{P}^{\emptyset}_{G,\beta}\otimes\mathbf{P}^{\emptyset}_{G,\beta}[\mathbf{n}_1+\mathbf{n}_2\in\mathcal{F}_A] = E^{\text{Ising}}_{G,\beta}\left[\prod_{v\in A}\sigma_v\right]^2,$$

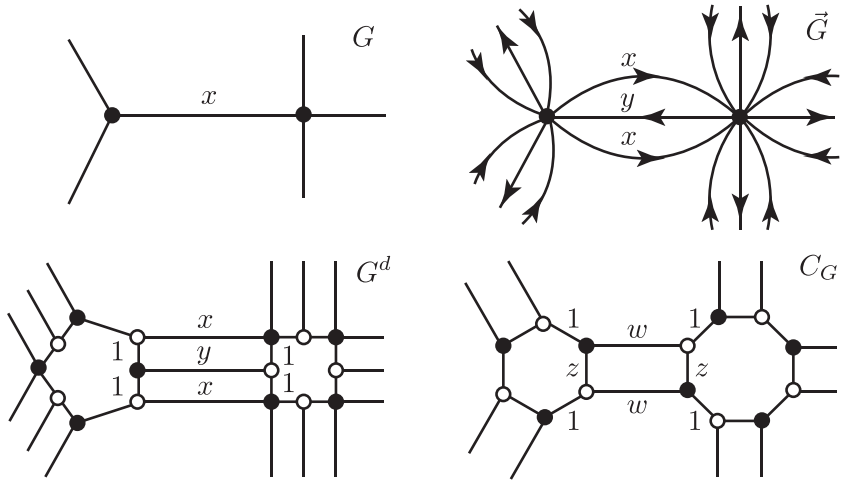

FIGURE 3.3 One can construct the graphs $\vec{G}$, G^d and C_G ($\vec{G}$ is formally a multigraph) locally around each vertex of G. The weights satisfy $y = \frac{2x}{1-x^2}$, $w = \frac{2x}{1+x^2}$, $z = \frac{1-x^2}{1+x^2}$. Here, $x = x_e$ is the high-temperature weight equal to $\tanh(\beta J_e)$. The edges carrying weight 1 in G^d (resp. in C_G) are called short (resp. roads), and the remaining edges are called long (resp. streets).

where σ denotes the Ising spins. The last expression is by definition the correlation function of XOR Ising spins at A. Since the spins are ± 1-valued, this implies that the law of τ under $\mathbb{P}_{G,\beta}$ is the law of the XOR-Ising model (e.g. one can look at the characteristic function of the random vector τ and expand it into a finite sum of correlation functions as above). □

3.2 | Mappings between discrete models

In this section, we recall the combinatorial equivalences between DRCs, alternating flows and bipartite dimers established in [21, 43]. We will later use them to derive a version of Dubédat's bosonisation identity [17]. An additional black-white symmetry for correlators of monomer insertions is established that is not apparent in [17]. This will yield a representation of the inverse Kasteleyn matrix as the fermionic observable of Chelkak and Smirnov [15].

The results here are stated for general Ising models on arbitrary planar graphs $G = (V, E)$ and with arbitrary coupling constants $(J_e)_{e\in E}$. We focus on the free boundary conditions case and the wired boundary conditions can be treated analogously, replacing G with G^+. We will actually mostly consider wired boundary conditions on the dual graph G^* which one can think of as $(G^\dagger)^+$, where $G^\dagger$ is the weak dual of G whose vertex set does not contain the unbounded face of G.

We start by describing the relevant decorated graphs: the DRC model on a graph G will be related to the alternating flow model on a directed graph $\vec{G}$, and the dimer model on two different bipartite graphs G^d and C_G. All these graphs are planar and weighted, and their local structure together with the corresponding edge weights are shown in Figure 3.3. We now describe their construction in detail. Even though this is ultimately not relevant, we note that the structure of G^d and $\vec{G}$ is determined by G *together with* a choice of an orientation for each edge.

Given G, $\vec{G}$ is obtained by replacing each edge e of G by three parallel directed edges e_{s1}, e_m, e_{s2} such that the orientation of the side (or outer) edges e_{s1} and e_{s2} is opposite to the orientation of the middle edge e_m. The orientation of the middle edge can be chosen arbitrarily.

To obtain G^d from $\vec{G}$, we replace each vertex v of $\vec{G}$ by a cycle of vertices of even length which is given by the number of times the orientation of edges in $\vec{G}$ incident on v changes when going around v. We colour the new vertices black if the corresponding edges are incoming into v and white otherwise. We then connect the white vertices in a cycle corresponding to v with the appropriate black vertices in a cycle corresponding to v', where v and v' are adjacent in $\vec{G}$. We call *long* all the edges of G^d that correspond to an edge of $\vec{G}$, and *short* the remaining edges connecting the vertices in the cycles.

The last graph C_G can be constructed directly from G by replacing each edge of G by a quadrangle of edges, and then connecting two quadrangles by an edge if the corresponding edges of G share a vertex and are incident to the same face (see Figure 3.3). Following [17], we call *streets* the edges in the quadrangles and *roads* those connecting the quadrangles (which represent cities).

We note that the set of faces U (resp. vertices V) of G naturally embeds into the set of faces of $\vec{G}$, G^d and C_G (resp. G^d and C_G). We therefore think of U and V as subsets of the set of faces of the respective decorated graphs (e.g. when we talk about equality in distribution of the height function on C_G and the nesting field on G).

In the remainder of this section, we describe the mappings between the different models in the following order: In Section 3.2.1, alternating flows on $\vec{G}$ are mapped under a map θ to a pair composed of the odd and even part of a DRC on G. In Section 3.2.2, dimers on G^d are mapped under a map π to alternating flows on $\vec{G}$. In Section 3.2.3, dimers on G^d are mapped to dimers on C_G. The corresponding statements for wired boundary conditions can be recovered by replacing G with G^+.

The first two maps yield relations between configurations of the associated models, and the last map is described as a sequence of local transformations (urban renewals) of the graphs C_G or G^d that does not change the distribution of the height function on a certain subset of the faces of these two graphs.

We first describe relations on the level of distributions on configurations where no sources or disorders are imposed. Later on (in Section 3.3), we increase the complexity by introducing sources.

3.2.1 | Double random currents on G and alternating flows on $\vec{G}$

A *sourceless alternating flow* F is a set of edges of the directed graph $\vec{G}$ satisfying the *alternating condition*, that is, for each vertex v, the edges in F that are incident to v alternate between being oriented towards and away from v when going around v (see Figure 3.4). In particular, the same number of edges enters and leaves v. We denote the set of sourceless alternating flows on $\vec{G}$ by $\mathcal{F}^{\emptyset}$, and following [43], we define a probability measure on $\mathcal{F}^{\emptyset}$ by the formula, for every $F \in \mathcal{F}^{\emptyset}$,

$$\mathbf{P}^{\emptyset}_{\text{flow}}(F) := \frac{1}{Z^{\emptyset}_{\text{flow}}} \mathrm{w}_{\text{flow}}(F), \tag{3.3}$$

where $Z^{\emptyset}_{\text{flow}}$ is the partition function of sourceless flows and, if $V(F)$ denotes the set of vertices in the graph (V, F) that have at least one incident edge,

$$\mathrm{w}_{\text{flow}}(F) := 2^{|V|-|V(F)|} \prod_{e \in F} x_e, \tag{3.4}$$

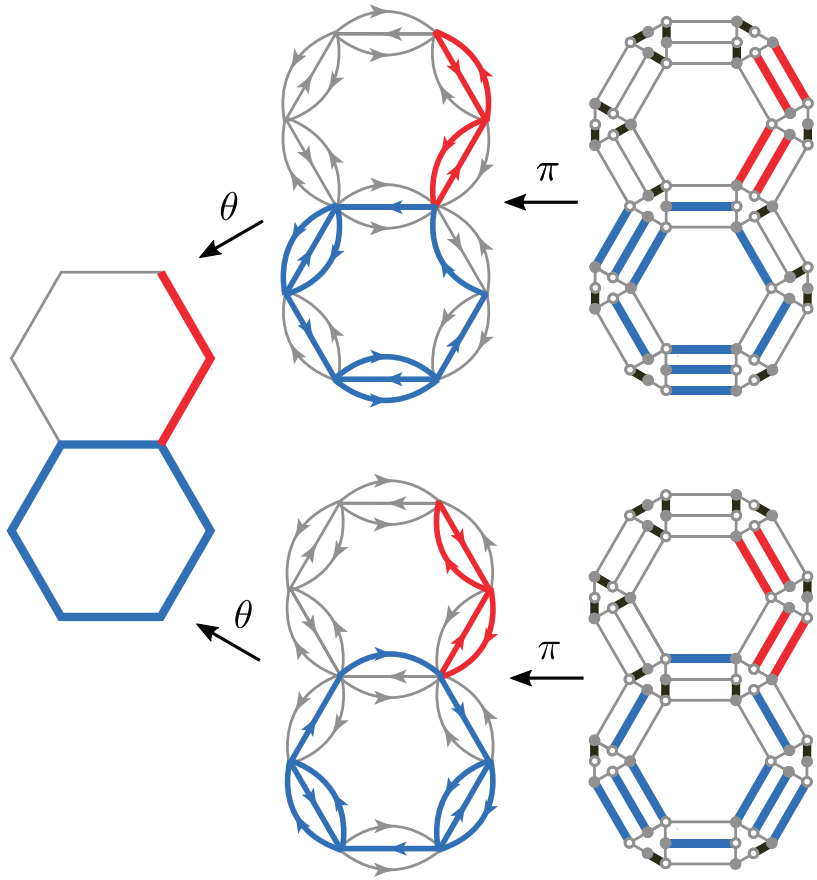

FIGURE 3.4 Left: A configuration $(\mathbf{n}_{\text{odd}}, \mathbf{n}_{\text{even}})$ on a piece of the hexagonal lattice G. The blue edges represent $\mathbf{n}_{\text{odd}}$ and the red edges represent $\mathbf{n}_{\text{even}}$. The blue and red edges together form one cluster $\mathscr{C}$. Middle: Two alternating flow configurations on $\vec{G}$ mapped to $(\mathbf{n}_{\text{odd}}, \mathbf{n}_{\text{even}})$ under θ. The two clusters have opposite orientations of the outer boundary. Depending on this orientation, the height function either increases or decreases by one when going from the outside to the inside of the lower hexagon. This corresponds to two different outcomes for the label $\epsilon_{\mathscr{C}}$ in the definition of the nesting field (1.6). Right: Two dimer configurations on G^d that map to the corresponding alternating flows under π. Note that the parity of the height function on G^d restricted to the vertices of $\mathscr{C}$ and shifted by $1/2$ changes whenever the sign of $\epsilon_{\mathscr{C}}$ changes. This can be seen from the placement of the dimers on the short edges. This property is used in the proof of Theorem 3.1. On the other hand, the parity of the height function on the faces of G is independent of $\epsilon_{\mathscr{C}}$. We also note that both π and θ are many-to-one maps.

with the weights $x_{\vec{e}}$ as in Figure 3.3. We also define the *height function* of a flow F to be a function $h = h_F$ defined on the faces of $\vec{G}$ in the following way:

(i) $h(u_0) = 0$ for the unbounded face u_0,
(ii) for every other face u, choose a path γ connecting u_0 and u, and define $h(u)$ to be total flux of F through γ, that is, the number of edges in F crossing γ from left to right minus the number of edges crossing γ from right to left.

The function h is well defined, that is, independent of the choice of γ, since at each $v \in V$, the same number of edges of F enters and leaves v (and so the total flux of F through any closed path of faces is zero).

We are ready to state the correspondence between DRCs and alternating flows. To this end, consider a map $\theta : \mathcal{F}^{\emptyset} \to \Omega^{\emptyset}$ defined as follows. For every $F \in \mathcal{F}^{\emptyset}$ and every $e \in E$, count the number of the corresponding directed edges e_m, e_{s1}, e_{s2} that are present in F. Let $F_{\text{odd}} \subseteq E$ be the set with one or three such present edges, and $F_{\text{even}} \subseteq E$ the set with exactly two such edges, and set

$$\theta(F) := (F_{\text{odd}}, F_{\text{even}}).$$

Denote by $\theta_* \mathbf{P}^{\emptyset}_{\text{flow}}$ the pushforward measure on $\Omega^{\emptyset}$. The following result was first proved in [43].

Lemma 3.4 Corollary 4.3 of [43]. *Let* $\mathbf{n}$ *be distributed according to* $\mathbf{P}^{\emptyset}_{\text{dcur}}$*, and let* $h_{\mathbf{n}}$ *be its nesting field. Let* F *be distributed according to* $\mathbf{P}^{\emptyset}_{\text{flow}}$*. Then*

$$(F_{\text{odd}}, F_{\text{even}}, h_F) = (\mathbf{n}_{\text{odd}}, \mathbf{n}_{\text{even}}, h_{\mathbf{n}}) \qquad \text{in law.}$$

Proof. This is a consequence of the fact that the total weight of all alternating flows corresponding to a cluster in the DRC, and whose outer boundary is oriented clockwise is the same as those oriented counterclockwise (see also the proof of Lemma 3.10). This corresponds to the fact that the nesting field is defined using symmetric coin flip random variables $\epsilon_{\mathscr{C}}$. Moreover, the sum of these two weights is the same as the weight of the cluster in the DRC model. More details are provided in the proof of Theorem 2.1 in [21]. □

3.2.2 | Alternating flows on $\vec{G}$ and dimers on G^d

We first shortly recall the dimer model in its full generality. To this end, consider a finite weighted graph $\mathcal{G}$. Recall that a *dimer cover* (or *perfect matching*) M of $\mathcal{G}$ is a subset of edges such that every vertex of the graph is incident to exactly one edge of M. We write $\mathcal{M}(\mathcal{G})$ for the set of all dimer covers of $\mathcal{G}$. The *dimer model* is a probability measure on $\mathcal{M}(\mathcal{G})$ which assign a probability to a dimer cover that is proportional to the product of the edge weights over the dimer cover.

To each dimer cover M on a bipartite planar finite graph $\mathcal{G}$ (coloured in black and white in a bipartite fashion), one can associate a *1-form* f_M (i.e. a function defined on directed edges which is antisymmetric under a change of orientation) satisfying $f_M((v,v')) = -f_M((v',v)) = 1$ if $\{v,v'\} \in M$ and v is white, and $f_M((v,v')) = 0$ otherwise. For a 1-form f and a vertex v, let $df(v) = \sum_{v' \sim v} f((v,v'))$ be the *divergence* of f at v. Note that for a dimer cover M, $df_M(v) = 1$ if v is white, and $df_M(v) = -1$ if v is black. Fixing a reference 1-form f_0 with the same divergence, we define the *height function* $h = h_M$ by

(i) $h(u_0) = 0$ for the unbounded face u_0,
(ii) for every other face u, choose a dual path γ connecting u_0 and u, and define $h(u)$ to be the total flux of $f_M - f_0$ through γ, that is, the sum of values of $f_M - f_0$ over the edges crossing γ from left to right.

The height function is well defined, that is, independent of the choice of γ, since $f_M - f_0$ is a divergence-free flow, that is, $d(f_M - f_0) = 0$.

We now go back to the specific case of $\mathcal{G} = G^d$. We will write $\mathbf{P}^{\emptyset}_{G^d}$ for the dimer model measure on G^d with weights as in Figure 3.3. We also fix a reference 1-form f_0 on G^d given by

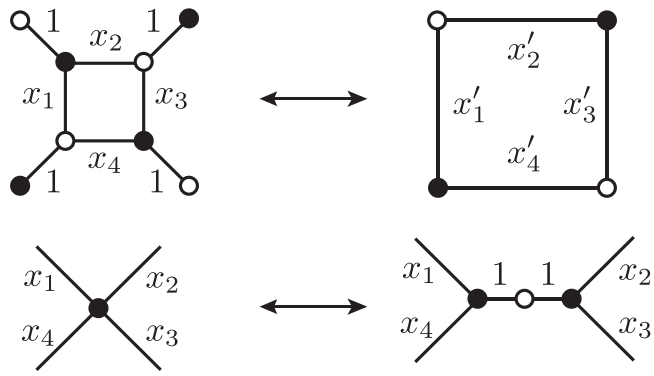

FIGURE 3.5 Urban renewal and vertex splitting are transformations of weighted graphs preserving the distribution of dimers and the height function outside the modified region. The weights in urban renewal satisfy $x_1' = \frac{x_3}{x_1x_3+x_2x_4}$, $x_2' = \frac{x_4}{x_1x_3+x_2x_4}$, $x_3' = \frac{x_1}{x_1x_3+x_2x_4}$, $x_4' = \frac{x_2}{x_1x_3+x_2x_4}$.

- $f_0((w,b)) = -f_0((b,w)) = 1/2$ if $\{w,b\}$ is a short edge and w is white,
- $f_0((w,b)) = f_0((b,w)) = 0$ if $\{w,b\}$ is a long edge.

We now describe a straightforward map π from the dimer covers on G^d to alternating flows on $\vec{G}$ that preserves the law of the height function. We note that one could carry out the same discussion and make a connection with DRCs directly, without introducing alternating flows. However, we find the language of alternating flows particularly convenient to express some of the crucial steps discussed later on (especially Lemmata 3.10 and 3.11). To this end, to each matching $M \in \mathcal{M}(G^d)$, associate a flow $\pi(M) \in \mathcal{F}^\emptyset$ by replacing each long edge in M by the corresponding directed edge in $\vec{G}$. One can check that this always produces an alternating flow. Indeed, assuming otherwise, there would be two consecutive edges in $F(M)$ of the same orientation, and therefore, the path of short edges connecting them in a cycle would be of odd length and therefore could not have a dimer cover, which is a contradiction. Let $\pi_* \mathbf{P}^\emptyset_{G^d}$ be the pushforward measure on $\mathcal{F}^\emptyset$ under the map π.

Lemma 3.5 [21]. *We have $\pi_* \mathbf{P}^\emptyset_{G^d} = \mathbf{P}^\emptyset_{\text{flow}}$. Moreover, under this identification, the restriction to U of the height function of the dimer model is exactly the height function of the resulting alternating flow.*

Proof. This is a consequence of the fact that the reference 1-form vanishes on the long edges, and hence its contribution to the increment of the height function across a long edge of G^d is equal to zero, and the fact that the weights of the edges of $\vec{G}$ and the long edges of G^d are the same. Moreover, if a vertex v has zero flow through it, that is, $v \in V \setminus V(F)$, then there are exactly 2 dimer covers of the cycle of short edges of G^d corresponding to v. Since both of these covers have total edge weight 1, this accounts for the factor $2^{|V|-|V(F)|}$ in (3.4). □

3.2.3 | Dimers on G^d and on C_G

We will write $\mathbf{P}^\emptyset_{C_G}$ for the dimer model measure on C_G with weights as in Figure 3.3. The dimer models on G^d and $(G^*)^d$ are closely related to the dimer model on C_G (as was described in [21]) using standard dimer model transformations called the vertex splitting and urban renewal, see Figure 3.5. The main two results of this section are Proposition 3.6 below where we relate the

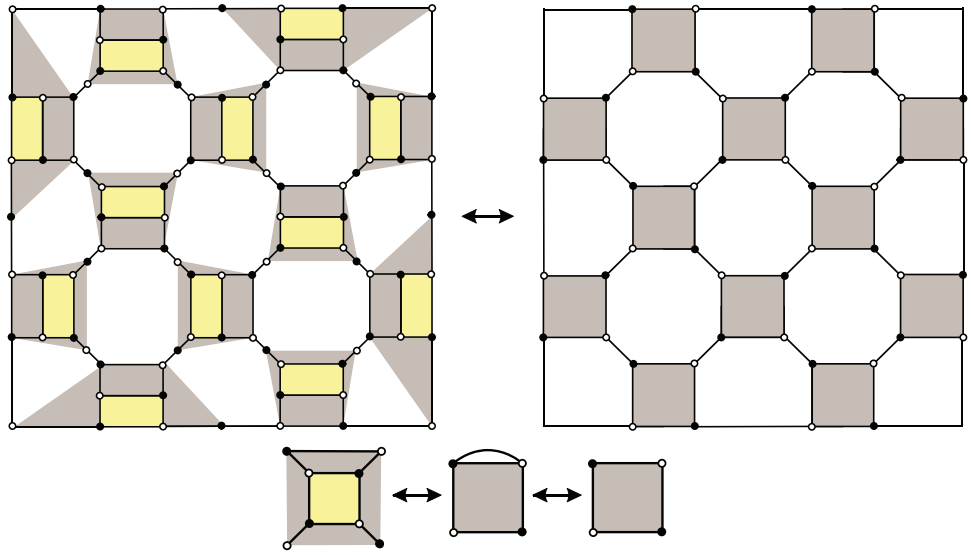

FIGURE 3.6 An example of the correspondence between dimer models on G^d and C_G. The yellow quadrilaterals within grey quadrilaterals are transformed using urban renewal moves, and then collapsing one doubled edge to a single edge as shown at the bottom of the figure. The underlying graph G is a 3×3 piece of the square lattice.

height functions on G^d and C_G, and the proof Theorem 3.1 (existence of the master coupling) that relies on Proposition 3.6.

Proposition 3.6. *The height function on C_G restricted to the faces and vertices of G is distributed as the height functions on G^d and $(G^*)^d$ restricted to the faces and vertices of G. In particular, the height function on C_G restricted to the faces of G has the law of the nesting field of the DRC with free boundary conditions on G, and restricted to the vertices of G has the law of the nesting field of the DRC with wired boundary conditions on $G^\dagger$ (or free boundary conditions on G^*).*

To prove the proposition, we start with a crucial lemma that first appeared in [21].

Lemma 3.7 [21]. *One can transform G^d and $(G^*)^d$ to C_G (and the other way around) using urban renewals and vertex splittings.*

Proof. We will describe how to transform G^d to C_G (see Figure 3.6 for an illustration). The second part follows since C_G is symmetric with respect to G and G^*.

To this end, fix a bipartite black-white colouring of both G^d and C_G. Note that for each edge e in G, there is one quadrilateral Q in C_G and two quadrilaterals Q_1, Q_2 in G^d corresponding to e. For each such edge e, choose for the internal quadrilateral of urban renewal the quadrilateral Q_i in G^d with the opposite colours of vertices when compared to Q. Then, split each vertex that the chosen quadrilateral shares with a quadrilateral corresponding to a different edge of G. In this way, we find ourselves in the situation from the upper left panel in Figure 3.5. After performing urban renewal and collapsing the doubled edge, we are left with one quadrilateral as desired. One can check that the weights that we obtain match those from Figure 3.3. We then repeat the procedure for every edge of G. The resulting graph is C_G. □

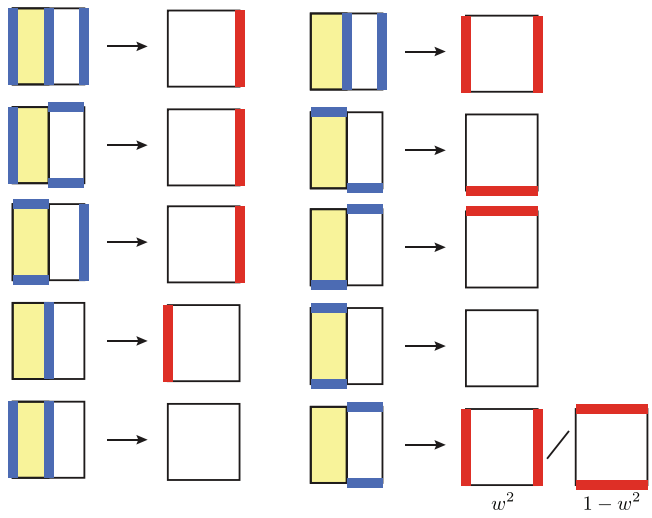

FIGURE 3.7 The figure shows the measure-preserving mapping of local configurations on G^d (corresponding to a single edge e of G) to local configurations on the streets of C_G under urban renewal performed on the left-hand-side quadrilateral in G^d. The last case involves additional random choice between two possible configurations. These choices are independent for local configurations corresponding to different edges of G and the probabilities are as in the figure with $w = 2x/(1+x^2)$.

A choice of quadrilaterals where urban renewals are applied for a rectangular piece of the square lattice is depicted in Figure 3.6. In this way, the DRC model on the square lattice is related to a (weighted) dimer model on the square-octagon lattice. In Figure 3.7, we illustrate the behaviour of local dimer configurations under one urban renewal performed in the construction described in the lemma above.

As the reference 1-form for the dimer model on C_G, we choose the canonical one given by

$$f_0((w,b)) = -f_0((b,w)) = \mathbf{P}^{\emptyset}_{C_G}(\{w,b\} \in M), \tag{3.5}$$

where w is a white vertex. Note that this makes the height function centred as all its increments become centred by definition. This is the same 1-form as used in [9] on the infinite square-octagon lattice $C_{\mathbb{Z}^2}$. In [36], two crucial properties of f_0 were established when G is an infinite isoradial graph and the Ising model on G is critical. In the next lemma, we show that both of these properties hold for arbitrary Ising weights on general finite planar graphs.

Lemma 3.8. *We have*

- $\mathbf{P}^{\emptyset}_{C_G}(e \in M) = 1/2$, *if e is a road, that is, e corresponds to a corner of G,*
- $\mathbf{P}^{\emptyset}_{C_G}(e \in M) = \mathbf{P}^{\emptyset}_{C_G}(e' \in M)$, *if e and e' are two parallel streets corresponding to the same edge of G (or of the dual G^*).*

In the proof, which is postponed to the end of Section 3.3, we actually compute the probability from the second item in terms of the underlying Ising measure. However, the exact value will not be important for our considerations. We note that the first bullet of the lemma above is the reason why the nesting field with free boundary conditions on G is defined to be integer-valued and the one with wired boundary conditions on G^* to be half-integer valued.

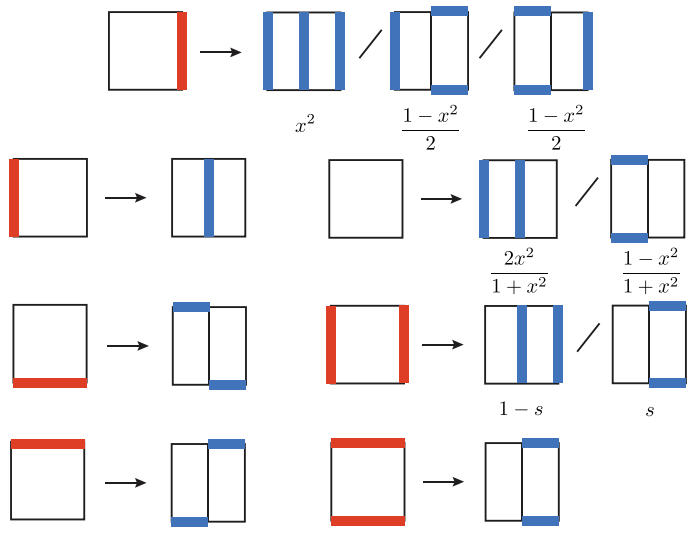

FIGURE 3.8 The reverse mapping to that in Figure 3.7. Again, urban renewal is performed on the left-hand-side quadrangle of the local configuration on G^d. Whenever there is ambiguity, we use additional randomness which is independent for each local configuration and with probabilities as in the figure with $s = \frac{2(1-x^2)}{3+x^4}$. These probabilities are simply obtained from Figure 3.7 using the definitions of the weights in both dimer models on C_G and G^d and elementary conditional probability computations.

A crucial observation now is that the height function on the faces of G^d corresponding to the faces and vertices of G is not modified by vertex splitting and urban renewal. This follows from basic properties of these transformations, and the fact that the reference 1-form on the short edges of G^d is the same as the one on the roads of C_G (by the first item of the lemma above). Indeed, one can compute the height function on the faces of G^d and C^G corresponding to the faces and vertices of G using only increments across short edges and roads, respectively. This means that the resulting height function on these faces of C_G has the same distribution as the one on G^d. Since C_G plays the same role with respect to G^* as to G, we immediately conclude Proposition 3.6.

This observation is at the heart of the proof of the master coupling from Theorem 3.1. However, one has to be careful since there is loss of information between the dimer model on G^d and the one on C_G. Indeed, we have already seen that knowing a dimer configuration on G^d allows one to fully recover the triple $(\mathbf{n}_{\text{odd}}, \mathbf{n}_{\text{even}}, h_{\mathbf{n}})$. However, a dimer configuration M on C_G only gives access to $(\mathbf{n}_{\text{odd}}, h_{\mathbf{n}})$ (since M determines the height function, and $\mathbf{n}_{\text{odd}}$ are the edges where the height function has a non-trivial increment) and does not contain information about $\mathbf{n}_{\text{even}}$. To recover it, one needs to add additional randomness in the form of independent coin flips for each edge of G with an appropriate success probability.

Proof of Theorem 3.1. We will use a procedure reverse to that from the proof of Lemma 3.7. This procedure induces a measure-preserving mapping between local configurations on C_G and G^d, see Figure 3.8, where in certain cases additional randomness is used to decide on the exact configuration on G^d.

As mentioned, the graph C_G plays a symmetric role with respect to G and G^*. Hence, taking the Kramers–Wannier dual parameters $x_e^* = (1-x_e)/(1+x_e)$ and rotating the local configuration on C_G by $\pi/2$, one can use the same mapping from Figure 3.8 to generate local dimer

configurations on $(G^*)^d$ that will correspond to dual random current configurations. Recall that part of our aim is to couple the DRC on G with its dual on G^* so that no edge and its dual are open at the same time. The idea is to first sample a dimer configuration on C_G, and then using the rules from Figure 3.8 to choose, possibly introducing additional randomness, the dimer configurations on both G^d and $(G^*)^d$. The desired property of the coupling will follow from the way we use the additional randomness for G^d and $(G^*)^d$.

We now explain this in more detail. In the coupling between DRCs and dimers on G^d, an edge in the current has value zero if and only if there is no long edge present in the corresponding local dimer configuration. From Figure 3.8, we see that the only possibility to have non-zero values of double currents for both a primal edge e and its dual e^* is when the quadrangle in C_G that corresponds to both e and e^* has no dimer in the dimer cover. In that case, we have a probability of $2x_e^2/(1+x_e^2)$ to get a non-zero (and even) value of the primal double current and a probability of $2(x_e^*)^2/(1+(x_e^*)^2)$ to get a non-zero (and even) value of the dual double current. However, since these choices are independent of the possible choices for other local configurations, and since

$$\frac{2x_e^2}{1+x_e^2}+\frac{2(x_e^*)^2}{1+(x_e^*)^2}=1-\frac{2x_e(1-x_e)}{1+x_e^2}<1,$$

we can couple the results so that the primal and dual currents are never both open (non-zero) at e. Together establishes Property 1 from the statement of the theorem.

We now focus on Property 2. Note that the spins $\tau^\dagger$ defined by the interfaces of odd current in $\mathbf{n}$ satisfy

$$\tau_u^\dagger=(-1)^{H(u)} \tag{3.6}$$

for $u\in U$, where H is the height function on C_G. By Proposition 3.6, we already know that H restricted to U has the law of the height function on $(G^*)^d$ restricted to U. From the relationship between the DRC $\mathbf{n}^\dagger$ on G^* and the alternating flow model on $\vec{G}^*$, one can see that the parity of this height function at a face u changes with the change of the orientation of the outer boundary of the cluster of $\mathbf{n}^\dagger$ containing u (see Figure 3.4 for a dual example). Therefore, $(-1)^{H(u)}$ is distributed as an independent assignment of a sign to each cluster of $\mathbf{n}^\dagger$. This yields Property 2. A dual argument for

$$\tau_v=i(-1)^{H(v)} \tag{3.7}$$

with $v\in V$, and i the imaginary unit, yields the dual correspondence. Here, the factor i appears due to the fact that the height function takes half-integer values on V.

Furthermore, (3.6) and (3.7) together imply Property 3.

Finally, for Property 4, we make the following observations. First of all, when an edge is empty (has zero current) in $\mathbf{n}$, then in the dimer model on G^d, the corresponding three long edges are not part of the dimer configuration. We can therefore remove them, and proceed similarly for all other empty edges encountered during the exploration of a cluster of $\mathbf{n}$. This means that the unexplored part dimer configuration on $\tilde{G}^d$ is independent of the explored part, and moreover is in a measure-preserving correspondence with DRCs with free boundary conditions on $\tilde{G}$. Furthermore, the (random) maps from Figures 3.7 and 3.8, when composed together, map from dimers on $\tilde{G}^d$ to dimers on $(\tilde{G}^*)^d$ (and hence to DRCs with wired boundary conditions on the weak dual $(\tilde{G}^\dagger)^d$) are local. Therefore, the distribution of $\mathbf{n}^\dagger$ inside $(\tilde{G}^*)^d$ is not affected by the explored part of the primal current $\mathbf{n}$ outside $\tilde{G}$, and is that of an independent DRC with wired boundary conditions

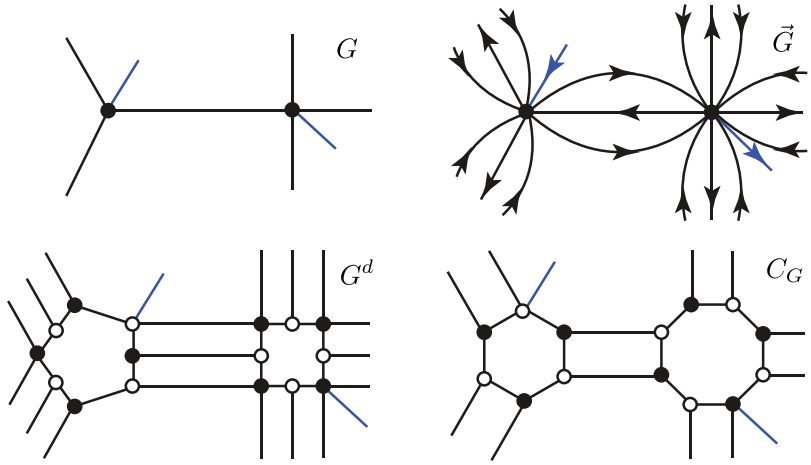

FIGURE 3.9 Corner insertions in the relevant models can be realised by considering additional edges connecting a vertex and a neighbouring face.

on $(\tilde{G}^\dagger)^d$. We also note that a proof without using the dimer representation can also be given using the construction from [42]. □

We leave it to the interested reader to check that the resulting coupling of the primal and dual DRC model is the same as the one described in [42] (where no connection with the dimer model is used, and where all the properties above can as well be deduced).

3.3 | Disorder and source insertions

It will be important for our analysis to introduce the so-called sources in dimers, alternating flows, and DRCs, and to see how they relate to order-disorder variables in the Ising model.

A *corner* $c = (u, v)$ of a planar graph G is a pair composed of a face $u = u(c)$ (also seen as a vertex of the dual graph) and a vertex $v = v(c)$ bordering u. One can visualise corners as segments from the centre of the face u to the vertex v (see Figure 3.9). In this section, we discuss correlations of disorder insertions, by which we mean modifications of the state space of the appropriate model that are localised at the corners of G, and describe their mutual relationships. In what follows, consider two corners c_i and c_j, and a simple dual path γ connecting $u(c_i)$ to $u(c_j)$. For a collection of edges E_0 of G, $\vec{G}$, G^d or C_G, we define $\mathrm{sgn}_\gamma(E_0) = -1$ if the number of edges in E_0 crossed by γ is odd and $\mathrm{sgn}_\gamma(E_0) = 1$ otherwise.

In the following subsections, we introduce correlation functions of corner insertions in the relevant models and relate them to each other.

3.3.1 | Kadanoff–Ceva fermions via double random currents

The two-point correlation function of *Kadanoff–Ceva fermions* is defined by

$$\langle \chi_{c_i} \chi_{c_j} \rangle^\gamma := \frac{1}{Z^\emptyset_{\mathrm{hT}}} \sum_{\eta \in \mathcal{E}^{\{v(c_i), v(c_j)\}}} \mathrm{sgn}_\gamma(\eta) \prod_{e \in \eta} x_e, \tag{3.8}$$

where $Z^{\emptyset}_{\mathrm{hT}} := \sum_{\eta\in\mathcal{E}^{\emptyset}} \prod_{e\in\eta} x_e$. Here, $\mathcal{E}^{\emptyset}$ is the collection of sets of edges $\eta \subseteq E$ such that each vertex in the graph (V,η) has even degree, and $\mathcal{E}^{\{v(c_i),v(c_j)\}}$ is the collection of sets of edges such that each vertex has even degree except for $v(c_i)$ and $v(c_j)$ that have odd degree. We note that the sign of this correlator depends on the choice of γ. However, its amplitude depends only on the corners c_i and c_j.

The next lemma was proved in [4, Lemma 6.3]. It expresses Kadanoff–Ceva correlators in terms of double currents for which $u(c_i)$ is connected to $u(c_j)$ in the dual configuration. Below, for $\mathbf{n} \in \Omega^B$, let

$$\mathrm{w}_{\mathrm{dcur}}(\mathbf{n}) := \sum_{\substack{\mathbf{n}_1\in\Omega^B,\mathbf{n}_2\in\Omega^{\emptyset}\\ \mathbf{n}_1+\mathbf{n}_2=\mathbf{n}}} \mathrm{w}(\mathbf{n}_1)\mathrm{w}(\mathbf{n}_2),$$

where $\mathrm{w} = \mathrm{w}_G$ is the random current weight defined in (1.4). For a current $\mathbf{n}$, let $\mathbf{n}^*$ be the set of dual edges e^* with $\mathbf{n}_e = 0$. For two faces u and u', let $u \overset{\mathbf{n}^*}{\longleftrightarrow} u'$ mean that u is connected to u' in $\mathbf{n}^*$, that is, that u and u' belong to the same connected component of the graph $(U,\mathbf{n}^*)$.

Lemma 3.9 Fermions via double currents [4]. *We have*

$$\langle \chi_{c_i}\chi_{c_j}\rangle^{\gamma} = \frac{1}{Z^{\emptyset}_{\mathrm{dcur}}} \sum_{\mathbf{n}\in\Omega^{\{v(c_i),v(c_j)\}}} \mathrm{sgn}_{\gamma}(\mathbf{n}_{\mathrm{odd}})\mathrm{w}_{\mathrm{dcur}}(\mathbf{n})\mathbf{1}\{u(c_i) \overset{\mathbf{n}^*}{\longleftrightarrow} u(c_j)\}.$$

3.3.2 | Sink and source insertions in alternating flows

Consider the graph $\vec{G}$ with two additional directed edges $c_i = (u(c_i), v(c_i))$ and $-c_j = (v(c_j), u(c_j))$, and let $\mathcal{F}^{c_i,-c_j}$ be the set of alternating flows on this graph that contain both c_i and $-c_j$. By an alternating flow, here we mean a subset of edges of the extended graph that satisfies the alternating condition at every vertex of $\vec{G}$. The weights of c_i and $-c_j$ are set to 1. With γ defined as above, introduce

$$Z^{\gamma}_{\mathrm{flow}}(c_i,-c_j) := \sum_{F\in\mathcal{F}^{c_i,-c_j}} \mathrm{sgn}_{\gamma}(F)\mathrm{w}_{\mathrm{flow}}(F).$$

Here, c_i plays the role of the *source* and $-c_j$ is the *sink* of the flow F.

Recall that $\theta : \mathcal{F}^{\emptyset} \to \Omega^{\emptyset}$ is the measure-preserving map sending sourceless alternating flows on $\vec{G}$ to sourceless double current configurations on G, where as before, we identify a current $\mathbf{n}$ with the pair $(\mathbf{n}_{\mathrm{odd}}, \mathbf{n}_{\mathrm{even}})$. With a slight abuse of notation, we also write θ for the analogous map from $\mathcal{F}^{c_i,-c_j}$ to the set $\Omega^{\{v(c_i),v(c_j)\}}$ of currents on G with sources at $v(c_i)$ and $v(c_j)$ (for currents, there is no distinction between sources and sinks).

The next lemma is closely related to [43, Theorem 4.1].

Lemma 3.10 (Symmetry between sinks and sources). *We have*

$$Z^{\gamma}_{\mathrm{flow}}(c_i,-c_j) = Z^{\gamma}_{\mathrm{flow}}(c_j,-c_i).$$

Proof. Note that the flow's weights on $\vec{G}$ are invariant under the reversal of direction of the flow, that is, the weights of the three directed edges e_{s1}, e_m, e_{s2} of $\vec{G}$ corresponding to a single edge e of G satisfy $x_{e_{s1}} + x_{e_{s2}} + x_{e_{s1}} x_{e_{s2}} x_{e_m} = x_{e_m}$ by construction. Hence, for a fixed $(\mathbf{n}_{\text{odd}}, \mathbf{n}_{\text{even}}) \in \Omega^{\{v(c_i), v(c_j)\}}$, we have

$$\sum_{F \in \mathcal{F}^{c_i, -c_j} \,:\, \theta(F) = (\mathbf{n}_{\text{odd}}, \mathbf{n}_{\text{even}})} \mathrm{w}_{\text{flow}}(F) = \sum_{F \in \mathcal{F}^{c_j, -c_i} \,:\, \theta(F) = (\mathbf{n}_{\text{odd}}, \mathbf{n}_{\text{even}})} \mathrm{w}_{\text{flow}}(F).$$

We finish the proof by summing both sides of this identity over $(\mathbf{n}_{\text{odd}}, \mathbf{n}_{\text{even}}) \in \Omega^{\{v(c_i), v(c_j)\}}$, and using the fact that $\mathrm{sgn}_\gamma(F)$ depends only on $\theta(F)$. □

The next result is a direct analogue of Lemma 3.9 with an additional factor of $1/2$ that corresponds to the fact that the connected component of the flow that connects c_i to $-c_j$ has a fixed orientation.

Lemma 3.11 (Dual connection in alternating flows). *We have*

$$\theta(\mathcal{F}^{c_i, -c_j}) = \{\mathbf{n} \in \Omega^{\{v(c_i), v(c_j)\}} \,:\, u(c_i) \overset{\mathbf{n}^*}{\longleftrightarrow} u(c_j)\},$$

and moreover,

$$Z^\gamma_{\text{flow}}(c_i, -c_j) = \frac{1}{2} \sum_{\mathbf{n} \in \Omega^{\{v(u_i), v(c_j)\}}} \mathrm{sgn}_\gamma(\mathbf{n}_{\text{odd}}) \mathrm{w}_{\text{dcurr}}(\mathbf{n}) \mathbf{1}\{u(c_i) \overset{\mathbf{n}^*}{\longleftrightarrow} u(c_j)\}.$$

Proof. We first argue that for each $(\mathbf{n}_{\text{odd}}, \mathbf{n}_{\text{even}}) = \theta(F)$ with $F \in \mathcal{F}^{c_i, -c_j}$, we have that $u(c_i) \overset{\mathbf{n}^*}{\longleftrightarrow} u(c_j)$. This follows from topological arguments and the alternating condition for flows. Indeed, assume by contradiction that there is a cycle of edges in F separating $u(c_i)$ from $u(c_j)$, and choose the innermost such cycle surrounding $u(c_i)$. Consider the vertex v of this cycle that is first visited on a path from c_i to $-c_j$. The alternating condition implies that the edges of the cycle on both sides of v should be oriented away from v. Following that orientation around the cycle, we must arrive at another vertex v' of the cycle where both incident edges are oriented towards v'. That is in contradiction with the alternating condition and the fact that the cycle is minimal. The fact that the image of the map is $\{u(c_i) \overset{\mathbf{n}^*}{\longleftrightarrow} u(c_j)\}$ follows from the same arguments as in [43, Lemma 5.4].

The second part of the statement follows from the proof of [43, Theorem 4.1] or [21, Theorem 1.7] (the weights of flows in [43] are the same as ours up to a global factor). The multiplicative constant $1/2$ is a consequence of the fact that the orientation of the cluster containing the corners is fixed to one of the two possibilities, and in the DRC measure, there is an additional factor of 2 for each cluster (see [43, Theorem 3.2]). □

Corollary 3.12. *We have*

$$\langle \chi_{c_i} \chi_{c_j} \rangle^\gamma = 2 \frac{Z^\gamma_{\text{flow}}(c_i, -c_j)}{Z^\gamma_{\text{flow}}} = 2 \frac{Z^\gamma_{\text{flow}}(c_j, -c_i)}{Z^\gamma_{\text{flow}}}.$$

Proof. This follows directly from Lemmata 3.9 and 3.11. □

3.3.3 | Monomer insertions on G^d and C_G

We identify the faces and vertices of the graphs G and $\vec{G}$ with the corresponding subsets of the faces of the dimer graphs G^d and C_G. We say that a vertex of G^d or C_G is a *corner (vertex)* corresponding to $c = vu$ if it is incident both on the vertex v and the face u of G in this identification. Analogously to the discussion above, for $\mathcal{G} \in \{G^d, C_G\}$ and v, v' two vertices of $\mathcal{G}$, we define $Z^\gamma_{\mathcal{G}}$ to be the partition function of dimer covers of the graph $\mathcal{G}$ with v and v' removed, where moreover each dimer crossed by the path γ contributes an additional factor of -1 to the weight of the cover.

Lemma 3.13 (Symmetry between white and black corners). *Let b_i and w_i (resp. b_j and w_j) be a black and white corner vertex of G^d corresponding to the corner c_i (resp. c_j). If there is no such vertex of the chosen colour, we modify G^d by splitting the corner vertex of the opposite colour (using the vertex splitting operation from Figure 3.5). Then,*

$$Z^\gamma_{G^d}(b_i, w_j) = Z^\gamma_{G^d}(w_i, b_j) = Z^\gamma_{\text{flow}}(c_i, c_j).$$

Proof. By the definition of the measure-preserving map F_* between dimers and alternating flows, a corner monomer insertion in dimers is a source or sink insertion in alternating flows, which yields

$$Z^\gamma_{\text{flow}}(c_i, c_j) = Z^\gamma_{G^d}(b_i, w_j).$$

The statement then follows immediately from Lemma 3.10. □

Lemma 3.14 (Monomer insertions in G^d and C_G). *Let b and w be, respectively, black and white corner vertices of G^d, and let $\tilde{b}$ and $\tilde{w}$ be the corresponding black and white vertices of C_G. Then,*

$$Z^\gamma_{G^d}(b, w) = Z^\gamma_{C_G}(\tilde{b}, \tilde{w}).$$

Proof. We use urban renewal as in Figure 3.10 to transform G^d with monomer insertions to C_G with monomer insertions. Note that here we use urban renewal with some of the long edges having negative weight. However, this is not a problem since the opposite edges in a quadrilateral being transformed by urban renewal always have the same sign, which results in a non-zero multiplicative constant for the partition functions. The resulting weights of C_G are negative if and only if the edge crosses γ. This implies the claim readily. □

We finally combine the previous results to obtain the following identity. We note that it can also be derived using the approach of [17] after taking into account the symmetry of the underlying six-vertex model (that we do not discuss here and that is also not discussed in [17]).

Corollary 3.15. *In the setting of Lemma 3.13, we have*

$$\langle \chi_{c_i} \chi_{c_j} \rangle^\gamma = 2\frac{Z^\gamma_{C_G}(w_i, b_j)}{Z_{C_G}} = 2\frac{Z^\gamma_{C_G}(w_j, b_i)}{Z_{C_G}}.$$

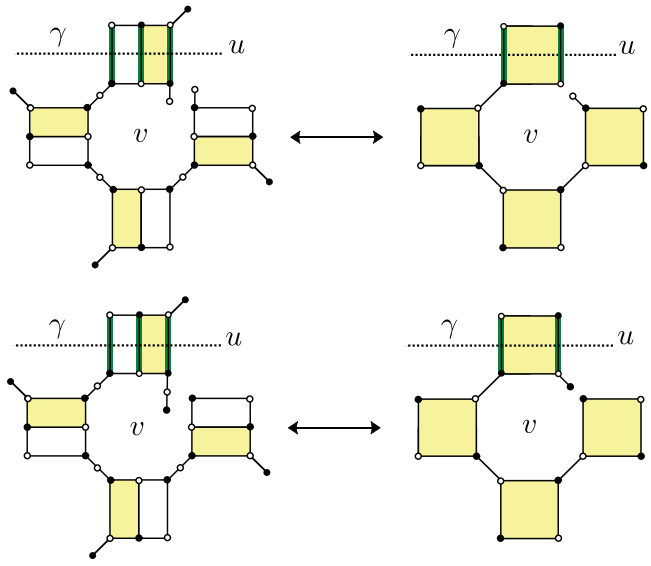

FIGURE 3.10 Behaviour of corner monomer insertions under urban renewal. Insertion of a monomer is modelled by the addition of edges with weight one into the dimer model: above (resp. below), the insertion of a black (resp. white) monomer at the corner $c = uv$ with a disorder operator at u. The green edges crossing γ are assigned negative weights. Urban renewal is applied to the yellow quadrilaterals on the left-hand side yielding the yellow quadrilaterals on the right-hand side. Note that the colour of the monomer insertions on the left-hand and right-hand sides agree.

Proof. This follows from Lemmata 3.14 and 3.13, as well as Corollary 3.12. □

The final item of this section is the proof of Lemma 3.5 which explicitly computes the canonical reference 1-form (3.8) on C_G in terms of the underlying Ising measures.

Proof of Lemma 3.8. By the corollary above, for a street $\{w, b\}$ of C_G corresponding to an edge $e = \{v, v'\}$ of G, we have

$$\mathbf{P}^{\emptyset}_{C_G}(\{w,b\} \in M) = \frac{2x}{1+x^2} \frac{Z^{\gamma}_{C_G}(w,b)}{Z_{C_G}} = \frac{x}{1+x^2} \langle \chi_c \chi_{c'} \rangle^{\gamma}, \tag{3.9}$$

where $x = x_e = \tanh \beta J_e$ is the high-temperature Ising weight, $\frac{2x}{1+x^2}$ is the weight of the edge $\{w, b\}$ in the dimer model on C_G as in Figure 3.3, and where c and c' are the two corners of G corresponding to the two roads of C_G that are incident on w and b, respectively. Indeed, the first identity is a consequence of the fact that in this case the path γ can be chosen empty and therefore the numerator $Z^{\gamma}_{C_G}(w, b)$ is actually the *unsigned* partition function of dimer covers of the graph where w and b are removed.

We now compute $\langle \chi_c \chi_{c'} \rangle^{\gamma}$ in terms of the Ising two-point function $\mu_G[\sigma_v \sigma_{v'}]$. To this end, recall that $\mathcal{E}^{\emptyset}$ is the collection of sets of edges $\eta \subseteq E$ such that each vertex in the graph (V, η) has even degree, and $\mathcal{E}^{\{v,v'\}}$ is the collection of sets of edges such that each vertex has even degree except

for v and v' that have odd degree. Let

$$Z_+ := \sum_{\substack{\eta\in\mathcal{E}^\emptyset \\ e\in\eta}} \prod_{e'\in\eta} x_{e'}, \qquad \text{and} \qquad Z_- := \sum_{\substack{\eta\in\mathcal{E}^\emptyset \\ e\notin\eta}} \prod_{e'\in\eta} x_{e'},$$

and $Z = Z^\emptyset_{\mathrm{hT}}$. By definition (3.8) of Kadanoff–Ceva fermions with γ empty, the high-temperature expansion of spin correlations, and the fact that $\eta \mapsto \eta \triangle \{e\}$ is a bijection between $\mathcal{E}^\emptyset$ and $\mathcal{E}^{\{v,v'\}}$, (3.9) gives

$$\mathbf{P}^\emptyset_{C_G}(\{w,b\}\in M) = \frac{x}{1+x^2}\frac{1}{Z}(x^{-1}Z_+ + xZ_-) = \frac{x}{1+x^2}\mu_G[\sigma_v\sigma_{v'}]. \tag{3.10}$$

The same argument applied to the other street $\{w',b'\}$ corresponding to the same edge e yields $\mathbf{P}^\emptyset_{C_G}(\{w,b\}\in M) = \mathbf{P}^\emptyset_{C_G}(\{w',b'\}\in M)$ as the last displayed expression depends only on e. Moreover, by the Kramers–Wannier duality and the same computation for the dual Ising model on the dual graph G^*, we have

$$\mathbf{P}^\emptyset_{C_G}(\{w,b'\}\in M) = \mathbf{P}^\emptyset_{C_G}(\{w',b\}\in M) = \frac{x^*}{1+(x^*)^2}\mu_{G^*}[\sigma_u\sigma_{u'}] = \frac{1-x^2}{2(1+x^2)}\mu_{G^*}[\sigma_u\sigma_{u'}], \tag{3.11}$$

where $x^* := (1-x)/(1+x)$ is the dual weight, and where $\{u,u'\}$ is the dual edge of $\{v,v'\}$. This yields the second bullet of the lemma.

To prove the first bullet of the lemma, we need to relate the dual energy correlators $\mu_G[\sigma_v\sigma_{v'}]$ and $\mu_{G^*}[\sigma_u\sigma_{u'}]$ with each other. Interpreting the graphs in $\mathcal{E}^\emptyset$ as interfaces between spins of different value on the vertices of G^*, and using the low-temperature expansion, we get

$$\mu_{G^*}[\sigma_u\sigma_{u'}] = \frac{Z_- - Z_+}{Z}.$$

This together with the second equality of (3.10), and the fact that $Z_+ + Z_- = Z$, yields

$$2x\mu_G[\sigma_v\sigma_{v'}] + (1-x^2)\mu_{G^*}[\sigma_u\sigma_{u'}] = 1+x^2.$$

Therefore adding (3.10) and (3.11) gives

$$\mathbf{P}^\emptyset_{C_G}(\{w,b\}\in M) + \mathbf{P}^\emptyset_{C_G}(\{w,b'\}\in M) = 1/2.$$

This means that the probability of seeing the road containing w in the dimer configuration is $1/2$. By symmetry, this is true for all roads of C_G. This finishes the proof. □

3.4 | Kasteleyn theory and complex-valued fermionic observables

In this section, we introduce a Kasteleyn orientation which will be directly related to complex-valued observables introduced by Chelkak and Smirnov [15].

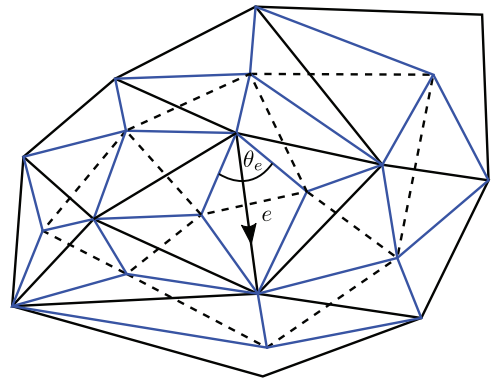

FIGURE 3.11 A piece of the primal graph G and its dual G^* (black solid and dashed edges respectively) and the corresponding diamond graph (blue edges) used to define the Kasteleyn weighting. We assume that the edges of G and G^* are drawn as straight line segments. Each street e of C_G can be identified with a directed edge of G or G^*. Then, the angle θ_e is the angle in the diamond graph at the origin of this directed edge as depicted in the figure. By definition, these angles sum up to 2π around every vertex and face of G, and around every face of the diamond graph. This guarantees that the associated weighting satisfies the Kasteleyn condition.

3.4.1 | A choice of Kasteleyn's orientation

A *Kasteleyn weighting* of a planar bipartite graph is an assignment of complex phases $\varsigma_e \in \mathbb{C}$ with $|\varsigma_e| = 1$ to the edges of the graph satisfying the *alternating product condition* meaning that for each cycle $e_1, e_2, \dots, e_{2k}$ in the graph, we have

$$\prod_{i=1}^{k} \varsigma_{e_{2i-1}} \varsigma_{e_{2i}}^{-1} = (-1)^{k+1}. \tag{3.12}$$

Note that it is enough to check the condition around every bounded face of the graph.

To define an explicit Kasteleyn weighting for C_G, consider the *diamond graph* of G, that is, the graph whose vertices are the vertices and faces of G, and whose edges are the corners of G (see Figure 3.11). Recall that the edges of C_G that correspond to the corners of G are called roads and the remaining edges (forming the quadrangles) are called streets. To each street, there is assigned an angle θ_e between the two neighbouring corners in the diamond graph. We now define

- $\varsigma_e = -1$ if e is a road,
- $\varsigma_e = \exp(\frac{\mathrm{i}}{2}\theta_e)$ if e is a street that crosses a primal edge of G,
- $\varsigma_e = \exp(-\frac{\mathrm{i}}{2}\theta_e)$ if e is a street that crosses a dual edge of G^*.

That ς is a Kasteleyn orientation of C_G follows from the fact that the angles sum up to 2π around every vertex and face of G, and around every face of the diamond graph. Note that if G is a finite subgraph of an embedded infinite graph Γ, then one can as well use the angles from the diamond graph of Γ since, as already mentioned, one needs to check condition (3.12) only on the bounded faces of C_G. In particular, for subgraphs of the square lattice with the standard embedding, we will take $\theta_e = \pi/2$ for all edges e.

Fix a bipartite colouring of C_G, and let $K = K_{C_G}$ be a Kasteleyn matrix for a dimer model on the bipartite graph C_G with the weighting as above, that is, the matrix whose rows are indexed by the

black vertices and the columns by the white vertices, and whose entries are

$$K(b,w) := \varsigma_{bw} x_{bw}$$

if bw is an edge of C_G and $K(b,w) = 0$ otherwise, where b and w are respectively black and white vertices, and x is the edge weight for C_G as in Figure 3.3.

We assume that the set of corners of G comes with a prescribed order $c_1, \dots, c_m$, and we order the rows and columns of K according to this order (for each white and black vertex of C_G, there is exactly one corner of G that the vertex corresponds to). We denote by b_i and w_i the black and white vertex of C_G corresponding to c_i.

The following lemma is a known observation.

Lemma 3.16. *We have that*

$$K^{-1}(w_i, b_j) = \mathrm{i}\kappa_\gamma \frac{Z^\gamma_{C_G}(w_i, b_j)}{Z_{C_G}}, \tag{3.13}$$

where γ is any dual path connecting a face u_i adjacent to b_i with a face u_j adjacent to w_j, κ_γ is a complex phase depending only on γ, w_j and b_i (see the proof for a concrete formula), and $Z^\gamma_{C_G}(b_i, w_j)$ is, as before, the partition function of dimers on C_G with b_i and w_j removed, and with negative weights assigned to the edges crossing γ.

The factor i is due to an arbitrary choice of κ_γ which is made for later convenience. We will now justify (3.13) and explicitly identify the complex phase κ_γ in this expression.

Proof. To compute the inverse matrix, we use the cofactor representation as a ratio of determinants:

$$K^{-1}(w_i, b_j) = (-1)^{i+j} \frac{\det K^{b_j, w_i}}{\det K},$$

where $K^{w_i, b_j} =: \tilde{K}$ is the matrix K with the jth row and ith column removed.

By definition of the determinant, we have

$$\det K = \sum_{\pi \in S_m} \operatorname{sgn}(\pi) \prod_{k=1}^{m} \varsigma_{b_k w_{\pi(k)}} x_{b_k w_{\pi(k)}}.$$

In this sum, only terms where π corresponds to a perfect matching on C_G are non-zero. Moreover, by a classical theorem of Kasteleyn [33], the complex phase $\operatorname{sgn}(\pi) \prod_{i=1}^m \varsigma_{b_i w_{\pi(i)}}$ is constant for such π. In particular, we can take π to be the identity. Since $\varsigma_{b_i w_i} = -1$, we get that

$$\det K = (-1)^N Z_{C_G},$$

where N is the number of corner edges in C_G.

We now want to interpret $\tilde{K}$ as a Kasteleyn matrix for the graph $\tilde{C}_G$ obtained from C_G by removing the vertices w_i and b_j. To this end, if w_i and b_j are not incident on the same face $u_i = u_j$, we

need to introduce a sign change to the Kasteleyn weighting along a dual path γ which connects u_i to u_j. We do it as follows. Define modified weights $\tilde{\varsigma}$ and $\tilde{x}$ by $\tilde{\varsigma}_e = -\varsigma_e$ (resp. $\tilde{x}_e = -x_e$), if e is crossed by γ, and $\tilde{\varsigma}_e = \varsigma_e$ (resp. $\tilde{x}_e = x_e$) otherwise. Then $\varsigma_e x_e = \tilde{\varsigma}_e \tilde{x}_e$, and hence $\tilde{K}(b,w) = \tilde{\varsigma}_{bw}\tilde{x}_{bw}$ if bw is an edge of $\tilde{C}_G$, and $\tilde{K}(b,w) = 0$ otherwise. We leave it to the reader to verify that $\tilde{\varsigma}$ is indeed a Kasteleyn weighting for $\tilde{C}_G$.

We can therefore again apply Kasteleyn's theorem to obtain

$$\det \tilde{K} = \sum_{\pi \in S_{m-1}} \operatorname{sgn}(\pi) \prod_{k=1}^{m-1} \tilde{\varsigma}_{\tilde{b}_k \tilde{w}_{\pi(k)}} \tilde{x}_{b_k w_{\pi(k)}} = \tilde{\kappa}_\gamma Z^\gamma_{C_G}(w_i, b_j),$$

where $\tilde{b}_1, \dots, \tilde{b}_{m-1}$ (resp. $\tilde{w}_1, \dots, \tilde{w}_{m-1}$) is an order-preserving renumbering of the black (resp. white) vertices where b_j (resp. w_i) is removed, and

$$\tilde{\kappa}_\gamma = \operatorname{sgn}(\pi) \prod_{k=1}^{m-1} \tilde{\varsigma}_{\tilde{b}_k \tilde{w}_{\pi(k)}}$$

is a constant complex factor independent of the permutation π defining a perfect matching of $\tilde{C}_G$. Setting

$$\kappa_\gamma = (-1)^{i+j+1+N} \mathrm{i} \tilde{\kappa}_\gamma \tag{3.14}$$

justifies (3.13). □

We now proceed to giving κ_γ a concrete representation in terms of the winding angle of γ. To this end, we first need to introduce some complex factors. We follow [13] and for each directed edge or corner e, we fix a square root of the corresponding direction in the complex plane and denote by η_e its *complex conjugate*. Recall that we always assume that a corner c is oriented towards its vertex $v(c)$, and we write $-c$ whenever we consider the opposite orientation. For two directed edges or corners e, g that do not point in opposite directions, we define $\angle(e,g)$ to be the *turning angle* from e to g, that is, the number in $(-\pi, \pi)$ satisfying

$$e^{-\mathrm{i}\angle(e,g)} = (\overline{\eta_e}\eta_g)^2.$$

Lemma 3.17. *Let c_i, c_j and γ be as above. Define $\tilde{\gamma}$ to be the extended path starting at $-c_j$, following γ, and ending at c_i. Then,*

$$\kappa_\gamma = \exp\left(\frac{\mathrm{i}}{2}\operatorname{wind}(\tilde{\gamma})\right),$$

where wind$(\tilde{\gamma})$ *is the total* winding angle *of the path $\tilde{\gamma}$, that is, the sum of all turning angles along the path.*

Proof. Let ρ be a simple primal path starting at $v(c_i)$ and ending at $v(c_j)$, and let $\tilde{\rho}$ be the extended path that starts at c_i, then follows ρ, and ends at $-c_j$. We will define a perfect matching M_ρ of $\tilde{C}_G$ that corresponds to ρ in a natural way (see Figure 3.12). Note that there is a unique sequence of streets S_ρ such that the first edge contains b_i and the last edge contains w_j, and where all the

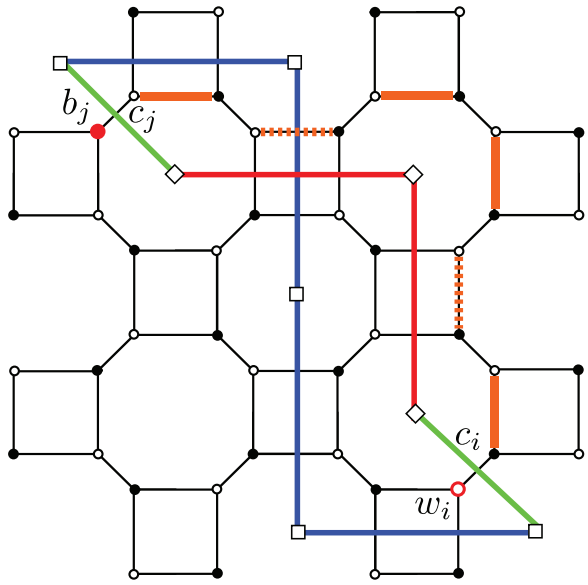

FIGURE 3.12 An illustration of the proof of Lemma 3.17 in the case where G is a piece of the square lattice. The green lines represent corners c_i and c_j, the red lines represent the primal path ρ from $v(c_i)$ to $v(c_j)$ and the blue lines show the dual path γ from $u(c_j)$ to $u(c_i)$. The red vertices w_i and b_j are removed in the graph $C_{\tilde{G}}$. The matching M_ρ corresponding to ρ contains the orange streets and all remaining roads. The dashed (resp. solid) orange edges carry a phase $\exp(\frac{i\pi}{4})$ (resp. $\exp(-\frac{i\pi}{4})$) in the original Kasteleyn weighting ς of C_G. The orange edge crossed by γ gets an additional -1 sign in the Kasteleyn weighting $\tilde{\varsigma}$ of $\tilde{C}_G$.

edges are directly to the right of the oriented path $\tilde{\rho}$ (the orange edges in Figure 3.12). We define M_ρ to contain S_ρ and all the remaining roads denoted by R_ρ.

Moreover, let ℓ be the loop (closed path) which is the concatenation of $\tilde{\rho}$ and $\tilde{\gamma}$. We claim that

$$\prod_{bw\in S_\rho} \tilde{\varsigma}_{bw} = (-1)^{t(\ell)} \prod_{bw\in S_\rho} \varsigma_{bw} = (-1)^{t(\ell)+1} \mathrm{i} \exp\left(-\frac{\mathrm{i}}{2}\mathrm{wind}(\tilde{\rho})\right), \tag{3.15}$$

where $t(\ell)$ is the number of self-crossings of ℓ. Indeed, the first identity follows since the self-crossings of ℓ only come from a crossing between γ and ρ, and each such edge gets an additional -1 factor in the Kasteleyn weighting $\tilde{\sigma}$. We now argue for the second inequality by inspecting the contribution of the phases ς at each turn of $\tilde{\rho}$.

To this end, we consider all the corners adjacent to ρ. We denote by α_k (resp. α_k^*), $k = 1, 2, \ldots$, the unsigned angles between two consecutive corners that share a vertex (resp. a face) of G, and by β_k, we denote the angles between the edges of ρ and the corners (see Figure 3.13). Note that there is exactly $|\rho|$ angles of type α^*, and $2|\rho|$ angles of type β (there can be more angles of type α). Moreover, $\alpha_k^* = \pi - \beta_{2k-1} - \beta_{2k}$ for each $k \in \{1, \ldots, |\rho|\}$. Finally, the sum of all angles of type α and β around a vertex of G is by definition equal to π plus the turning angle of ρ at that vertex. Writing A (resp. B) for the sum of all angles of type α (resp. β), and using the definition of ς, we find

$$\prod_{bw\in S_\rho} \varsigma_{bw} = \prod_k e^{-\frac{\mathrm{i}\alpha_k}{2}} \prod_k e^{\frac{\mathrm{i}\alpha_k^*}{2}} = e^{-\frac{\mathrm{i}}{2}(A+B-|\rho|\pi)} = e^{-\frac{\mathrm{i}}{2}(\mathrm{wind}(\tilde{\rho})+\pi)} = -\mathrm{i}\exp\left(-\frac{\mathrm{i}}{2}\mathrm{wind}(\tilde{\rho})\right),$$

which justifies (3.15).

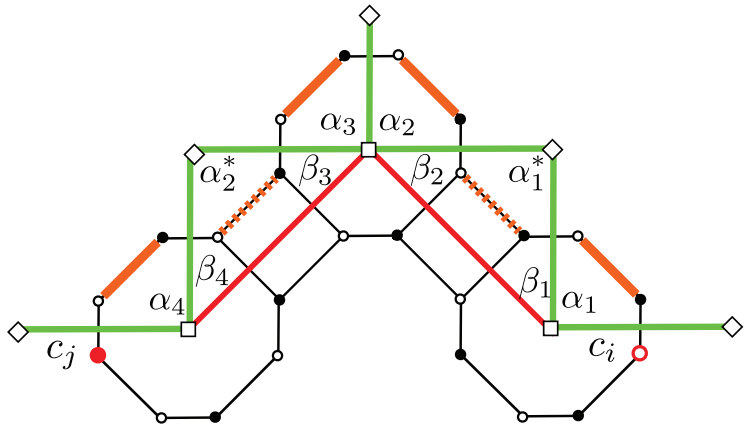

FIGURE 3.13 An illustration of the proof of (3.15). The path ρ goes from c_i to $-c_j$, and is composed of the two red edges. The orange edges represent S_ρ.

On the other hand, a classical fact due to Whitney [67] (see also [13, Lemma 2.2]) says that

$$\exp\left(\frac{\mathrm{i}}{2}\mathrm{wind}(\ell)\right) = (-1)^{t(\ell)+1}. \tag{3.16}$$

Factorising the left-hand side into the contributions coming from $\tilde{\rho}$ and $\tilde{\gamma}$, we get

$$\exp\left(\frac{\mathrm{i}}{2}\mathrm{wind}(\ell)\right) = \kappa_\gamma \exp\left(\frac{\mathrm{i}}{2}\mathrm{wind}(\tilde{\rho})\right).$$

Combining with (3.15), we arrive at

$$\prod_{bw\in M_\rho} \tilde{\varsigma}_{bw} = \prod_{bw\in S_\rho} \tilde{\varsigma}_{bw} \prod_{bw\in R_\rho} \tilde{\varsigma}_{bw} = (-1)^{|R_\rho|}\mathrm{i}\kappa_\gamma,$$

where the second equality holds true since roads have complex phase $\varsigma = -1$. On the other hand, by (3.14), we have

$$\kappa_\gamma = (-1)^{i+j+1+N}\mathrm{sgn}(\pi)\mathrm{i}\prod_{k=1}^{m-1}\tilde{\varsigma}_{b_k w_{\pi(k)}} = (-1)^{i+j+1+N}\mathrm{sgn}(\pi)\mathrm{i}\prod_{bw\in M_\rho}\tilde{\varsigma}_{bw},$$

where $\pi \in S_{k-1}$ is the permutation defining the matching M_ρ, and N is the number of all corner edges in C_G. Therefore, to finish the proof, it is enough to show that

$$\mathrm{sgn}(\pi) = (-1)^{i+j+N+|R_\rho|}. \tag{3.17}$$

To this end, first note that M_ρ naturally defines a bijection $\tilde{\pi}$ of the set of corners of G with the two corners c_i and c_j identified as one corner, called from now on $\tilde{c}$, where $\tilde{\pi}(c) = c'$ if the black vertex corresponding to c is connected by an edge in M_ρ to the white vertex corresponding to c'. This bijection can be thought of as a permutation of $\{1, \dots, k-1\}$ where the index corresponding to $\tilde{c}$ is $m-1$, and where the first $m-2$ indices respect the original order on the remaining corners of C_G. Clearly, $\tilde{\pi}$ has only one non-trivial cycle whose length is $|S_\rho|+1$, and hence, $\mathrm{sgn}(\tilde{\pi}) = (-1)^{|S_\rho|}$. Without loss of generality, let $j > i$ and for an index $l \in \{1, \dots, k-1\}$, let $p_l \in S_{k-1}$ be the

permutation such that $p_l(l) = k-1$ and that does not change the order of the remaining indices. Note that $\mathrm{sgn}(p_l) = (-1)^{k-1-l}$ as p_l is a composition of $k-1-l$ transpositions. One can check that $\pi = p_i^{-1}\tilde{\pi}p_{j-1}$, and as a result $\mathrm{sgn}(\pi) = (-1)^{i+j-1+|S_\rho|}$. To show (3.17) and finish the proof, we count the roads whose both endpoints are covered by a street in S_ρ, to get that $N = |S_\rho| + 1 + |R_\rho|$. □

All in all, from (3.13) together with Corollary 3.15, we obtain the following statement.

Corollary 3.18. *We have*

$$K^{-1}(w_i, b_j) = \frac{1}{2}\mathrm{i}\kappa_\gamma \langle \chi_{c_i}\chi_{c_j}\rangle^\gamma, \tag{3.18}$$

where the complex phase κ_γ is as in Lemma 3.17.

3.4.2 | Complex-valued fermionic observables

In this section, we rewrite $\langle \chi_{c_i}\chi_{c_j}\rangle$, and hence the right-hand side of (3.18), in terms of complex-valued fermionic observables of Chelkak–Smirnov [15], and Hongler–Smirnov [31]. This correspondence is well known (and can be, e.g. found in [13]) but we choose to present the details for completeness of exposition. In the next section, we will use it together with the available scaling limit results to derive the scaling limit of K^{-1} for the critical model on C_{D^δ}.

We first define the complex version of the Kadanoff–Ceva observable for two corners c_i and c_j by

$$f(c_i, c_j) := \frac{1}{Z^{\emptyset}_{\mathrm{hT}}} \sum_{\eta \in \mathcal{E}^{\upsilon(c_i),\upsilon(c_j)}} \exp\left(-\frac{\mathrm{i}}{2}\mathrm{wind}(\rho_\eta)\right) \prod_{e\in\eta} x_e, \tag{3.19}$$

where $\mathrm{wind}(\rho_\eta)$ is again the total winding angle of the path ρ_η, that is, the sum of all turning angles along the path, and where ρ_η is a simple path contained in $\eta \cup \{c_i, c_j\}$ that starts at c_i and ends at $-c_j$, and is defined as follows: for each vertex υ of degree larger than two in η, one connects the edges around υ into pairs in a non-crossing way, thus giving rise to a collection of non-crossing cycles $\mathcal{C}_\eta$ and a path from c_i to $-c_j$ that we call ρ_η.

It is a standard fact that the definition of $f(c_i, c_j)$ does not depend on the way the connections at each vertex of η are chosen (as long as they are non-crossing). Moreover, for all $\eta \in \mathcal{E}^{\upsilon(c_i),\upsilon(c_j)}$, we have

$$-\overline{\kappa}_\gamma \exp\left(-\frac{\mathrm{i}}{2}\mathrm{wind}(\rho_\eta)\right) = \mathrm{sgn}_\gamma(\eta), \tag{3.20}$$

where as before, γ is a fixed dual path connecting $u(c_i)$ and $u(c_j)$, and $\kappa_\gamma = \exp(\frac{\mathrm{i}}{2}\mathrm{wind}(\tilde{\gamma}))$, with $\tilde{\gamma}$ being the path starting at $-c_j$, then following γ, and ending at c_i. To justify this identity, we consider the loop ℓ which is the concatenation of ρ_η and the path $\tilde{\gamma}$, and write

$$\exp\left(-\frac{\mathrm{i}}{2}\mathrm{wind}(\ell)\right) = \overline{\kappa}_\gamma \exp\left(-\frac{\mathrm{i}}{2}\mathrm{wind}(\rho_\eta)\right).$$

We then again use Whitney's identity (3.16) and the fact that the collection of cycles C_η must, by construction, cross γ an even number of times (since C_η does not cross ρ_η, and C_η crosses ℓ an even number of times for topological reasons). This justifies (3.20) and implies that

$$\langle \chi_{c_i} \chi_{c_j} \rangle^\gamma = -\overline{\kappa}_\gamma f(c_i, c_j),$$

which together with Corollary 3.18 gives the following proposition.

Proposition 3.19. *We have*

$$K^{-1}(w_i, b_j) = -\frac{\mathrm{i}}{2} f(c_i, c_j). \tag{3.21}$$

To make the connection with the scaling limit results of [31], we still need to introduce an observable that is indexed by two directed edges of G instead of two corners. To this end, for each edge e of G, let z_e be its midpoint. Also, for a directed edge $e = (v_1, v_2)$, let $h(e)$ be the *half-edge*$\{z_e, v_2\}$, let $-e = (v_2, v_1)$ be its reversal and let $\bar{e} = \{v_1, v_2\}$ be its undirected version. Moreover, for two directed edges $e = (v_1, v_2)$ and $g = (\tilde{v}_1, \tilde{v}_2)$, let $\mathcal{E}^{e,g}$ be the collections of edges $\tilde{\eta} \in \mathcal{E}^{v_2, \tilde{v}_1}$ that *do not contain* $\bar{e}$ and $\bar{g}$. We define

$$f(e, g) := \frac{1}{Z^{\emptyset}_{\mathrm{hT}}} \sum_{\tilde{\eta} \in \mathcal{E}^{e,g}} \exp\left(-\frac{\mathrm{i}}{2} \mathrm{wind}(\rho_{\tilde{\eta}})\right) \prod_{e \in \tilde{\eta}} x_e,$$

where $\rho_{\tilde{\eta}}$ is a simple path in $\tilde{\eta} \cup \{h(e), h(-g)\}$ that starts at z_e and ends at z_g, and is analogous to ρ_η from (3.19). Note that the winding of $\rho_{\tilde{\eta}}$ is constant (independent of $\tilde{\eta}$) modulo 2π and equal to $\angle(e, g)$, and therefore,

$$f(e, g) \in \overline{\eta}_e \eta_g \mathbb{R}. \tag{3.22}$$

4 | CONVERGENCE OF THE NESTING FIELD (PROOF OF THEOREM 1.4)

Let $D \subset \mathbb{C}$ be a Jordan domain, and let D^δ approximate D, that is, $d(\partial D^\delta, \partial D) \to 0$ as $\delta \to 0$ (where d is as in (1.2)). We consider the critical DRC model with free boundary conditions on D^δ, and the corresponding dimer model on Dubédat's square-octagon graph C_{D^δ}. We call U^δ and V^δ the set of faces of C_{D^δ} that correspond to the faces and vertices of D^δ respectively. In this section, we show that the moments of the associated height function h^δ converge to the moments of $\frac{1}{\sqrt{\pi}}$ times the Dirichlet GFF.

4.1 | Scaling limit of inverse Kasteleyn matrix

We start by establishing the scaling limit of the inverse Kasteleyn matrix on C_{D^δ}. This is crucial for the computation of the moments of the height function that is done in the next section.

Our method is to use Proposition 3.19 obtained in the previous section, as well as the existing scaling limit results for discrete s-holomorphic observables in the Ising model [14, 31]. It is

important to note that to prove our main results, we need to work with continuum domains D with an arbitrary (possibly fractal) boundary. Therefore, we state a generalised version of the scaling limit results of Hongler and Smirnov [31] for the critical fermionic observable with two points in the bulk of the domain. Their result, as stated, is valid only for domains whose boundary is a rectifiable curve (see also [30]). Even though the stronger result that we need is most likely known to the experts, for the sake of completeness, we will outline its proof, which is a direct consequence of the robust framework of Chelkak, Hongler and Izyurov [14] that was used to establish scaling limits for critical spin correlations.

From now on, we assume that the observables are critical, that is, the weight x_e is constant and equal to $x_c = \sqrt{2} - 1$ so that $\prod_{e\in\eta} x_e = x_c^{|\eta|}$. Also, we define

$$f(e, z_g) := x_c(f(e, g) + f(e, -g)), \tag{4.1}$$

which is the observable of Hongler and Smirnov [31] (when e is a horizontal edge pointing to the right) that is indexed by a directed edge e and a midpoint of an edge z_g. The next lemma relates this observable to the corner observable in a linear fashion. This type of identities is well known (see, e.g. [13]) and is closely related to the notion of *s-holomorphicity* introduced by Smirnov [65] for the square lattice, and generalized by Chelkak and Smirnov [15], and Chelkak [11, 12]. We omit the proof.

Lemma 4.1. *Let c_i and c_j be two corners that do not share a vertex, and let e and g be directed edges incident to $v(c_i)$ and $v(c_j)$, respectively. Then,*

$$f(c_i, c_j) = \frac{1}{\sqrt{2}} \sum_{e'\in\{e,-e\}} \Big(1 + (\overline{\eta_{c_i}}\eta_{e'})^2\Big)\Big(f(e', z_g) - (\overline{\eta_{e'}}\eta_{c_j})^2\overline{f(e', z_g)}\Big).$$

We also need to introduce the continuum counterparts of the discrete holomorphic observables. To this end, let $D \subsetneq \mathbb{C}$ be a simply connected domain different from $\mathbb{C}$, and let $\psi_w = \psi_w^D$ be the unique conformal map from D to the unit disk with $\psi_w(w) = 0$ and $\psi_w'(w) > 0$. For $w, z \in D$, we define

$$f_-^D(w, z) := \frac{1}{2\pi}\sqrt{\psi_w'(w)\psi_w'(z)} \quad \text{and} \quad f_+^D(w, z) := \frac{1}{2\pi}\sqrt{\psi_w'(w)\psi_w'(z)}\frac{1}{\psi_w(z)}.$$

Lemma 4.2 (Conformal covariance of $f_\pm^D$). *Let $\varphi : D \to D'$ be a conformal map. Then,*

$$f_-^D(w, z) = \overline{\varphi'(w)}^{\frac{1}{2}}\varphi'(z)^{\frac{1}{2}} f_-^{D'}(\varphi(w), \varphi(z)),$$

$$f_+^D(w, z) = \varphi'(w)^{\frac{1}{2}}\varphi'(z)^{\frac{1}{2}} f_+^{D'}(\varphi(w), \varphi(z)).$$

Moreover, for the upper half-plane $\mathbb{H}$, we have

$$f_-^{\mathbb{H}}(w, z) = \frac{\mathrm{i}}{2\pi(z - \overline{w})} \quad \textit{and} \quad f_+^{\mathbb{H}}(w, z) = \frac{1}{2\pi(z - w)}.$$

Proof. To prove the first part, note that $\psi^{D'}_{\varphi(w)}(z) = \psi^{D}_{w}(\varphi^{-1}(z))\frac{\varphi'(w)}{|\varphi'(w)|}$. Indeed, the right-hand side is a conformal map with a positive derivative $(\psi^{D}_{w})'(w)/|\varphi'(w)|$ and vanishing at $\varphi(w)$. Hence, we have

$$\begin{aligned} f^{D'}_{-}(\varphi(w),\varphi(z)) &= \left[\left(\psi^{D'}_{\varphi(w)}\right)'(\varphi(w))\left(\psi^{D'}_{\varphi(w)}\right)'(\varphi(z))\right]^{\frac{1}{2}} \\ &= \left[\left(\psi^{D}_{w}\right)'(w)\left(\psi^{D}_{w}\right)'(z)\right]^{\frac{1}{2}}\left[\varphi'(w)\varphi'(z)\right]^{-\frac{1}{2}}\frac{\varphi'(w)}{|\varphi'(w)|} \\ &= f^{D}_{-}(w,z)\overline{\varphi'(w)}^{-\frac{1}{2}}\varphi'(z)^{-\frac{1}{2}}, \end{aligned}$$

and similarly for f^{D}_{+}. The second part follows from the fact that $\psi^{\mathbb{H}}_{w}(z) = i\frac{z-w}{z-\overline{w}}$ and the definition of $f^{\mathbb{H}}_{\pm}$. □

We now proceed to the generalisation of [31, Theorem 8] mentioned at the beginning of the section. In the proof, we will very closely follow the proof of [14, Theorem 2.16] dealing with the convergence of discrete s-holomorphic spinors.

Theorem 4.3. *Let $D \subset \mathbb{C}$ be a bounded simply connected domain, and let D^δ approximate D as $\delta \to 0$. Fix $w, z \in D$, and let $e = e^\delta$ and $g = g^\delta$ be edges of D^δ whose midpoints converge to w and z, respectively, as $\delta \to 0$. Then,*

$$f^\delta(e, z_g) = \delta\Big(f^{D}_{-}(w,z) + \overline{\eta}^2_e f^{D}_{+}(w,z) + o(1)\Big) \qquad \text{as } \delta \to 0,$$

where f^δ is the observable from (4.1) defined on D^δ. Moreover, the convergence is uniform on compact subsets of $\{(w,z) \in D^2 : w \neq z\}$.

Before giving a sketch of the proof of this theorem, we state a corollary that will be convenient for us when computing moments of the height function in the next section.

Corollary 4.4. *Consider the setting from the theorem above and let $c_i = c_i^\delta$ and $c_j = c_j^\delta$ be two corners of D^δ whose vertices converge to w and z, respectively. Then*

$$K^{-1}(w_i, b_j) = -\frac{1}{\sqrt{2}}\delta \mathrm{i}\Big(f^{D}_{-}(w,z) - \overline{\eta}^2_{c_i}\eta^2_{c_j}\overline{f^{D}_{-}(w,z)} + \overline{\eta}^2_{c_i} f^{D}_{+}(w,z) - \eta^2_{c_j}\overline{f^{D}_{+}(w,z)} + o(1)\Big),$$

where K^{-1} is the inverse Kasteleyn matrix on C_{D^δ}.

Proof. To simplify the notation, we drop D from the superscripts. We combine Lemmas 4.3 and 4.1 to get that $\frac{\sqrt{2}}{\delta}f(c_i, c_j)$ equals to

$$\sum_{e' \in \{e,-e\}} \Big(1 + (\overline{\eta}_{c_i}\eta_{e'})^2\Big)\big(f(e', z_g) - (\overline{\eta}_{e'}\eta_{c_j})^2\overline{f(e', z_g)}\big)$$

$$= \sum_{e' \in \{e,-e\}} \Big(1 + (\overline{\eta}_{c_i}\eta_{e'})^2)(f_-(w,z) + \overline{\eta}_{e'}^2 f_+(w,z) - (\overline{\eta}_{e'}\eta_{c_j})^2\overline{f_-(w,z)} - \eta_{c_j}^2\overline{f_+(w,z)}) + o(1)$$

$$= 2\Big(f_-(w,z) + \overline{\eta}_{c_i}^2 f_+(w,z) - \overline{\eta}_{c_i}^2\eta_{c_j}^2\overline{f_-(w,z)} - \eta_{c_j}^2\overline{f_+(w,z)}\Big) + o(1),$$

where the last equality holds due to cancellations resulting from $\eta_e^2 = -\eta_{-e}^2$. On the other hand, by (3.21), $K^{-1}(w_i, b_j) = -\frac{\mathrm{i}}{2}f(c_i, c_j)$ which finishes the proof. □

Sketch of proof of Theorem 4.3. Based on the scaling limit results of Hongler–Smirnov [31], we first argue that the statement holds true for a domain D with a smooth boundary. Indeed, in [31], it is assumed that $\eta_e^2 = 1$ and hence, in that case, the result follows directly from [31, Theorem 8]. Applying this to a rotated domain together with the conformal covariance properties from Lemma 4.2 yields the statement for a general direction of e.

We now briefly describe how to use the robust framework of Chelkak, Hongler and Izyurov to extend this to general simply connected domains. In [14, Theorem 2.16], a scaling limit result was established for a discrete holomorphic spinor F^δ defined on an approximation D^δ of an arbitrary bounded simply connected domain D. The two observables F^δ and f^δ satisfy the same boundary conditions (of [31, Proposition 18] and [14, (2.7)]). Moreover, both observables are s-holomorphic away from the diagonal. The difference, however, is their singular behaviour near the diagonal. In [14], the full plane version $F_{\mathbb{C}}^\delta$ (the discrete analog of $1/\sqrt{z-w}$) of the observable is subtracted from F^δ in order to cancel out the discrete-holomorphic singularity on the diagonal. The details of the proof of [14, Theorem 2.16] can be carried out verbatim for f^δ instead of F^δ and its full plane version $f_{\mathbb{C}}^\delta$ (the discrete analog of $1/(z-w)$) introduced in [31] instead of $F_{\mathbb{C}}^\delta$. Indeed, the arguments in [14] depend only on the fact that the observables in question are s-holomorphic and satisfy the correct boundary value problem.

Since the scaling limit is conformally invariant and was uniquely identified for domains with a smooth boundary by the argument above, this finishes the proof. □

4.2 | Moments of h^δ

Throughout this section, and as before, let $D \subset \mathbb{C}$ be a Jordan domain, and let D^δ approximate D, that is, $d(\partial D^\delta, \partial D) \to 0$ as $\delta \to 0$ (where d is as in (1.2)). For simplicity of exposition, we only consider the height function on C_{D^δ} restricted to U^δ which has the same distribution as the nesting field of the critical DRC on D with free boundary conditions. The case of mixed moments (for the joint height function on both the faces and vertices of D^δ) follows in the same manner as the faces and vertices of D^δ play a symmetric role in the graph C_{D^δ}. To this end, let $a_1, a_2, \dots, a_n$ be distinct points in D, and let $h^\delta(a_i)$ $(i = 1, \dots, n)$ be the height function evaluated at the face $u_i^\delta = u_i^\delta(a_i) \in U^\delta$ of D^δ, in which the point a_i lies (we choose a face arbitrarily if a_i lies on an edge of D^δ).

Let $G_D(z,w)$ be the Dirichlet Green's function in D, that is, the Green's function of standard Brownian motion in D killed upon hitting ∂D. In particular, for the upper-half plane $\mathbb{H}$, we have

$$G_{\mathbb{H}}(z,w) = \frac{1}{2\pi}\ln\left|\frac{z-\overline{w}}{z-w}\right|.$$

This section is devoted to the proof of the following theorem. Below, $\mathbf{P}^{\emptyset,\emptyset}_{D^\delta,D^\delta}$ denotes the probability measure of the DRC model with free boundary conditions together with the independent labels used to define the nesting field.

Theorem 4.5. *For every even integer n and any distinct points $a_1, a_2, \dots, a_n \in D$, we have*

$$\lim_{\delta\to 0} \mathbf{E}^{\emptyset,\emptyset}_{D^\delta,D^\delta}\left[\prod_{i=1}^n h^\delta(a_i)\right] = \sum_{\pi \text{ pairing of } \{a_1,\dots,a_n\}} \prod_{\{z,w\}\in\pi} \frac{1}{\pi} G_D(z,w),$$

where a pairing is a partition into sets of size two.

Note that the field h^δ is symmetric, and therefore, the corresponding moments for n odd vanish.

Kasteleyn theory classically allows to compute all moments of the height function in terms of the inverse Kasteleyn matrix K^{-1}. In the proof of the theorem, we follow the line of computation due to Kenyon [34] but with several adjustments to our setting. In particular, we start with an algebraic manipulation to take care of the behaviour of K^{-1} near the boundary of D^δ: for $a_1^0, \dots, a_n^0 \in D$, write

$$\mathbf{E}^{\emptyset,\emptyset}_{D^\delta,D^\delta}\left[\prod_{i=1}^n h^\delta(a_i)\right] = \mathbf{E}^{\emptyset,\emptyset}_{D^\delta,D^\delta}\left[\prod_{i=1}^n (h^\delta(a_i) - h^\delta(a_i^0))\right] - \sum_{\substack{t\in\{0,1\}^n \\ t\neq(1,\dots,1)}} (-1)^{\sum_i (1-t_i)} \mathbf{E}^{\emptyset,\emptyset}_{D^\delta,D^\delta}\left[\prod_{i=1}^n h^\delta(a_i^{t_i})\right], \tag{4.2}$$

where $a_i^1 = a_i$ for $i = 1, \dots, n$.

The advantage of this formulation is that the first term on the right-hand side can be computed using Kasteleyn theory, and that the others are small when $a_1^0, \dots, a_n^0$ are close to the boundary. This latter fact is not obvious and is relying on discrete properties of the DRC obtained in [22] (note that it is basically saying that the field is uniformly small — in terms of moments — near the boundary).

We start by proving that the remaining terms are small.

Proposition 4.6. *For any $\varepsilon > 0$ and $a_1, \dots, a_n \in D$, one may choose $a_1^0, \dots, a_n^0 \in D$ so that*

$$\left|\mathbf{E}^{\emptyset,\emptyset}_{D^\delta,D^\delta}\left[\prod_{i=1}^n h^\delta(a_i)\right] - \mathbf{E}^{\emptyset,\emptyset}_{D^\delta,D^\delta}\left[\prod_{i=1}^n (h^\delta(a_i) - h^\delta(a_i^0))\right]\right| < \varepsilon \tag{4.3}$$

uniformly in $\delta > 0$.

Remark 4.7. This proposition, which basically claims that the second term on the right-hand side of (4.2) is close to zero provided the a_i^0 are close enough to the boundary, is a restatement of the fact that boundary conditions for the limiting height function are zero. It is therefore the main place where we identify boundary conditions. Note that this proposition relies heavily on the main results from [22] (Theorems 2.1 and 2.4 from Section 2), and is as such non-trivial.

To prove this proposition, we need to introduce some auxiliary notions. We say that a cluster of the DRC is *relevant* for $A = \{a_1, \dots, a_n\} \subsetneq D$ if it is odd around u_i^δ for at least two different $i \in$

$\{1, \dots, n\}$ (it is possible that $u_i^\delta = u_j^\delta$ even though $a_i \neq a_j$). We denote by $\mathsf{R}^\delta(A)$ the number of relevant clusters for A in D^δ, and by $\mathsf{I}^\delta(A)$ the event that all faces $u_1^\delta, \dots, u_n^\delta$ are surrounded by at least one relevant cluster for A. We start with three lemmata.

Lemma 4.8. *For every $n \geqslant 2$ even, there exists $P_n \in (0, \infty)$ such that for all sets of points $A = \{a_1, \dots, a_n\} \subsetneq D$, we have*

$$\mathbf{E}^{\emptyset,\emptyset}_{D^\delta, D^\delta}\left[\prod_{i=1}^n h^\delta(a_i)\right] \leqslant P_n \sqrt{\mathbf{E}^{\emptyset,\emptyset}_{D^\delta, D^\delta}[\mathsf{R}^\delta(A)^n]\mathbf{P}^{\emptyset,\emptyset}_{D^\delta, D^\delta}[\mathsf{I}^\delta(A)]}.$$

Proof. For a cluster $\mathcal{C}$ of the DRC, let

$$\mathrm{Odd}(\mathcal{C}) := \{a_i \in A : \mathcal{C} \text{ is odd around } u_i^\delta\}.$$

We denote a partition of A by $\{A_1, \dots, A_k\}$. We call such a partition even if all its elements have even cardinality. Using the correspondence with the nesting field of the critical DRC on D^δ with free boundary conditions defined in (1.6), we have

$$\begin{aligned}
\mathbf{E}^{\emptyset,\emptyset}_{D^\delta, D^\delta}\left[\prod_{i=1}^n h^\delta(a_i)\right] &= \mathbf{E}^{\emptyset,\emptyset}_{D^\delta, D^\delta}\left[\prod_{i=1}^n \left(\sum_{\mathcal{C}_i} \epsilon_{\mathcal{C}_i} \mathbf{1}_{\{\mathcal{C}_i \text{ odd around } u_i^\delta\}}\right)\right] \\
&= \mathbf{E}^{\emptyset,\emptyset}_{D^\delta, D^\delta}\left[\sum_{(\mathcal{C}_1, \dots, \mathcal{C}_n)} \prod_{i=1}^n \epsilon_{\mathcal{C}_i} \mathbf{1}_{\{\mathcal{C}_i \text{ odd around } u_i^\delta\}}\right] \\
&= \sum_{\{A_1, \dots, A_k\} \text{ even}} \mathbf{E}^{\emptyset,\emptyset}_{D^\delta, D^\delta}\left[\sum_{(\mathcal{C}_1, \dots, \mathcal{C}_k)} \mathbf{1}_{\{A_i \subseteq \mathrm{Odd}(\mathcal{C}_i),\ \mathcal{C}_i \text{ distinct } \forall i \in \{1, \dots, k\}\}}\right] \\
&\leqslant \sum_{\{A_1, \dots, A_k\} \text{ even}} \mathbf{E}^{\emptyset,\emptyset}_{D^\delta, D^\delta}\left[\sum_{(\mathcal{C}_1, \dots, \mathcal{C}_k)} \mathbf{1}_{\{\mathcal{C}_i \text{ relevant for } A\}} \mathbf{1}_{\mathsf{I}^\delta(A)}\right] \\
&\leqslant P_n \mathbf{E}^{\emptyset,\emptyset}_{D^\delta, D^\delta}\left[\mathsf{R}^\delta(A)^{n/2} \mathbf{1}_{\mathsf{I}^\delta(A)}\right] \\
&\leqslant P_n \sqrt{\mathbf{E}^{\emptyset,\emptyset}_{D^\delta, D^\delta}[\mathsf{R}^\delta(A)^n]\mathbf{P}^{\emptyset,\emptyset}_{D^\delta, D^\delta}[\mathsf{I}^\delta(A)]},
\end{aligned}$$

where P_n is the number of even partitions of a set of size n (we used that $k \leqslant n/2$), and where in the last inequality we used the Cauchy–Schwarz inequality. □

Lemma 4.9 (Logarithmic bound on the number of clusters). *There exists $C \in (0, \infty)$ such that for every bounded domain D and every $A = \{a_1, \dots, a_n\} \subsetneq D$ and $N \geqslant 1$,*

$$\mathbf{E}^{\emptyset,\emptyset}_{D^\delta, D^\delta}[\mathsf{R}^\delta(A)^N] \leqslant \frac{1}{N!}\left[Cn \log\left(\frac{\mathrm{diam}(D)}{\min_{i \neq j} |a_i - a_j|}\right)\right]^N,$$

uniformly in $\delta > 0$.

Proof. Consider the constant C given by Theorem 2.1. Set $\kappa := \frac{1}{2}\min_{i\neq j}|a_i - a_j|$ and $d := \mathrm{diam}(D)$.

Consider the family $\mathcal{B} = (\Lambda_{r_k}(x_k) : k \in \mathcal{K})$ containing the boxes $\Lambda_{\frac{r}{4C}}(x)$ with $r := 2^j\kappa$, $x \in \frac{r}{4C}\mathbb{Z}^2 \cap \mathrm{Ann}(a_i, r, 2r)$ for every $1 \leqslant i \leqslant n$ and $0 \leqslant j \leqslant \lfloor \log_2(d/\kappa)\rfloor$. One may easily check that every cluster that surrounds at least two vertices in A must contain, for some $k \in \mathcal{K}$, a crossing from $\Lambda_{r_k}(x_k)$ to $\Lambda_{2Cr_k}(x_k)$. We deduce that if X_k is the number of disjoint $\Lambda_{Cr_k}(x_k)$-clusters crossing $\mathrm{Ann}(x_k, r_k, 2Cr_k)$ from inside to outside, then

$$\mathsf{R}^\delta(A) \leqslant \sum_{k\in\mathcal{K}} X_k.$$

Now, for each $k \in \mathcal{K}$, $\Lambda_{3Cr_k}(x_k)$ intersects at most $O(C^2)$ boxes $\Lambda_{3Cr_l}(x_l)$ for $l \in \mathcal{K}$. We may therefore partition $\mathcal{K}$ in $I = O(C^2)$ disjoint sets $\mathcal{K}_1, \dots, \mathcal{K}_I$ for which the $\Lambda_{3Cr_k}(x_k)$ with $k \in \mathcal{K}_i$ are all disjoint. Set $S_i := \sum_{k\in\mathcal{K}_i} X_k$. Hölder's inequality implies that

$$\mathbf{E}^{\emptyset,\emptyset}_{D^\delta,D^\delta}[\mathsf{R}^\delta(A)^N] \leqslant \mathbf{E}^{\emptyset,\emptyset}_{D^\delta,D^\delta}[(S_1 + \cdots + S_{|I|})^N] \leqslant |I|^{N-1}\sum_{i=1}^{|I|}\mathbf{E}^{\emptyset,\emptyset}_{D^\delta,D^\delta}[S_i^N].$$

The mixing property of the DRC proved in [22] and Theorem 2.1 imply the existence of $C_{\mathrm{mix}} \in (0,\infty)$ (independent of everything) such that S_i is stochastically dominated by $C_{\mathrm{mix}}\widetilde{S}_i$, where $\widetilde{S}_i$ is the sum of $|\mathcal{K}_i|$ independent geometric random variables $(\widetilde{X}_k : k \in \mathcal{K}_i)$ of parameter $1/2$. We deduce that

$$\mathbf{E}^{\emptyset,\emptyset}_{D^\delta,D^\delta}[S_i^N] \leqslant C_{\mathrm{mix}}^N \times \frac{(C_0|\mathcal{K}_i|)^N}{N!}.$$

Since $|\mathcal{K}_i| \leqslant |\mathcal{K}| \leqslant C_1 n\log(d/\kappa)$, we deduce that

$$\mathbf{E}^{\emptyset,\emptyset}_{D^\delta,D^\delta}[\mathsf{R}^\delta(A)^N] \leqslant \frac{(C_2 n\log(d/\kappa))^N}{N!}.$$

This concludes the proof. □

We now turn to the third lemma that we will need. Let $\partial_\alpha\Omega$ be the set of points in Ω that are exactly at a Euclidean distance equal to α away from $\partial\Omega$.

Lemma 4.10 (Large DRC clusters do not come close to the boundary). *For every $C, \alpha, \varepsilon > 0$, there exists $\beta = \beta(C,\alpha,\varepsilon) > 0$ such that for every $D \subseteq \Lambda_C$,*

$$\mathbf{P}^{\emptyset,\emptyset}_{D^\delta,D^\delta}[\partial_\alpha D \overset{\mathbf{n}_1+\mathbf{n}_2}{\longleftrightarrow} \partial_\beta D] \leqslant \varepsilon. \tag{4.4}$$

Proof. Assume that $\partial_\alpha D$ is not empty otherwise there is nothing to prove. Since $D \subseteq \Lambda_C$, one may find a collection of $k = O((C/\alpha)^2)$ vertices $x_1, \dots, x_k \in \frac{1}{3}\alpha\mathbb{Z}^2$ such that

- $\Lambda_{2\alpha/3}(x_i) \subseteq D$ for $1 \leqslant i \leqslant k$;
- $\Lambda_\alpha(x_i) \not\subseteq D$ for $1 \leqslant i \leqslant k$;
- $\partial_\alpha D \subseteq \Lambda_{\alpha/3}(x_1) \cup \cdots \cup \Lambda_{\alpha/3}(x_k)$.

Then, Theorem 2.4 implies that

$$\mathbf{P}^{\emptyset,\emptyset}_{D^\delta,D^\delta}[\partial_\alpha D \overset{\mathbf{n}_1+\mathbf{n}_2}{\longleftrightarrow} \partial_\beta D] \leqslant \sum_{i=1}^{k} \mathbf{P}^{\emptyset,\emptyset}_{D^\delta,D^\delta}[\Lambda_{\alpha/3}(x_i) \overset{\mathbf{n}_1+\mathbf{n}_2}{\longleftrightarrow} \partial_\beta D] \leqslant k\epsilon(\beta/\alpha). \tag{4.5}$$

We then choose β so that the right-hand side is smaller than ε. □

These ingredients are enough for the proof of Proposition 4.6.

Proof of Proposition 4.6. Firstly, Lemma 4.9 shows that for every $n \geqslant 2$, there exist $C_n, M_n < \infty$ such that for all sets of points $A = \{a_1, \dots, a_n\} \subsetneq D$, we have

$$\mathbf{E}^{\emptyset,\emptyset}_{D^\delta,D^\delta}[\mathrm{R}^\delta(A)^n] \leqslant C_n \left|\log(\min_{i\neq j}|a_i - a_j|) \wedge \log\frac{1}{\delta}\right|^{M_n}. \tag{4.6}$$

Lemma 4.10 implies that for every $n \geqslant 2$ and every $\eta > 0$, there exists a function $\rho : [0,\infty) \to [0,\infty)$ satisfying $\rho(0) = 0$ and continuous at 0, and such that for all δ and all sets of points $A = \{a_1, \dots, a_n\} \subsetneq D$ that are pairwise at least η away from each other, we have

$$\mathbf{P}^{\emptyset,\emptyset}_{D^\delta,D^\delta}[\mathrm{I}^\delta(A)] \leqslant \rho(\min_i \mathrm{dist}(u_i, \partial D)).$$

The proof is then a direct combination of these two inequalities with Lemma 4.8 and (4.2). □

We now turn to the computation of the first term on the right-hand side of (4.2) using the approach of Kenyon [34]. The next result is an analog of [34, Proposition 20].

Proposition 4.11. *Let $a_1, a_1^0, \dots, a_n, a_n^0$ be distinct points in D, and let $\gamma_1, \dots, \gamma_n$ be pairwise disjoint curves in D connecting a_i^0 to a_i for $i = 1, \dots, n$. Then,*

$$\lim_{\delta\to 0} \mathbf{E}^{\emptyset,\emptyset}_{D^\delta,D^\delta}\left[\prod_{i=1}^{n}(h^\delta(a_i) - h^\delta(a_i^0))\right] = \mathrm{i}^n \sum_{\epsilon\in\{\pm1\}^n}\prod_{k=1}^{n}\epsilon_k \int_{\gamma_1}\cdots\int_{\gamma_n} \det\left[f_{\epsilon_i,\epsilon_j}(z_i,z_j)\right]_{1\leqslant i,j\leqslant n} dz_1^{(\epsilon_1)}\cdots dz_n^{(\epsilon_n)},$$

where $dz_i^{(1)} = dz_i$, $dz_i^{(-1)} = d\overline{z_i}$, and

$$f_{\epsilon_i,\epsilon_j}(z_i,z_j) = \begin{cases} 0 & \text{if } i = j, \\ f_-(z_i,z_j) & \text{if } (\epsilon_i,\epsilon_j) = (-1,1), \\ f_+(z_i,z_j) & \text{if } (\epsilon_i,\epsilon_j) = (1,1), \\ \overline{f_-(z_i,z_j)} & \text{if } (\epsilon_i,\epsilon_j) = (1,-1), \\ \overline{f_+(z_i,z_j)} & \text{if } (\epsilon_i,\epsilon_j) = (-1,-1). \end{cases}$$

Moreover the limit is conformally invariant.

Proof. We start by proving a stronger version of the conformal invariance statement. Namely, if one expands the determinant under the integrals as a sum of terms over permutations ι, then each multiple integral of the term $T_{\epsilon,\iota}$ corresponding to a fixed ϵ and ι is conformally invariant. This follows from the conformal covariance of the functions $f_{\pm}(z_i, z_j)$ stated in Lemma 4.2 and an integration by substitution. Indeed, it is enough to notice that $T_{\epsilon,\iota}$ is a product of n functions $f_{\pm}(z_i, z_j)$ or their conjugates with the property that each variable z_i appears in it exactly twice and in a way that, under a conformal map φ, it contributes a factor $\varphi'(z_i)$ if $\epsilon_i = 1$ and $\overline{\varphi'(z_i)}$ if $\epsilon_i = -1$.

We now turn to the convergence part. To this end, for $i = 1, \dots, n$ and every δ small enough, we fix a dual path γ_i^δ connecting $(u_i^0)^\delta$ with u_i^δ that converges uniformly to γ_i. It will be convenient to choose the paths γ_i^δ in such a way that:

- the faces of C_{D^δ} visited by each γ_i^δ alternate with each step between U^δ and V^δ (by definition, the paths start and end in U^δ),
- the restriction of each γ_i^δ to U^δ is a path in the dual of D^δ, meaning that consecutive faces share an edge in D^δ,
- the restriction of each γ_i^δ to V^δ is a path in D^δ given by the left endpoints of the edges of D^δ crossed by the path.

Note that such paths exist (for δ small enough), and they only cross corner edges of C_{D^δ}.

We enumerate the edges crossed by γ_i^δ (there is always an even number of them) using the symbols $c_{i,1}^+, c_{i,1}^-, \dots, c_{i,l_i}^+, c_{i,l_i}^-$. With a slight abuse of notation we will also write $c_{i,t}^\pm$ for the indicator functions that the edge belongs to the dimer cover, and $\hat{c}_{i,t}^\pm := c_{i,t}^\pm - \mathbf{E}[c_{i,t}^\pm]$ for the centred version. Since the height increments are centred by the choice of the reference 1-form f_0 (3.5) and since $|f_0| = 1/2$ on all roads, we find

$$\begin{aligned}
\mathbf{E}^{\emptyset,\emptyset}_{D^\delta,D^\delta}\left[\prod_{i=1}^n (h^\delta(a_i) - h^\delta(a_i^0))\right] &= \mathbf{E}^{\emptyset,\emptyset}_{D^\delta,D^\delta}\left[\prod_{i=1}^n \sum_{t=1}^{l_i} (c_{i,t}^+ - c_{i,t}^-)\right] \\
&= \mathbf{E}^{\emptyset,\emptyset}_{D^\delta,D^\delta}\left[\prod_{i=1}^n \sum_{t=1}^{l_i} (\hat{c}_{i,t}^+ - \hat{c}_{i,t}^-)\right] \\
&= \sum_{t_i=1}^{l_1} \cdots \sum_{t_n=1}^{l_n} \sum_{s\in\{\pm\}^n} (-1)^{\#_(s)} \mathbf{E}\left[\prod_{i=1}^n \hat{c}_{i,t_i}^{s_i}\right], \qquad (4.7)
\end{aligned}$$

where $\#\_(s)$ is the number of minuses in s.

Fix $t_1, \dots, t_n$ and $s \in \{\pm\}^n$, and let $\hat{c}_i := \hat{c}_{i,t_i}^{s_i}$. By [34, Lemma 21], the determinant of the inverse Kasteleyn matrix gives correlations of height increments, hence

$$\mathbf{E}^{\emptyset,\emptyset}_{D^\delta,D^\delta}\left[\prod_{i=1}^n \hat{c}_i\right] = \left(\prod_{i=1}^n K(b_i, w_i)\right) \det \hat{C} = (-1)^n \det \hat{C} = \det \hat{C}, \qquad (4.8)$$

where $\hat{C}$ is the $n \times n$ matrix given by

$$\hat{C}_{i,j} = \begin{cases} K^{-1}(w_i, b_j) & \text{if } i \neq j, \\ 0 & \text{otherwise.} \end{cases}$$

Here, we used that the edges of C^δ (roads) corresponding to the corners in D^δ are assigned weight -1 in the Kasteleyn weighting as defined in Section 3.4.1.

Let e_i be the edge satisfying $c^\pm(e_i) = c^\pm_{i,t_i}$, and let z_i be its midpoint. We write $f_\pm := f^D_\pm$ and $f^\delta := f^{D_\delta}$. Proposition 4.4 gives

$$K^{-1}(w_i, b_j) = -\frac{\delta \mathrm{i}}{\sqrt{2}}\Big(f_-(z_i,z_j) - \overline{\eta}^2_{c_i}\eta^2_{c_j}\overline{f_-(z_i,z_j)} + \overline{\eta}^2_{c_i} f_+(z_i,z_j) - \eta^2_{c_j}\overline{f_+(z_i,z_j)} + o(1)\Big).$$

We now expand the determinant from (4.8) as a sum over permutations. Let us investigate the term in this expansion coming from a fixed permutation ι, and for simplicity of notation, let us assume that ι is the cycle $\iota(i) = i+1 \pmod n$. The case of a general permutation will follow in a similar manner. The term under consideration reads

$$\begin{aligned}
&\mathrm{sgn}(\iota)\frac{\delta^n}{\sqrt{2}^n}\mathrm{i}^n\prod_{i=1}^n\Big(f_-(z_i,z_{i+1}) + \overline{\eta}^2_{c_i} f_+(z_i,z_{i+1}) - \\
&\qquad\qquad \overline{\eta}^2_{c_i}\eta^2_{c_{i+1}}\overline{f_-(z_i,z_{i+1})} - \eta^2_{c_{i+1}}\overline{f_+(z_i,z_{i+1})}\Big) + o(\delta^n)\\
&= \mathrm{sgn}(\iota)\frac{\delta^n}{\sqrt{2}^n}\mathrm{i}^n\prod_{i=1}^n\Big(f_{-1,1}(z_i,z_{i+1}) + \eta^{-2}_{c_i} f_{1,1}(z_i,z_{i+1}) - \\
&\qquad\qquad \eta^{-2}_{c_i}\eta^2_{c_{i+1}} f_{1,-1}(z_i,z_{i+1}) - \eta^2_{c_{i+1}} f_{-1,-1}(z_i,z_{i+1})\Big) + o(\delta^n).
\end{aligned} \tag{4.9}$$

We can now expand the product into a sum of 4^n terms. Note that for each corner c_i, the factors $\eta^2_{c_i}$ and $\eta^{-2}_{c_i}$ appear in exactly one out of n brackets, meaning that each final term contains a multiplicative factor of $\eta^{r_{c_i}}_{c_i}$, where $r_{c_i} \in \{-2, 0, 2\}$.

The first important observation is that the terms for which there exists i such that $r_{c_i} = 0$ cancel out to $o(\delta^n)$ after summing over all sign choices $s \in \{-1,1\}^n$ in (4.7). Indeed, for each such term, take the smallest i for which $r_{c_i} = 0$ and consider the corresponding term assigned in (4.7) to a different sign choice s' which differs from s only at the coordinate i. By (4.9), the two terms differ by $o(\delta^n)$, and the cancellation in (4.7) is caused by the fact that $\#_-(s) = -\#_-(s')$.

There are exactly 2^n remaining terms indexed by $\epsilon \in \{-1,1\}^n$ that satisfy $r_{c_i} = -2\epsilon_i$ for all i. Note that in the embedding of the square lattice $\delta\mathbb{Z}^2$, all corners have length $\delta\sqrt{2}/2$, and therefore,

$$\eta^{\pm 2}_{c_i} = \sqrt{2}\delta^{-1} dc_i^{(\mp 1)},$$

where $dc_i^{(1)} := dc_i$ and $dc_i^{(-1)} := \overline{dc_i}$. Hence, the $\sqrt{2}$-terms cancel out, and each such term is of the form

$$\mathrm{sgn}(\iota)\mathrm{i}^n\Big(\prod_{i=1}^n \epsilon_i\Big)\Big(\prod_{i=1}^n f_{\epsilon_i,\epsilon_{i+1}}(z_i,z_{i+1})\Big) dc_i^{(\epsilon_1)}\cdots dc_n^{(\epsilon_n)} + o(\delta^n). \tag{4.10}$$

The term $\prod_{i=1}^n \epsilon_i$ arises as the product of the signs from the expansion of (4.9).

Since

$$d(c^+_{i,t_i})^{(\epsilon_i)} - d(c^-_{i,t_i})^{(\epsilon_i)} = d(z^\delta_i)^{(\epsilon_i)},$$

keeping the permutation ι and the signs ϵ fixed, and summing (4.10) over all $s \in \{-1,1\}^n$, we obtain

$$\operatorname{sgn}(\iota)\mathrm{i}^n\left(\prod_{i=1}^n \epsilon_i\right)\left(\prod_{i=1}^n f_{\epsilon_i,\epsilon_{i+1}}(z_i,z_{i+1})\right)d(z^\delta_1)^{(\epsilon_1)}\cdots d(z^\delta_n)^{(\epsilon_n)} + o(\delta^n).$$

Finally, summing back over all permutations and using that $\gamma^\delta_i \to \gamma_i$ as $\delta \to 0$, we obtain that (4.7) is equal to

$$\begin{aligned}&\mathrm{i}^n \sum_{t_i=1}^{l_1}\cdots\sum_{t_n=1}^{l_n}\left(\sum_{\epsilon\in\{\pm\}^n}\left(\prod_{i=1}^n\epsilon_i\right)\det\left[f_{\epsilon_i,\epsilon_j}(z_i,z_j)\right]_{1\leqslant i,j\leqslant n} d(z^\delta_1)^{(\epsilon_1)}\cdots d(z^\delta_n)^{(\epsilon_n)} + o(\delta^n)\right)\\ &\quad= \mathrm{i}^n\sum_{\epsilon\in\{\pm\}^n}\left(\prod_{i=1}^n\epsilon_i\right)\int_{\gamma_1}\cdots\int_{\gamma_n}\det\left[f_{\epsilon_i,\epsilon_j}(z_i,z_j)\right]_{1\leqslant i,j\leqslant n} dz_1^{(\epsilon_1)}\cdots dz_n^{(\epsilon_n)} + o(1). \qquad (4.11)\end{aligned}$$

This concludes the proof of Proposition 4.11. □

Proof of Theorem 4.5. We already proved in Proposition 4.11 that the desired limit exists and is conformally invariant. Hence, it is enough to identify it for the upper half-plane $\mathbb{H}$. In this case, by Lemma 4.2, we have an explicit formula

$$f_{\epsilon_i,\epsilon_j}(z_i,z_j) = \frac{\mathrm{i}^{\frac{\epsilon_j-\epsilon_i}{2}}}{2\pi\left(z_j^{(\epsilon_j)} - z_i^{(\epsilon_j)}\right)},$$

where $z_i^{(1)} = z_i$ and $z_i^{(-1)} = \overline{z_i}$. Up to conjugation by a diagonal matrix with entries $\mathrm{i}^{\frac{\epsilon_i}{2}}$, this is the same matrix as in [35, Lemma 3.1], and hence,

$$\det\left[f_{\epsilon_i,\epsilon_j}(z_i,z_j)\right]_{1\leqslant i,j\leqslant n} = \frac{1}{(2\pi)^n}\sum_{\pi \text{ pairing of } \{1,\dots,n\}}\prod_{\{i,j\}\in\pi}\frac{1}{\left(z_j^{(\epsilon_j)} - z_i^{(\epsilon_i)}\right)^2}.$$

This means that, after exchanging the order of summations, integrals and products, (4.11) is equal to

$$\begin{aligned}&\frac{\mathrm{i}^n}{(2\pi)^n}\sum_{\pi \text{ pairing of } \{1,\dots,n\}}\prod_{\{i,j\}\in\pi} 2\Re e\left[\int_{\gamma_j}\int_{\gamma_i}\frac{dz_i dz_j}{(z_j-z_i)^2} - \frac{d\overline{z_i}dz_j}{(z_j-\overline{z_i})^2}\right]\\ &= \pi^{-\frac{n}{2}}\sum_{\pi \text{ pairing of } \{1,\dots,n\}}\prod_{\{i,j\}\in\pi}\frac{1}{2\pi}\ln\left|\frac{(u_j-u_i)(u_j^0-u_i^0)(u_j^0-\overline{u_i})(u_j-\overline{u_i^0})}{(u_j^0-u_i)(u_j-u_i^0)(u_j-\overline{u_i})(u_j^0-\overline{u_i^0})}\right|.\end{aligned}$$

Note that the terms in the product above converge to $G_{\mathbb{H}}(u_i, u_j)$ as u_i^0 and u_j^0 get close to $\partial\mathbb{H}$. This together with (4.3) implies that, up to the explicit multiplicative constant, the moments have the same scaling limit as in [35], which ends the proof. □

4.3 | Convergence of h^δ as a random distribution

Recall that for $a \in D$, we write $h^\delta(a)$ for the evaluation of the nesting field at a face $u^\delta = u^\delta(a)$ of D^δ containing a. (Here, we talk only about the graph D^δ where the nesting field is defined, and not about C_{D^δ} which is used as an intermediate tool to prove this convergence.) For a test function $g : D \to \mathbb{R}$, define

$$h^\delta(g) := \int_D g(a)h^\delta(a)da. \tag{4.12}$$

Theorem 4.12. *Let h_D be the GFF in D with zero boundary conditions, and let $g_1, \dots, g_k : D \to \mathbb{R}$ be continuous and bounded test functions. Then, for $l_1, \dots, l_k \in \mathbb{N}$,*

$$\lim_{\delta\to 0} \mathbf{E}^{\emptyset,\emptyset}_{D^\delta,D^\delta}\left[\prod_{i=1}^k h^\delta(g_i)^{l_i}\right] = \mathbf{E}\left[\prod_{i=1}^k \left(\frac{1}{\sqrt{\pi}}h_D(g_i)\right)^{l_i}\right],$$

Proof. We first note that if $\sum_{i=1}^k l_i$ is odd, then the corresponding moments of h^δ and h vanish and there is nothing to prove. Moreover, to simplify notation, we only consider moments $\mathbf{E}[h^\delta(g)^l]$ of one test function g for l even. The general case follows in a similar way. To this end, we fix $l \geqslant 2$, and define

$$D^l_\delta := \{(a_1, \dots, a_l) \in D^l : |a_i - a_j| < \delta \text{ for some } i \neq j\}.$$

Then, by Lemma 4.8 and (4.6), we have

$$\int_D \cdots \int_D \mathbf{E}^{\emptyset,\emptyset}_{D^\delta,D^\delta}\left[\prod_{i=1}^l g(a_i)h^\delta(a_i)\right]\mathbf{1}_{(a_1,\dots,a_l)\in D^l_\delta} da_1 \cdots da_l \leqslant C\|g\|^l_\infty (\log\frac{1}{\delta})^{lM}\boldsymbol{\lambda}^{2l}(D^l_\delta)$$
$$\leqslant C'\|g\|^l_\infty \boldsymbol{\lambda}^2(D)^{l-1}(\log\frac{1}{\delta})^{lM}\delta^2$$

for some constants C, C' and M that depend on l, where $\boldsymbol{\lambda}^{2l}$ is the $2l$-dimensional Lebesgue measure. Note that the right-hand side tends to zero as $\delta \to 0$. The function

$$(a_1, \dots, a_l) \mapsto |\log(\min_{i\neq j}|a_i - a_j|)|^{lM}$$

is integrable over D^l, and hence by dominated convergence, Lemma 4.8 and (4.6) again, we have

$$\lim_{\delta\to 0}\mathbf{E}^{\emptyset,\emptyset}_{D^\delta,D^\delta}\left[h^\delta(g)^l\right] = \lim_{\delta\to 0}\int_D\cdots\int_D \mathbf{E}^{\emptyset,\emptyset}_{D^\delta,D^\delta}\left[\prod_{i=1}^l g(a_i)h^\delta(a_i)\right]da_1\cdots da_l$$
$$= \lim_{\delta\to 0}\int_D\cdots\int_D \mathbf{E}^{\emptyset,\emptyset}_{D^\delta,D^\delta}\left[\prod_{i=1}^l g(a_i)h^\delta(a_i)\right]\mathbf{1}_{(a_1,\dots,a_l)\in D^l\setminus D^l_\delta} da_1\cdots da_l$$

$$= \int_D \cdots \int_D \left(\prod_{i=1}^{l} g(a_i) \right) \lim_{\delta \to 0} \mathbf{E}^{\emptyset,\emptyset}_{D^\delta, D^\delta} \left[\prod_{i=1}^{n} h^\delta(a_i) \right] \mathbf{1}_{(a_1,\dots,a_l) \in D^l \setminus D^l_\delta} da_1 \cdots da_l$$

$$= \int_D \cdots \int_D \left(\prod_{i=1}^{l} g(a_i) \right) \sum_{\pi \text{ pairing}} \prod_{\{i,j\} \in \pi} \frac{1}{\pi} G_D(a_i, a_j) da_1 \cdots da_l$$

$$= \mathbf{E}[(\frac{1}{\sqrt{\pi}} h_D(g))^l],$$

where the second last equality follows from Theorem 4.5. □

Remark 4.13. We note that the same convergence as in Theorem 4.12 holds if the height function is considered as a function on all faces of C_{G^δ} and not only on the faces of G^δ.

We are now ready to conclude the proof the main theorem of this section.

Proof of Theorem 1.4. By Theorem 4.12, all moments of h^δ converge to the corresponding moments of $\frac{1}{\sqrt{\pi}} h_D$. Since h_D is a Gaussian process, its moments identify its law uniquely. Since convergence of the second moment implies tightness, we conclude that h^δ tends to $\frac{1}{\sqrt{\pi}} h_D$ in distribution as δ tends to 0 in the space of generalised functions acting on continuous test functions with compact support. □

5 | FURTHER PRELIMINARIES

In this section, we recall some background on the continuum side.

In this section, we recall some background on the continuum side, notably on the GFF, the local sets and the two-valued sets. Throughout, let $D \subsetneq \mathbb{C}$ be a simply connected domain whose boundary is a Jordan curve.

The SLE was introduced by Schramm in [57]. It is a family of non-self-crossing random curves which depend on a parameter $\kappa > 0$. For many discrete models, free or wired/monochromatic boundary conditions force the interfaces to take the form of loops. The loop interfaces are conjectured (and sometimes proved) to converge to a conformal loop ensemble (CLE) in the continuum, which is a random collection of loops contained in D that do not cross each other. The family of CLE was introduced by Sheffield in [62] and further studied by Sheffield and Werner in [63]. It depends on a parameter $\kappa \in (8/3, 8)$ and can be constructed using variants of SLE_κ.

In [58, 59], Schramm and Sheffield made the important discovery that level lines of the discrete GFF converge in the scaling limit to SLE_4 curves, and that the limiting SLE_4 curves are coupled with the continuum GFF as its *local sets* (i.e. a set with a certain spatial Markov property, see Definition 5.1). More generally, the theory of local sets developed in [59] allows one to couple SLE_κ with the GFF for all $\kappa \in (0, 8)$. The coupling between SLE_κ and GFF was further developed in [19, 49–52] (also, see references therein).

In this work, we are only concerned with the case $\kappa = 4$. It was shown in [59] that SLE_4-type curves are coupled with the GFF with a height gap 2λ in such a way that they are local sets of the GFF with boundary values, respectively, $a - \lambda$ and $a + \lambda$ on the left- and right-hand sides

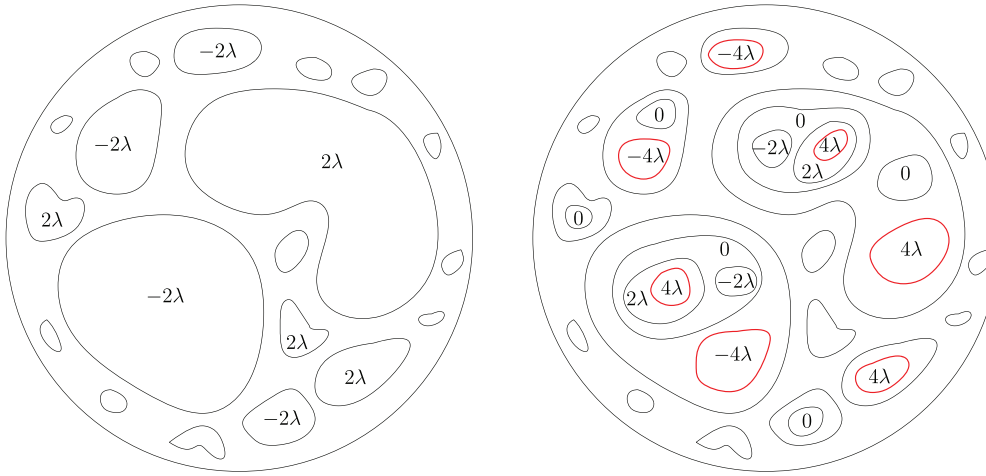

FIGURE 5.1 Left: A sketch of CLE_4 coupled with the GFF. The loops have boundary values -2λ or 2λ. Right: We depict a few layers of the nested CLE_4 coupled with the same GFF. We mark in red the outermost loops that have boundary values -4λ or 4λ, which belong to $\mathcal{L}_{-4\lambda,4\lambda}$.

of the curve. A crucial property shown in [59] is that such SLE_4-type curves are deterministic functions of the GFF. We call these curves level lines, to keep the same terminology as in the discrete. The value $a \in \mathbb{R}$ is called the *height* of the level line. The coupling between SLE_4 and GFF was extended to CLE_4 and GFF by Miller and Sheffield [48] (a more general coupling between CLE_κ and GFF for all $\kappa \in (0,8)$ was established in [53]; a proof for the case $\kappa = 4$ was also provided in [7]).

Let us fix some notation that will be used throughout this work. For any simply connected domain U, we say that its boundary ∂U is a *contour*. If γ is a simple loop, then let $O(\gamma)$ denote the domain encircled by γ, which is equal to the unique bounded connected component of $\mathbb{C} \setminus \gamma$. Let $\overline{O}(\gamma)$ be the closure of $O(\gamma)$. Every simple loop is a contour, but a contour need not be a loop or a curve. Let h be a zero boundary GFF in D. For every simply connected domain $U \subseteq D$, let $h|_U$ denote the restriction of h to the domain U. If $h|_U$ is equal to a GFF in U with constant boundary conditions, say equal to c, then let $h^0|_U$ be the zero boundary GFF so that $h|_U$ is equal to $h^0|_U$ plus c. This constant c is also called the *boundary value* of U, or the *boundary value* of ∂U. Let Γ denote a collection of simple loops which do not cross each other. Let $\mathrm{gask}(\Gamma)$ denote the *gasket* of Γ, which is equal to $\overline{D} \setminus \cup_{\gamma\in\Gamma} O(\gamma)$. Given a connected set $A \subseteq \overline{D}$ such that $\partial D \subseteq A$, let $\mathcal{L}(A)$ denote the collection of outer boundaries of the connected components of $D \setminus A$.

The Miller–Sheffield coupling between the GFF and CLE_4 states that h a.s. uniquely determines a random collection Γ of simple loops which do not cross each other and satisfy the following property (see Figure 5.1, left): conditionally on $\mathrm{gask}(\Gamma)$, for each loop $\gamma \in \Gamma$, there exists $\epsilon(\gamma) \in \{-1,1\}$ such that $h|_{O(\gamma)}$ is equal to $\epsilon(\gamma)2\lambda$ plus a zero-boundary GFF. In addition, the fields $h|_{O(\gamma)}$ for different γ's are (conditionally) independent of each other. In other words, $\mathrm{gask}(\Gamma)$ is a *local set* of h with boundary values in $\{-2\lambda, 2\lambda\}$. It turns out that Γ has the law of a CLE_4. In addition, $\mathrm{gask}(\Gamma)$ carries no mass of the GFF: for all test function f on D, we have

$$\int_D f(x)h(x)dx = \sum_{\gamma\in\Gamma} \int_{O(\gamma)} f(x)h|_{O(\gamma)}(x)dx. \tag{5.1}$$

Each loop γ in CLE_4 is a level line (we also call it a level loop) of the GFF with boundary value $\epsilon(\gamma)2\lambda$ on the inner side of the loop and 0 on the outer side of the loop (so it is at height $\epsilon(\gamma)\lambda$).

It is also natural to consider level loops of h at other heights than those of CLE_4. For example, the previous coupling can be extended to the nested CLE_4 (by sampling the CLE_4 coupled to $h^0|_{O(\gamma)}$ for each $\gamma \in \Gamma$), so that the further layers of CLE_4 loops are at heights $(2k+1)\lambda$ for $k \in \mathbb{Z}$. For $a \in (-\lambda, \lambda)$, the outermost level loops of h at height a are given by boundary conformal loop ensembles (BCLE) [53], and one can then also consider nested versions of BCLE to obtain level loops of h at a continuum range of heights.

The gaskets of CLEs and BCLEs belong to a particular class of local sets called *two-valued sets* introduced by Aru, Sepúlveda and Werner in [7]: a two-valued set is a *thin local set* (a terminology in [60] meaning that the local set carries no mass of the GFF, described by (5.1)) with two boundary values in $\{-a, b\}$, denoted by $\mathbb{A}_{-a,b}$. For example, the gasket of CLE_4 is equal to $\mathbb{A}_{-2\lambda,2\lambda}$, and the gaskets of BCLEs correspond to $\mathbb{A}_{-a,b}$ with $a+b=2\lambda$. It was shown in [7] that the sets $\mathbb{A}_{-a,b}$ exist for $a, b > 0$ with $a+b \geqslant 2\lambda$, and are a.s. unique and determined by h. Let us use $\mathcal{L}_{-a,b}$ to denote $\mathcal{L}(\mathbb{A}_{-a,b})$. Throughout, we denote by $\mathcal{L}^+_{-a,b}$ (resp. $\mathcal{L}^-_{-a,b}$) the set of loops in $\mathcal{L}_{-a,b}$ with boundary value b (resp. $-a$). We will also use notations like $\mathrm{CLE}_4(h)$ and $\mathcal{L}_{-a,b}(h)$ to represent these sets coupled to h (especially when there are different GFFs involved).

The loops in $\mathcal{L}_{-a,b}$ are composed of SLE_4-type curves which are level lines of h, hence are a.s. simple and do not cross each other (but can intersect each other). The law of $\mathcal{L}_{-a,b}$ is invariant under all conformal automorphisms from D onto itself, since h is invariant under those conformal maps. The geometric properties of the loops in $\mathcal{L}_{-a,b}$ are well understood (see, e.g. [6, 7, 56] and Lemma 5.6).

Let us now give a simple and intuitive explanation of the two-valued sets, and postpone more details to the next subsection. As pointed out in [7], $\mathbb{A}_{-a,b}$ is a 2D analogue for GFF of the stopping time of a 1D Brownian motion upon exiting $[-a, b]$, and is intuitively the set of points that are connected to the boundary by a path on which the values of h remain in $[-a, b]$. Let us illustrate this by the following construction of $\mathbb{A}_{-2n\lambda,2n\lambda}$ via iterated CLE_4s (see Figure 5.1, right). For each point $z \in D$, the boundary values of the successive loops that encircle z in the nested CLE_4 perform a symmetric random walk with steps $\pm 2\lambda$. The loops in $\mathcal{L}_{-2n\lambda,2n\lambda}$ correspond to the first time that we obtain a nested CLE_4 loop with boundary value equal to $-2n\lambda$ or $2n\lambda$.

Let us give more details on GFF, local sets and two-valued sets. Here, we look at a GFF in the unit disk $\mathbb{U}$. For any other simply connected domain D, one can simply map D conformally onto $\mathbb{U}$. Let Γ be the space of all closed non-empty subsets of $\overline{\mathbb{U}}$. We view Γ as a metric space, endowed by the Hausdorff metric induced by the Euclidean distance. Note that Γ is naturally equipped with the Borel σ-algebra on Γ induced by this metric. Given $A \in \Gamma$, let A_δ denote the closure of the δ-neighbourhood of A in $\mathbb{U}$. Let $\mathcal{A}_\delta$ be the smallest σ-algebra in which A and the restriction of h to the interior of A_δ are measurable. Let

$$\mathcal{A} := \bigcap_{\delta \in \mathbb{Q}, \delta > 0} \mathcal{A}_\delta.$$

Intuitively, this is the smallest σ-algebra in which A and the values of h in an infinitesimal neighbourhood of A are measurable.

Definition 5.1 (Local set [59]). Let h be a GFF in $\mathbb{U}$. We say that a random set A is a *local set* of h if A is a closed subset of $\overline{\mathbb{U}}$ and one can write $h = h_A + h^A$, where

- h_A is an $\mathcal{A}$-measurable random distribution which is a.s. harmonic on $\mathbb{U} \setminus A$.
- Conditionally on $\mathcal{A}$, h^A is a random distribution which is independent of $\mathcal{A}$. It is a.s. zero on A and equal to an independent zero boundary GFF in each connected component of $\mathbb{U} \setminus A$.

Two-valued sets were introduced by Aru, Sepúlveda and Werner in [7]. More precisely, they denote thin local sets with two prescribed boundary values. Above we have mentioned the examples of CLE_4 (whose gasket is a thin local set of a GFF with two boundary values in $\{-2\lambda, 2\lambda\}$) and $\mathrm{BCLE}_4(-1)$ (whose gasket is a thin local set of a GFF with two boundary values in $\{-\lambda, \lambda\}$).

In [7], the authors first defined the more general family of *bounded-type thin local sets* (denoted by BTLS), as follows.

Definition 5.2 (BTLSs, [7]). Let h be a GFF in D. Let A be a relatively closed subset of D. For $K > 0$, we say that A is a K-BTLS of h if

1. (boundedness) A is a local set of h such that $|h_A(x)| \leqslant K$ for all $x \in D \setminus A$.
2. (thinness) for any smooth function f, we have $(h_A, f) = \int_{D\setminus A} h_A(x) f(x) dx$.

It was shown in [7] that a BTLS must be connected to the boundary of the domain.

Lemma 5.3 (Proposition 4, [7]). *If A is a BTLS, then $A \cup \partial D$ is a.s. connected.*

A two-valued set is defined to be a BTLS A such that $h_A \in \{-a, b\}$ for $a, b > 0$. The family of two-valued sets satisfies the properties of the following lemma.

Lemma 5.4 (Proposition 2 in [7]). *Let $-a < 0 < b$.*

- *When $a + b < 2\lambda$, it is not possible to construct a BTLS A such that $h_A \in \{-a, b\}$ a.s.*
- *When $a + b \geqslant 2\lambda$, there is a unique BTLS A coupled with h such that $h_A \in \{-a, b\}$ a.s. We denote this set A by $\mathbb{A}_{-a,b}$.*
- *If $[a, b] \subseteq [a', b']$, then $\mathbb{A}_{-a,b} \subseteq \mathbb{A}_{-a',b'}$ a.s.*

This lemma shows that two-valued sets are deterministic functions of the GFF h (when they exist), and this property will be instrumental in our proof.

When $a + b = 2\lambda$, the set $\mathcal{L}_{-a,b}$ is equal to $\mathrm{BCLE}_4(\rho)$ (where $\rho = -a/\lambda$) and can be constructed using the branching $\mathrm{SLE}_4(\rho, -2-\rho)$ process ([7, 53]). The loops in $\mathcal{L}^+_{-a,b}$ (resp. $\mathcal{L}^-_{-a,b}$) correspond to the loops traced in the clockwise (resp. counterclockwise) direction by the branching $\mathrm{SLE}_4(\rho, -2-\rho)$. Properties of such SLE processes directly imply the following lemma.

Lemma 5.5 [7, 53]. *If $a + b = 2\lambda$, every loop in $\mathcal{L}_{-a,b}$ intersects ∂D. The loops in $\mathcal{L}^-_{-a,b}$ are equal to the outer boundaries of the connected components of $D \setminus \overline{\cup_{\gamma\in\mathcal{L}^+_{-a,b}} O(\gamma)}$.*

For other values of a, b, $\mathbb{A}_{-a,b}$ is constructed by iterating the branching $\mathrm{SLE}_4(\rho, -2-\rho)$ processes. Using properties of the $\mathrm{SLE}_4(\rho, -2-\rho)$ processes, [6] has deduced the following intersecting behaviour of the loops in $\mathcal{L}_{-a,b}$, which will be useful for us later.

Lemma 5.6 (Intersecting behaviour of the loops [6]).

1. *There exists a loop in $\mathcal{L}^+_{-a,b}$ (resp. $\mathcal{L}^-_{-a,b}$) which intersects ∂D if and only if $b < 2\lambda$ (resp. $a < 2\lambda$).*
2. *If $a + b < 4\lambda$, then one can connect any two loops η_1 and η_2 in $\mathcal{L}_{-a,b}$ by a finite sequence of loops $(\gamma_1, \dots, \gamma_n)$ so that $\gamma_1 = \eta_1$, $\gamma_n = \eta_2$ and γ_{k+1} intersects γ_k for each $1 \leqslant k \leqslant n-1$. Only loops with different boundary values can intersect each other.*

We will also use the following lemmas to identify uniquely the law of the limiting interfaces in Section 6.1.

Lemma 5.7 (Lemma 3.8, [6]). *Let $a, b > 0$ with $a + b > 2\lambda$. Then almost surely, a loop ℓ of $\mathcal{L}_{-a,b}$ labelled $-a$ touches the boundary if and only if $a < 2\lambda$ and ℓ is a loop of $\mathcal{L}_{-a,-a+2\lambda}$ labelled $-a$. Moreover, the loops of $\mathcal{L}_{-a,b}$ which do not touch the boundary and are surrounded by a loop $\gamma \in \mathcal{L}_{-a,-a+2\lambda}$ labelled $-a + 2\lambda$ are exactly the loops of $\mathcal{L}_{-2\lambda,a+b-2\lambda}(h^0|_{O(\gamma)})$.*

Lemma 5.8. *Let $A_1, A_2, \dots$ be an increasing sequence of thin local set of a GFF h in a domain D with $A_1 = A_{-\sqrt{2}\lambda,\sqrt{2}\lambda}$, and such that for each k and each $\ell \in \mathcal{L}(A_k)$ with boundary value $m\sqrt{2}\lambda$, each loop in $\mathcal{L}(A_{k+1})$ encircled by ℓ has boundary value either $(m-1)\sqrt{2}\lambda$ or $(m+1)\sqrt{2}\lambda$. Then, for each k and each $\ell \in \mathcal{L}(A_k)$, the loops in $\mathcal{L}(A_{k+1})$ encircled by ℓ are exactly $\mathcal{L}_{-\sqrt{2}\lambda,\sqrt{2}\lambda}(h^0_{O(\ell)})$.*

Proof. Suppose that $\ell \in \mathcal{L}(A_k)$ has boundary value $m\sqrt{2}\lambda$. Since $A_1, A_2, \dots$ is an increasing sequence, every loop $\gamma \in \mathcal{L}(A_{k+1})$ is either encircled by ℓ or $O(\gamma) \cap O(\ell) = \emptyset$. Since A_{k+1} is a thin local set of h, we have for any smooth function f

$$\int_{O(\ell)} h_{O(\ell)}(x) f(x) dx = \int_{O(\ell)} h(x) f(x) dx = \sum_{\gamma \in \mathcal{L}(A_{k+1}), O(\gamma) \subseteq O(\ell)} \int_{O(\gamma)} h_{O(\gamma)}(x) f(x) dx.$$

Since ℓ has boundary value $m\sqrt{2}\lambda$ and each $\gamma \in \mathcal{L}(A_{k+1})$ encircled by ℓ has boundary value either $(m-1)\sqrt{2}\lambda$ or $(m+1)\sqrt{2}\lambda$, we can conclude the proof. □

Lemma 5.9. *Consider the following collection of loops defined iteratively.*

- *Let $\mathcal{L}_0(h)$ be the collection of loops resulting from replacing each $\ell \in \mathcal{L}^+_{-\sqrt{2}\lambda,\sqrt{2}\lambda}(h)$ (resp. $\ell \in \mathcal{L}^-_{-\sqrt{2}\lambda,\sqrt{2}\lambda}(h)$) by an independent (conditionally on ℓ) $\mathcal{L}_{-\sqrt{2}\lambda,(2-\sqrt{2})\lambda}(h|_{O(\ell)})$ (resp. $\mathcal{L}_{-(2-\sqrt{2})\lambda,\sqrt{2}\lambda}(h|_{O(\ell)})$).*
- *Given $\mathcal{L}_k(h)$, define $\mathcal{L}_{k+1}(h)$ by replacing each $\ell \in \mathcal{L}_k(h)$ with boundary value 0 by an independent (conditionally on ℓ) copy of $\mathcal{L}_0(h|_{O(\ell)})$.*

Then, $\liminf_{k\to\infty} \mathcal{L}_k(h) = \limsup_{k\to\infty} \mathcal{L}_k(h) = \mathcal{L}_{-2\lambda,2\lambda}(h) = \mathrm{CLE}_4(h)$.

Proof. For each k, $\mathrm{gask}(\mathcal{L}_k(h))$ is clearly a thin local set of h with boundary values in $\{-2\lambda, 0, 2\lambda\}$. It remains to prove that $\mathrm{gask}(\lim_{k\to\infty} \mathcal{L}_k(h))$ is a thin local set of h with boundary values in $\{-2\lambda, 2\lambda\}$. For this purpose, it is enough to prove that $\lim_{k\to\infty} \mathcal{L}_k(h)$ a.s. does not contain any loop with boundary value 0.

Let D be the domain on which h is defined. For $z \in D$, if z is encircled by a loop in $\mathcal{L}_k(h)$ with boundary value in $\{-2\lambda, 2\lambda\}$ for some $k \geqslant 0$, then z cannot be encircled by a loop in $\lim_{k\to\infty} \mathcal{L}_k(h)$ with boundary value 0. Let $E(z)$ be the event that z is encircled by a loop $\ell_k \in \mathcal{L}_k(h)$ with boundary value 0 for every $k \geqslant 0$. Then, z is encircled by a loop $\ell \in \lim_{k\to\infty} \mathcal{L}_k(h)$ if and only if $E(z)$ occurs. On this event, ℓ is a.s. encircled by ℓ_k for every $k \geqslant 0$.

On $E(z)$, for $k \geqslant 1$, let $r_k(z)$ be the conformal radius of ℓ_{k-1} seen from z. Let $r_0(z)$ be the conformal radius of ∂D seen from z. Then, for $k \geqslant 1$, conditionally on $E(z)$, the random variables $r_k(z)/r_{k-1}(z)$ are i.i.d. and their law does not depend on z (due to conformal invariance of $\mathcal{L}_0(h)$). Moreover, $r_k(z)/r_{k-1}(z)$ is a.s. strictly less than 1, since $\mathrm{gask}(\mathcal{L}_0(h))$ is a.s. non-empty. It follows that $r_k(z) \to 0$ as $k \to \infty$ a.s., hence ℓ a.s. has conformal radius 0, which is impossible. Therefore, z is a.s. not encircled by a loop in $\lim_{k\to\infty} \mathcal{L}_k(h)$ with boundary value 0. Since this is true for all z, we have proved that $\lim_{k\to\infty} \mathcal{L}_k(h)$ a.s. does not contain any loop with boundary value 0. □

6 | SCALING LIMIT OF THE DOUBLE RANDOM CURRENT CLUSTERS

In this section, we identify the scaling limit of the DRC clusters with free and wired boundary conditions. More precisely, we prove Theorems 6.2 and 6.4 which imply Theorems 1.1 and 1.2. As we have pointed out at the end of Section 1.2, Theorems 6.2 and 6.4 contain more information than Theorems 1.1 and 1.2.

Our proof crucially relies on the height function as defined in the master coupling in Theorem 3.1 which satisfies a strong form of spatial Markov property at the inner boundaries of the DRC clusters, namely one has an independent height function (which converges to a GFF) inside each domain encircled by the inner boundary of a cluster. The boundary values $\sqrt{2}\lambda$ and $2\sqrt{2}\lambda$ at the inner boundaries of the clusters come from the discrete height function (in the discrete, the height changes by ± 1 or $\pm 1/2$ between neighbouring sites and faces but the limiting field is $(2\sqrt{2}\lambda)^{-1}$ times the GFF, hence the values of the continuum field on the scaling limit of such inner boundaries are multiples of $\sqrt{2}\lambda$). For example, the scaling limit of the inner boundaries of the outermost cluster in a DRC model with wired boundary conditions follows directly from this spatial Markov property and the characterisation of two-valued sets (Lemma 5.4) [7].

In contrast, the discrete height function does *not* have this form of spatial Markov property at the outer boundaries of the clusters. However, we establish this spatial Markov property in the continuum limit, using additional information on the geometric properties of these loops and their interaction with other interfaces of the primal and dual models coupled through Theorem 3.1. More precisely, we show that the outer boundaries of the clusters in a free boundary DRC model converge to the CLE_4 coupled with the limiting GFF, so that each limiting loop has boundary value -2λ or 2λ. The value 2λ cannot be found in the height function of the discrete model, but only appears in the continuum limit. This is the same value as the height gap at the two sides of a level line, identified in [58].

Throughout, let D be a Jordan domain. Let U_1 and U_2 be two open and simply connected sets. We say that two contours ∂U_1 and ∂U_2 cross each other if $U_1 \not\subseteq U_2$, $U_2 \not\subseteq U_1$ and $U_1 \cap U_2 \neq \emptyset$. We say that a contour ∂U_1 encircles another contour ∂U_2 if $U_2 \subseteq U_1$, and we say ∂U_1 strictly encircles ∂U_2 if $U_2 \subsetneq U_1$.

6.1 | Main results

In this section, we state the main Theorems 6.2 and 6.4, which can be seen as enhanced versions of Theorems 1.1 and 1.2 presented in the introduction.

Let $D \subsetneq \mathbb{C}$ be a Jordan domain. Recall that we say that simply connected graphs $D^\delta \subset \delta\mathbb{Z}^2$ *approximate* D if $d(\partial D^\delta, \partial D) \to 0$ as $\delta \to 0$, where d is as in (1.2). We consider a critical DRC $\mathbf{n}^\delta$ on D^δ with free boundary conditions, and the dual DRC $(\mathbf{n}^\dagger)^\delta$ on $(D^\delta)^\dagger$ with wired boundary conditions, coupled together as in Theorem 3.1. Let $\mathbb{P}_{D^\delta}$ be this coupling that also encodes the joint height function H^δ composed of the nesting field h^δ of $\mathbf{n}^\delta$, and the nesting field $(h^\dagger)^\delta$ of $(\mathbf{n}^\dagger)^\delta$. The following collections of loops will be relevant in our proofs.

- Q_0^δ is the collection of loops in the inner boundary of the cluster of the ghost vertex of $(\mathbf{n}^\dagger)^\delta$. We proceed inductively. Having defined Q_k^δ, we define Q_{k+1}^δ in the following way. Recall that by property (4) of the master coupling from Theorem 3.1, if k is even, then in each loop ℓ of Q_k^δ, $\mathbf{n}^\delta$ restricted to the domain encircled by ℓ has wired boundary conditions. We modify the current by setting $\mathbf{n}_e^\delta = 2$ (the only important property is that the value is non-zero and even) for every primal edge e whose both endpoints are adjacent to ℓ from the inside. We denote this modified current restricted to ℓ by $\mathbf{n}_\ell^\delta$. We then define $Q_{k+1}^\delta(\ell)$ as the union of all the loops in the inner boundary of the external most (touching ℓ) cluster of $\mathbf{n}_\ell^\delta$ (see Figure 3.2 for an illustration). Finally, we set $Q_{k+1}^\delta = \bigcup_{\ell \in Q_k^\delta} Q_{k+1}^\delta(\ell)$. If k is odd, then we proceed analogously with $\mathbf{n}^\delta$ replaced by $(\mathbf{n}^\dagger)^\delta$, and the primal graph replaced by the dual graph. In particular, the loops in Q_k are on the primal (resp. dual) lattice for k even (resp. odd). We define $Q^\delta = \bigcup_{k=0}^\infty Q_k^\delta$.
- B_k^δ, for k even, is the collection of outer boundaries of the clusters of $\mathbf{n}^\delta$ that touch a loop of Q_k^δ from the inside. Moreover, for each loop $\ell \in B_k^\delta$, let $C(\ell)$ be the cluster of $\mathbf{n}^\delta$ with outer boundary ℓ, and let $A_k^\delta(\ell)$ be the collection of loops in the inner boundary of $C(\ell)$, and $A_k^\delta := \bigcup_{\ell \in B_k^\delta} A_k^\delta(\ell)$. The collection of loops B_k^δ, for k odd, is defined in the same way but with $\mathbf{n}^\delta$ exchanged for $(\mathbf{n}^\dagger)^\delta$. Finally, let $B^\delta = \bigcup_{k=0}^\infty B_k^\delta$ and $A^\delta = \bigcup_{k=0}^\infty A_k^\delta$.

Remark 6.1. Note that $A_k^\delta(\ell) \subset Q_{k+1}^\delta(\ell)$, and hence $A_k^\delta \subset Q_{k+1}^\delta$. Moreover, every loop in $Q_{k+1}^\delta(\ell) \setminus A_k^\delta(\ell)$ traces pieces of loops in B_k^δ that touch ℓ and/or the loop ℓ itself (see Figure 3.2 for an illustration). We also note that the outermost loops both in B^δ and A^δ can be of arbitrary level, that is, belong to B_k^δ and A_k^δ for any k.

For k odd (resp. even) and each $\gamma \in Q_k^\delta(\ell)$, we say that γ is the boundary of an *odd hole* if $\mathbf{n}_\ell^\delta$ (resp. $(\mathbf{n}^\dagger)_\ell^\delta$) is odd around every face encircled by γ (see definition in Section 1.3). Otherwise we say that γ is the boundary of an *even hole*. We define $c^\delta(\ell) = 1$ (resp. $c^\delta(\ell) = -1$) if ℓ is the boundary of an odd (resp. even) hole. Note that every loop in $Q_{k+1}^\delta(\ell) \setminus A_k^\delta(\ell)$ is the boundary of an even hole in by construction (since we modified the current by adding edges with value 2). Moreover, for each loop $\ell \in B^\delta$, let $\epsilon^\delta(\ell)$ be the label of the cluster $C(\ell)$ of $\mathbf{n}^\delta$ with outer boundary ℓ. The label is defined by the coupling with the nesting field h^δ as in Theorem 3.1.

We will prove the following theorems which clearly imply Theorem 1.1 and Theorem 1.2.

Theorem 6.2. *Let D and D^δ be as above, and such that ∂D is C^1. Let $\epsilon_{\mathfrak{g}}^\delta$ be the label of the cluster of the boundary in $(\mathbf{n}^\dagger)^\delta$. Then, as $\delta \to 0$, the family $(H^\delta, Q^\delta, c^\delta, \epsilon_{\mathfrak{g}}^\delta)$ defined above converges in distribution to a limit $(\frac{1}{\sqrt{\pi}}h, Q, c, \epsilon_{\mathfrak{g}})$ satisfying:*

- *h is a GFF with zero boundary conditions in D.*
- *For $k \geqslant 0$, let Q_k be the scaling limit of the loops in Q_k^δ. Then, Q_0 is equal to $\mathcal{L}_{-\sqrt{2}\lambda,\sqrt{2}\lambda}(h)$. Moreover, for every loop $\gamma \in Q_0$, h restricted to $O(\gamma)$ has boundary value $\epsilon_{\mathfrak{g}} c(\gamma)\sqrt{2}\lambda$.*
- *This picture repeats iteratively: if ℓ is a loop in Q_k, then all the loops in Q_{k+1} directly encircled by ℓ form $\mathcal{L}_{-\sqrt{2}\lambda,\sqrt{2}\lambda}(h^0|_{O(\ell)})$, and for each such loop γ, $h^0|_{O(\ell)}$ restricted to $O(\gamma)$ has boundary value*

$$(-1)^k c(\gamma)c(\ell)\sqrt{2}\lambda.$$

Remark 6.3. The difference in the gaps between the first layer and the remaining layers ($\epsilon_{\mathfrak{g}} c(\gamma)\sqrt{2}\lambda$ and $(-1)^k c(\gamma)c(\ell)\sqrt{2}\lambda$, respectively) comes from the fact that in the master coupling of Theorem 3.1, the label of the external most cluster of $\mathbf{n}^\dagger$ is chosen uniformly at random, whereas the increment of the heights between loops in consecutive layers is given by Property (3). Here, we also use Property 2 to see that for a primal cluster $\mathcal{C}$, one has $\epsilon_{\mathcal{C}} = -c(\gamma)$, where γ is the loop in Q^δ that surrounds and touches $\mathcal{C}$. An analogous formula holds for dual clusters. The alternating sign $(-1)^k$ appears since Q_k^δ alternate between primal and dual interfaces, and the formula in Property (3) changes sign depending if we compute the increment from a face or from a vertex of the original graph.

Theorem 6.4. *Let D and D^δ be as above and such that ∂D is C^1. As $\delta \to 0$, the family*

$$(H^\delta, B^\delta, A^\delta, \epsilon^\delta, c^\delta)$$

defined above converges in distribution to a limit $(\frac{1}{\sqrt{\pi}}h, B, A, \epsilon, c)$ satisfying (see Figure 6.1):

- *h is a GFF with zero boundary conditions in D.*
- *The collection of outermost loops in B is equal to $CLE_4(h)$. For each such loop ℓ, $h|_{O(\ell)}$ is equal to an independent zero-boundary GFF $h^0|_{O(\ell)}$ plus the constant $\epsilon(\ell)2\lambda$.*
- *For each such outermost loop ℓ of B, let $A(\ell)$ denote the collection of loops γ in A that are directly encircled by ℓ (no other loop in A encircles γ).*
  - *If $\epsilon(\ell) = 1$, then $A(\ell)$ is equal to $\mathcal{L}_{-2\lambda,(2\sqrt{2}-2)\lambda}(h^0|_{O(\ell)})$.*
  - *If $\epsilon(\ell) = -1$, then $A(\ell)$ is equal to $\mathcal{L}_{-(2\sqrt{2}-2)\lambda,2\lambda}(h^0|_{O(\ell)})$.*
  - *Each loop $\gamma \in A(\ell)$ has boundary value $\epsilon(\ell)(c(\gamma)+1)\sqrt{2}\lambda$.*
- *This picture repeats iteratively in each outermost loop ℓ of A (with $\partial D := \ell$, and with the loops of B and A encircled by ℓ).*

The relation between the loops in Q an A, B is illustrated in Figure 6.2.

Remark 6.5. We can deduce using crossing estimates from [22] that for each loop $\ell \in B_k$, two loops in $A_k(\ell)$ of the same parity (hence of the same boundary value and drawn in the same colour in Figure 6.1) never touch each other. Moreover, only the limit of the boundaries of odd holes can touch ℓ. This is consistent with Theorem 6.4 and the adjacency properties of the loops in a two-valued set (Lemma 5.6). Furthermore, Theorem 6.4 implies that each loop in $A_k(\ell)$ is connected to ℓ via a finite chain of loops of alternating parities (hence the length of this chain always has a fixed parity). In particular, the parity of the holes are determined by the shape of the clusters.

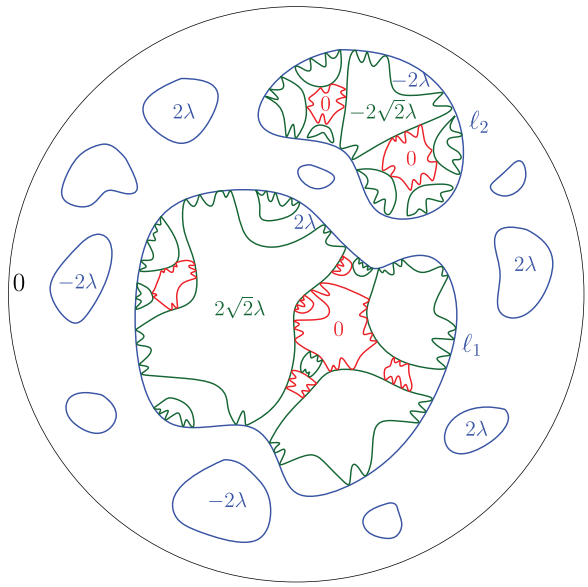

FIGURE 6.1 Scaling limit of the boundaries of the outermost clusters on the primal graph. We depicted the outermost loops of B in blue. For each blue loop ℓ, the loops in $A(\ell)$ have boundary value either 0 or $\epsilon(\ell)2\sqrt{2}\lambda$. For two blue loops ℓ_1 and ℓ_2 with labels $\epsilon(\ell_1) = 1$ and $\epsilon(\ell_2) = -1$, we depict the loops in $A(\ell_1)$ and $A(\ell_2)$. For $i = 1, 2$, we draw the loops in $A(\ell_i)$ with boundary value 0 (resp. $\epsilon(\ell_i)2\sqrt{2}\lambda$) in red (resp. green). Each green (resp. red) loop is the limit of the boundary of an odd (resp. even) hole.

Remark 6.6. We can deduce using crossing estimates from [22] that two loops in Q_0 of the same parity (hence of the same boundary value and drawn in the same colour in Figure 6.2) never touch each other. This is consistent with Theorem 6.2 and the adjacency properties of the loops in a two-valued set (Lemma 5.6).

6.2 | Pre-compactness and first properties of limiting curves

We now proceed to proving the two theorems. To this end, recall the tightness criterion [2, **H1**]: a family of random variables $\mathcal{F}^\delta$ (with law $\mathbb{P}_\delta$) taking values in $\mathfrak{C}(\Omega)$ satisfies condition **H1** if for every $k < \infty$ and every annulus $\mathrm{Ann}(x, r, R)$ with $\delta \leqslant r \leqslant R \leqslant 1$, the following bound holds uniformly in $\delta > 0$:

$$\mathbb{P}_\delta[N_{\mathcal{F}^\delta}(\mathrm{Ann}(x, r, R)) \geqslant k] \leqslant C(k)\left(\frac{r}{R}\right)^{\lambda(k)}, \tag{6.1}$$

with $C(k) > 0$ and $\lambda(k)$ tending to infinity as $k \to \infty$, and where

$$N_{\mathcal{F}^\delta}(\mathbf{A}) = \{k \text{ distinct pieces of curves in } \mathcal{F}^\delta \text{ cross the annulus } \mathbf{A}\}. \tag{6.2}$$

Here, by a *piece* (in $\mathbf{A}$) of a curve, we mean a connected component of the curve resulting from a restriction of the curve to the annulus $\mathbf{A}$. If $\mathcal{F}^\delta$ contains only one curve ℓ, we will simply write N_ℓ for $N_{\{\ell\}}$. Theorem 1.2 of [2] says that if $\mathcal{F}^\delta$ satisfies condition **H1**, then $\mathcal{F}^\delta$ is pre-compact for the topology of weak convergence with respect to the distance (1.1).

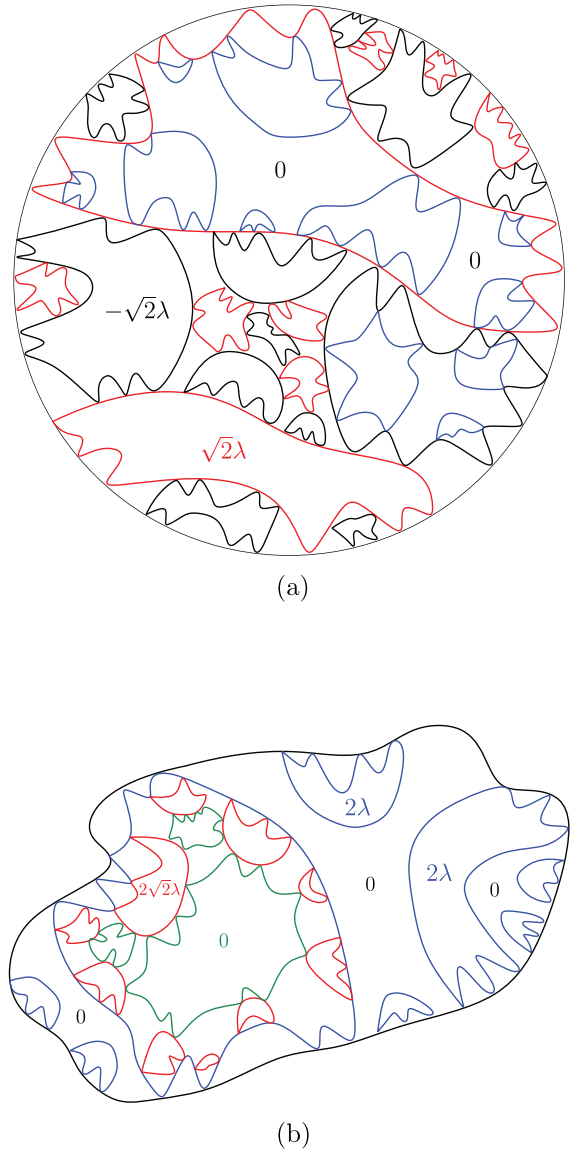

FIGURE 6.2 The nesting between the loops in Q, A, B and their coupling with h. For each set of discrete loops at mesh size δ, we take away the superscript δ to denote its scaling limit in the continuum. For example, A_k and B_k denote, respectively, the scaling limit of the loops in A_k^δ and B_k^δ. We point out that an outermost loop in B or A can be at an arbitrary level, that is, belongs to B_k or A_k for any k.

Proposition 6.7. *Let D, D^δ and $\mathbb{P}_{D^\delta}$ be as above. Let η^δ (resp. $\widehat{\eta}^\delta$) be the nested boundaries interface configuration of $\mathbf{n}^\delta$ (resp. $(\mathbf{n}^\dagger)^\delta$) as defined in Section 1.2. We view η^δ and $\widehat{\eta}^\delta$ as collections of loops, so that $\eta^\delta \cup \widehat{\eta}^\delta = A^\delta \cup B^\delta$. Then, η^δ satisfies condition **H1** under $\mathbb{P}_{D^\delta}$. Moreover, if ∂D is C^1, then $\widehat{\eta}^\delta$ also satisfies condition **H1** under $\mathbb{P}_{D^\delta}$.*

Proof. We apply criterion **H1** to the families η^δ and $\widehat{\eta}^\delta$. The event that $\mathrm{Ann}(x, r, R)$ is crossed by k separate pieces of interfaces in η^δ (resp. $\widehat{\eta}^\delta$) is included in the (rescaled version of the) event

$A_{2k}(r/\delta, R/\delta)$ for $\mathbf{n}$ (resp. $(\mathbf{n}^\delta)^\dagger$), so that we may apply Theorem 2.1 and Remark 7.3 of [22]. This concludes the proof. □

Lemma 6.8. *Let D, D^δ, $\mathbb{P}_{D^\delta}$, and Q_k^δ be as above. Assume, moreover, that ∂D is C^1. Then, for each $k \geqslant 0$, Q_k^δ satisfies condition **H1** under $\mathbb{P}_{D^\delta}$.*

Proof. We will say that two (pieces of) loops are *adjacent* if either they are both subsets of the same graph (primal or dual), and moreover, they intersect, or they are subsets of mutually dual graphs, and moreover, they visit at least one same corner (pair of vertex and face) of the primal graph.

We will proceed inductively. By Proposition 6.7, Q_0^δ satisfies **H1** since it is a subset of $\hat{\eta}^\delta$. Let us hence assume that Q_k^δ satisfies **H1**. Suppose that k is even (the case of k odd is treated analogously). Let us show that Q_{k+1}^δ also satisfies **H1** (with properly adjusted constants in (6.2)). For $\ell \in Q_k^\delta$, let $L(\ell) = Q_{k+1}^\delta(\ell) \setminus \eta^\delta$, and $L = Q_{k+1}^\delta \setminus \eta^\delta = \bigcup_{\ell \in Q_k^\delta} L(\ell)$. Note that by Proposition 6.7, it is enough to prove that L satisfies **H1**.

To this end, we will use the fact that the loops in L are constructed from (pieces of) a loop $\ell \in Q_k^\delta$ or/and pieces of the loops in η^δ that are adjacent to ℓ from the inside (see also Remark 6.1). Let us denote the latter collection of loops by $\eta^\delta(\ell)$. Consider annuli $\mathbf{A} = \mathrm{Ann}(x, r, R)$, and $\mathbf{A}_i = \mathrm{Ann}(x, rs^{i-1}, rs^i)$, where $i = 1, 2, 3, 4$ and $s = \sqrt[4]{R/r}$, so that $\mathbf{A} = \mathbf{A}_1 \cup \mathbf{A}_2 \cup \mathbf{A}_3 \cup \mathbf{A}_4$. Since $\eta^\delta(\ell)$ and $\eta^\delta(\ell')$ are disjoint for $\ell \neq \ell'$, by Proposition 6.7 and the induction assumption, it is enough to show that for each $\ell \in Q_k^\delta$,

$$N_{L(\ell)}(\mathbf{A}) \leqslant 2(N_{\eta^\delta(\ell)\cup\{\ell\}}(\mathbf{A}_1) + N_{\eta^\delta(\ell)}(\mathbf{A}_2) + N_{\eta^\delta(\ell)}(\mathbf{A}_3) + N_{\eta^\delta(\ell)\cup\{\ell\}}(\mathbf{A}_4)). \tag{6.3}$$

To this end, let $P_1(\ell)$ be the set of all pieces in $\mathbf{A}$ of the loops in $L(\ell)$ that cross $\mathbf{A}$ (as defined above). Then, the cardinality of $P_1(\ell)$ is equal to $N_{L(\ell)}(\mathbf{A})$. Moreover, let $P_2(\ell)$ be the set of all pieces in $\mathbf{A}$ of the loops in $\eta^\delta(\ell) \cup \{\ell\}$ (not necessarily crossing $\mathbf{A}$). Here, if a loop is fully contained in $\mathbf{A}$, then there is one piece which is equal to this loop. Furthermore, for each $p_1 \in P_1(\ell)$, let $P_2(p_1) \subset P_2(\ell)$ be the set of pieces in $P_2(\ell)$ that are adjacent to p_1, or are adjacent to another piece adjacent to p_1. As we mentioned earlier, the union of the pieces in $P_2(p_1)$ should entirely cover p_1, by Remark 6.1. The pieces in $P_2(\ell)$ are of two kinds: either they come from ℓ or $\eta^\delta(\ell)$. See Figure 6.3 for an illustration. Let $p_1 \in P_1(\ell)$. Since ℓ encircles all loops in $\eta^\delta(\ell)$, every piece in $P_2(p_1)$ that is a piece of a loop in $\eta^\delta(\ell)$ is either itself connected to the boundary of $\mathbf{A}$ or it is connected to it via a single piece of ℓ in $P_2(p_1)$. This means that there are two possibilities: either there exists a piece in $P_2(p_1)$ that crosses $\mathbf{A}_1$ or $\mathbf{A}_4$, or there exists a piece in $P_2(p_1)$ that is a full loop and crosses either $\mathbf{A}_2$ or $\mathbf{A}_3$. Indeed, suppose that none of the two possibilities is true, then there must exist a full loop γ in $P_2(p_1)$ that is entirely contained in $\mathbf{A}_2 \cup \mathbf{A}_3$. Note that γ must be connected to the boundary of $\mathbf{A}$ via a single piece of ℓ in $P_2(p_1)$. The latter piece in $P_2(p_1)$ then has to cross either $\mathbf{A}_1$ or $\mathbf{A}_4$, leading to a contradiction. Observe, moreover, that by planarity, each $p_2 \in P_2(p_1)$ belongs to at most two sets of the form $P_2(p_1')$ for some $p_1' \in P_1(\ell)$, since a crossing piece p_1 can follow p_2 from at most two sides (this bound is not optimal, but sufficient for our purpose), hence the constant 2 in (6.3). This shows (6.3) and finishes the proof of the lemma. □

Finally, we will need the following intersection properties of the limiting interfaces.

Lemma 6.9. *Let (A, B, c) be any subsequential limit of $(A^\delta, B^\delta, c^\delta)$. Then*

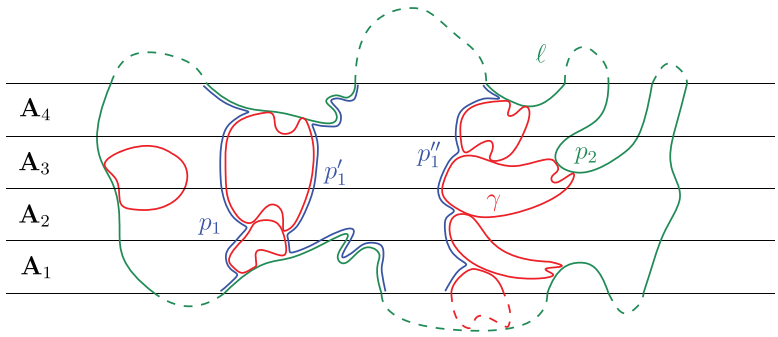

FIGURE 6.3 Illustration of the proof of (6.3). The proof is on the discrete lattice, but we depict curves in the continuum for convenience. Adjacent pieces of loops are depicted as curves that touch or trace each other. We depict in green the loop ℓ, and in red the loops in $\eta^\delta(\ell)$. Note that in the discrete, the loops in $\eta^\delta(\ell)$ can be adjacent to each other (i.e. the red loops can touch each other), even though Theorem 6.2 (that we will prove later) implies that the scaling limit of the loops in $\eta^\delta(\ell)$ a.s. do not touch each other (see Remark 6.6). The pieces in $P_2(\ell)$ are drawn in solid (green or red) curves. We depict in blue 3 pieces p_1, p_1', p_1'' in $P_1(\ell)$ (among several others). We can see that p_1 and p_1' are adjacent to the same pieces in $P_2(\ell)$, which is why the constant 2 in (6.3) is needed. In this picture, there are five pieces in $P_2(\ell)$ which are adjacent to p_1'', but none of them makes the required crossing across $\mathbf{A}_1, \dots, \mathbf{A}_4$. However, in this case, the pieces in $P_2(\ell)$ adjacent to p_1'' must contain at least one full loop γ from $\eta^\delta(\ell)$ which is strictly contained in $\mathbf{A}_2 \cup \mathbf{A}_3$. Then, γ must be adjacent to some piece p_2 of the loop ℓ which is connected to $\partial\mathbf{A}$. Here, p_2 crosses $\mathbf{A}_4$. Note that p_2 is not directly adjacent to p_1'', but is adjacent to some piece adjacent to p_1'', so it is contained in $P_2(p_1'')$ by our definition.

- *the loops in B are simple and do not intersect each other,*
- *the outermost loops in B do not intersect the outermost loops in A with $c = -1$.*

Proof. The fact that the loops in B do not intersect each other is a direct consequence of Theorem 2.2. Indeed, fix $\alpha, \beta, \varepsilon > 0$. For two loops of B^δ of diameter at least α to come within distance β of each other, there must be $x \in \Omega^\delta$ such that the translate by x of the rescaled version of the event $A_4^{\square}(\beta/\delta, \alpha/\delta)$ occurs. Yet, Theorem 2.2 implies that provided that $\beta \leqslant \beta_0(\alpha, \varepsilon)$, this occurs with probability smaller than ε. The fact that the loops in A and B are simple is also direct consequence of Theorem 2.2. Indeed, the event that a single loop comes within distance β of itself after going away to distance α also implies the same event. Letting β tend to zero, then α, and finally ε, we obtain the result.

Moreover, for a loop of A^δ of diameter at least α and with boundary value zero (and hence $c = -1$) to come within a distance β of an outermost loop in B^δ of diameter at least α, there must be $x \in D^\delta$ such that the translate by x of the rescaled version of the event $A_4^{\blacksquare}(\beta/\delta, \alpha/\delta)$ occurs. Yet, Theorem 2.3 implies that provided that $\beta \leqslant \beta_0(\alpha, \varepsilon)$, this occurs with probability smaller than ε. Letting β tend to zero, then α, and finally ε, we obtain the result. □

6.3 | Identification of limits

We start with a lemma that proves the first two bullets of Theorem 6.2.

Lemma 6.10. *Let D, D^δ, $\mathbb{P}_{D^\delta}$ and Q_0^δ be as above. Assume moreover that ∂D is C^1. Let $\epsilon_{\mathfrak{g}}^\delta$ be the label of the cluster of the boundary in $(\mathbf{n}^\dagger)^\delta$. Then the family $((h^\dagger)^\delta, Q_0^\delta, c^\delta, \epsilon_{\mathfrak{g}}^\delta)$ converges weakly to $(\frac{1}{\sqrt{\pi}}h, Q_0, c, \epsilon_{\mathfrak{g}})$ as $\delta \to 0$, where*

- *h is a GFF with zero boundary conditions in D.*
- *$Q_0 = \mathcal{L}_{-\sqrt{2}\lambda,\sqrt{2}\lambda}(h)$.*
- *For each $\ell \in Q_0$, h restricted to $O(\ell)$ has boundary value $\epsilon_{\mathfrak{g}} c(\ell)\sqrt{2}\lambda$.*

Proof. By Lemma 6.8, Theorem 1.4, and the compactness of $\{-1,1\}^{\mathbb{N}}$, $((h^\dagger)^\delta, Q_0^\delta, c^\delta, \epsilon_{\mathfrak{g}}^\delta)$ is pre-compact in the topology of week convergence. Let $(\frac{1}{\sqrt{\pi}}h, Q_0, c, \epsilon_{\mathfrak{g}})$ be a limit along a subsequence δ_n. We also know from Theorem 1.4 that h is the GFF in D with zero boundary conditions.

We will identify $\mathrm{gask}(Q_0)$ as the only two-valued set of h with boundary values $\pm\sqrt{2}\lambda$. To this end, we need to show that $\mathrm{gask}(Q_0)$ is thin for h, that is, for any smooth bounded function g, we have

$$\int_D g(x)h(x)dx = \sum_{\gamma\in Q_0}\int_{O(\gamma)} g(x)h|_{O(\gamma)}(x)dx.$$

Note that $\mathrm{gask}(Q_0^\delta) \subset \mathrm{gask}(A_0^\delta)$ by the master coupling from Theorem 3.1, and moreover h^δ is zero on $\mathrm{gask}(A_0^\delta)$. Furthermore, $(h^\dagger)^\delta$ and h^δ have a common scaling limit $\frac{1}{\sqrt{\pi}}h$ by Theorem 1.4. Therefore, it is enough to show the following (here we prefer to look at $\mathrm{gask}(A_0^\delta)$ as it deals with DRCs with free boundary conditions, and these are more amenable to analysis as already mentioned)

$$\lim_{\alpha\to 0}\lim_{n\to\infty}\int_{D^{\delta_n}} g(x)h^{\delta_n}(x)\mathbf{1}_{x\in E_\alpha^{\delta_n}}dx = 0, \tag{6.4}$$

where, if $\Lambda_\alpha(y) := y + [-\alpha,\alpha]^2$,

$$E_\alpha^{\delta_n} := \text{ union of the } \Lambda_\alpha(y) \text{ for } y \in \alpha\mathbb{Z}^2 \text{ such that } \Lambda_{2\alpha}(y) \text{ intersects some } \gamma \in A_0^{\delta_n}$$

(note that, in particular, every x that is within a distance α of some γ in $A_0^{\delta_n}$ must be in $E_\alpha^{\delta_n}$).

In order to prove this statement, we fix $\varepsilon > 0$ and see that

$$\begin{aligned}\varepsilon\mathbb{P}_{\delta_n}\left[\int_{D^{\delta_n}} g(x)h^{\delta_n}(x)\mathbf{1}_{x\in E_\alpha^{\delta_n}}dx \geqslant \varepsilon\right] &\leqslant \mathbb{E}_{\delta_n}\left[\left|\int_{D^{\delta_n}} g(x)h^{\delta_n}(x)\mathbf{1}_{x\in E_\alpha^{\delta_n}}dx\right|\right]\\ &\leqslant \sum_{y\in\alpha\mathbb{Z}^2}\mathbb{E}_{\delta_n}\left[\left|\int_{\Lambda_\alpha(y)} g(x)h^{\delta_n}(x)\mathbf{1}_{x\in E_\alpha^{\delta_n}}dx\right|\right]\\ &= \sum_{y\in\alpha\mathbb{Z}^2}\mathbb{E}_{\delta_n}\left[\mathbf{1}_{y\in E_\alpha^{\delta_n}}\left|\int_{\Lambda_\alpha(y)} g(x)h^{\delta_n}(x)dx\right|\right]\end{aligned}$$

$$\leqslant \sum_{y\in\alpha\mathbb{Z}^2} \mathbb{P}_{\delta_n}[y \in E_\alpha^{\delta_n}]^{1/2}\mathbb{E}_{\delta_n}\left[\left(\int_{\Lambda_\alpha(y)} g(x)h^{\delta_n}(x)dx\right)^2\right]^{1/2}$$

$$\leqslant \sum_{y\in\alpha\mathbb{Z}^2} \alpha^c \times C(g)\alpha^2\log(1/\alpha)$$

$$\leqslant C(g,D)\log(1/\alpha)\alpha^c.$$

Above, we used Markov's inequality in the first inequality, the triangle inequality in the second, the fact that $x \in E_\alpha^{\delta_n}$ is equivalent to $y \in E_\alpha^{\delta_n}$ in the third, and Cauchy–Schwarz in the fourth. In the fifth, we combine an easy estimate on the second moment of $\int_{\Lambda_\alpha(y)} g(x)h^{\delta_n}(x)dx$ based on the definition of the nesting field and RSW-type estimates from [22], together with the fact that for $\Lambda_\alpha(y)$ to intersect a loop γ in A^{δ_n}, there must be a primal path in $\mathbf{n}^\delta$ from $\Lambda_\alpha(x)$ to $\Lambda_\beta(x)$ or a path in $(\mathbf{n}^\delta)^*$ (the dual complement) from $\partial\Lambda_\beta(x)$ to $\partial\Lambda_{d(x,\partial D)}(x)$, where $\beta := \sqrt{\alpha d(x,\partial D)}$. This proves that gask$(Q_0^\delta)$ is thin for h.

Moreover, by the Markov property of the nesting field with wired boundary conditions (1.7) and Theorem 1.4 applied inside each loop of Q_0^δ, we know that gask(Q_0) is a local set of h, and that for each $\gamma \in Q_0$, the restriction of h to $O(\gamma)$ has boundary value equal to $\epsilon_{\mathfrak{g}}c(\ell)\sqrt{2\lambda} \in \{-\sqrt{2\lambda}, \sqrt{2\lambda}\}$ (since in the discrete the boundary value is equal to $\pm\frac{1}{2}$ and the scaling limit of h^δ is $\frac{1}{\sqrt{\pi}}h = \frac{1}{2\sqrt{2\lambda}}h$). By Lemma 5.4, this uniquely characterises Q_0 as the two-valued set $\mathcal{L}_{-\sqrt{2\lambda},\sqrt{2\lambda}}(h)$. □

Proof of Theorem 6.2. By the lemma above, we are left with proving the third bullet from the statement. By the definition of Q_k^δ and by the Markov property 4 of the master coupling from Theorem 3.1, we know that the loops of Q_{k+1}^δ contained in a single loop ℓ of Q_k^δ, have the same distribution as Q_0^δ in a domain D^δ whose outer boundary is ℓ. However, we cannot directly apply Lemma 6.10 since the assumption on the boundary of the domain being smooth is not satisfied by the scaling limits of the loops from Q_0^δ (as they are fractal loops by Lemma 6.10). Nonetheless, this assumption is only used to obtain subsequential limits of the loops. Indeed, the proof of convergence of the height function in Theorem 1.4 and of the fact that the gasket of the limiting collection of loops is thin in Lemma 6.10 works for Jordan domains with arbitrary boundaries as it goes through currents with free boundary conditions (and we have more control on them as already mentioned). The remaining ingredient of the proof is the Markov property that is the same both for random currents with free and wired boundary conditions.

Therefore, to prove the third bullet, it is enough to use pre-compactness of Q_k^δ (which follows directly from Lemma 6.8) and show that every subsequential limit of gask(Q_k^δ) is a thin local set (as in the proof of Lemma 6.10). Then, use Remark 6.3 to identify the signs of boundary values of the field on consecutive loops in the continuum, and use Lemma 5.8 to identify the limit uniquely. □

Proof of Theorem 6.4. By Theorem 1.4, Proposition 6.7 and compactness of $\{\pm1\}^{\mathbb{N}}$, we know that $(A^\delta, B^\delta, h^\delta, c^\delta, \epsilon^\delta)$ is pre-compact in the topology of weak convergence. Let (A, B, h, c, ϵ) be any subsequential limit.

Note that from Theorem 6.2 and Remark 6.1, we already know that the loops in A are a subset of all the loops in the union of nested iterations of $\mathcal{L}_{-\sqrt{2\lambda},\sqrt{2\lambda}}$. However, we need an

additional argument to uniquely determine exactly which subset they are. To be more precise, recall from Remark 6.1 that $A_k^\delta \subset Q_{k+1}^\delta$. Theorem 6.2 implies that if ℓ is a scaling limit of $\ell^\delta \in Q_k^\delta$, then the scaling limits of loops in $Q_{k+1}^\delta(\ell^\delta)$ is $\mathcal{L}_{-\sqrt{2}\lambda,\sqrt{2}\lambda}(h^0|_{O(\ell)})$. We claim that the scaling limit of $Q_{k+1}^\delta(\ell^\delta) \setminus A_k^\delta(\ell^\delta)$ is exactly the set of loops in $\mathcal{L}_{-\sqrt{2}\lambda,\sqrt{2}\lambda}(h^0|_{O(\ell)})$ that have label $(-1)^{k+1}c(\ell)\sqrt{2}\lambda$ and moreover intersect ℓ. Equivalently, by Lemma 5.7, this is exactly $\mathcal{L}^-_{-\sqrt{2}\lambda,(2-\sqrt{2})\lambda}(h^0|_{O(\ell)})$ if $c(\ell) = (-1)^k$, and $\mathcal{L}^+_{-(2-\sqrt{2})\lambda,\sqrt{2}\lambda}(h^0|_{O(\ell)})$ if $c(\ell) = (-1)^{k+1}$. Indeed, by property 2 of the master coupling from Theorem 3.1, the increment of the nesting field between ℓ^δ and $\gamma^\delta \in Q_{k+1}^\delta(\ell^\delta)$ is $(-1)^k c(\ell^\delta)c(\gamma^\delta)$. The loops in $Q_{k+1}^\delta(\ell^\delta) \setminus A_k^\delta(\ell^\delta)$ are boundaries of even holes as mentioned below Remark 6.1, and hence $c(\gamma^\delta) = -1$ for every such loop γ^δ. Altogether this means that all loops in the scaling limit of $Q_{k+1}^\delta(\ell^\delta) \setminus A_k^\delta(\ell^\delta)$ have label $(-1)^{k+1}c(\ell)\sqrt{2}\lambda$. To prove the claim, we still need to show that they are boundaries of exactly those even holes in $Q_{k+1}^\delta(\ell^\delta)$ whose scaling limit intersects ℓ. Here is where we use the intersection properties from Lemma 6.9. First of all, every loop $\gamma^\delta \in A_k^\delta(\ell^\delta)$ is by definition encircled by a loop in B_k^δ, which, in turn, is encircled by ℓ^δ. If γ^δ is the boundary of an even hole, then its scaling limit cannot intersect ℓ, as in this case, it would intersect the scaling limit of the corresponding loop in B_k^δ, which is forbidden by bullet two of Lemma 6.9. Hence, it is enough to show that every loop in $Q_{k+1}^\delta(\ell^\delta) \setminus A_k^\delta(\ell^\delta)$ has a scaling limit that intersects ℓ. To this end, recall from Remark 6.1 that each such loop traces pieces of loops in B_k^δ that touch ℓ^δ and/or pieces of ℓ^δ itself. If its scaling limit does not intersect ℓ, it means that it can only trace pieces of scaling limits of loops from B_k^δ that intersect ℓ. However, that would imply that these loops either touch each other or self-touch which is forbidden by bullet one of Lemma 6.9.

We now move on to the identification of the scaling limit of the outermost loops of B as $\mathrm{CLE}_4(h)$ using Lemmas 5.5 and 5.9. Our aim is to show that the continuum construction of Lemma 5.9 is mirrored in the discrete. Since we look at the outer boundaries of only the primal current $\mathbf{n}^\delta$, the relevant auxiliary collections of loops will be Q_{2k}^δ, $k = 0, 1, \ldots$. Let $\ell^\delta \in Q_{2k}^\delta$, and recall that $B_{2k}(\ell^\delta)$ is the set of outer boundaries of $\mathbf{n}^\delta$ that touch ℓ^δ from the inside, and let $B_{2k}(\ell)$ be the set of their scaling limits, where ℓ is the scaling limit of ℓ^δ. We claim that the restriction of the loops in $B_{2k}(\ell)$ to $O(\ell)$ agrees with the restriction of $\mathcal{L}^-_{-\sqrt{2}\lambda,(2-\sqrt{2})\lambda}(h^0|_{O(\ell)})$ to $O(\ell)$ if $c(\ell^\delta) = 1$, and with the restriction of $\mathcal{L}^+_{-(2-\sqrt{2})\lambda,\sqrt{2}\lambda}(h^0|_{O(\ell)})$ if $c(\ell^\delta) = -1$. Without loss of generality, let us assume that $c(\ell^\delta) = 1$. Indeed, by definition, the loops in $Q_{2k+1}^\delta(\ell^\delta) \setminus A_{2k}^\delta(\ell^\delta)$ restricted to the inside of ℓ^δ follow pieces of loops from $B_{2k}(\ell^\delta)$. Reversely, the loops in $B_{2k}(\ell^\delta)$ follow pieces of loops in $Q_{2k+1}^\delta(\ell^\delta) \setminus A_{2k}^\delta(\ell^\delta)$ unless the loops in $B_{2k}(\ell^\delta)$ come to distance one (see Figure 3.2 for an example). Since $B_{2k}(\ell)$ do not intersect each other, and by the paragraph above, inside $O(\ell)$, all loops from $B_{2k}(\ell)$ follow pieces of $O(\ell)$ if $c(\ell^\delta) = 1$. On the other hand, again by definition, the restriction of the loops in $B_{2k}(\ell)$ to ℓ is the closure of the complement of the restriction of $\mathcal{L}^-_{-\sqrt{2}\lambda,(2-\sqrt{2})\lambda}(h^0|_{O(\ell)})$ to ℓ. Hence, by Lemma 5.5, $B_{2k}(\ell)$ is equal to $\mathcal{L}^+_{-\sqrt{2}\lambda,(2-\sqrt{2})\lambda}(h^0|_{O(\ell)})$. This together with the construction of Lemma 5.9 that extracts the outermost loops from B proves that these outermost loops are $\mathrm{CLE}_4(h)$.

The fact that $A(\gamma)$ for every outermost loop $\gamma \in B$ is equal to $\mathcal{L}_{-2\lambda,(2\sqrt{2}-2)\lambda}(h^0|_{O(\gamma)})$ if $\epsilon(\gamma) = 1$, and to $\mathcal{L}_{-(2\sqrt{2}-2)\lambda,2\lambda}(h^0|_{O(\gamma)})$ if $\epsilon(\gamma) = -1$ follows directly from the discussion above and the second part of Lemma 5.7. □

6.4 | Asymptotic behaviour of the number of clusters

Let us now prove a lemma which leads to the asymptotic numbers of clusters in the DRC models that surround the origin.

Lemma 6.11. *In the scaling limit of the DRC model in the unit disk (with either the free or wired boundary conditions), let $N(\varepsilon)$ be the number of clusters surrounding the origin such that their outer boundaries have a conformal radius w.r.t. the origin at least ε. Then,*

$$N(\varepsilon)/\log(\varepsilon^{-1}) \underset{\varepsilon\to 0}{\longrightarrow} 1/(\sqrt{2}\pi^2).$$

Proof. By Theorems 1.1 and 1.2 and [7, Proposition 20], we know that the difference of log conformal radii between the outer boundaries of two successive DRC clusters that encircle the origin is given by $R := T_1 + T_2$, where T_1 is the first time that a standard Brownian motion exits $[-\pi, (\sqrt{2}-1)\pi]$ and T_2 is the first time that a standard Brownian motion exits $[-\pi, \pi]$. We have

$$\mathbb{E}(T_1 + T_2) = (\sqrt{2}-1)\pi^2 + \pi^2 = \sqrt{2}\pi^2.$$

The nth cluster which encircles the origin has log conformal radius equal to $-S_n$ where $S_n := -(R_1 + \cdots + R_n)$ and R_i are i.i.d. random variables distributed like R. Then, $N(\varepsilon)$ is the smallest $n \geqslant 1$ such that $S_{n+1} \geqslant \log(\varepsilon^{-1})$. By the law of large numbers, we know that S_n/n converges to $\mathbb{E}(R)$ a.s. as $n \to \infty$. Since $N(\varepsilon) \to \infty$ as $\varepsilon \to 0$, we also have that

$$S_{N(\varepsilon)+1}/(N(\varepsilon)+1) \to \mathbb{E}(R) \text{ a.s. as } \varepsilon \to 0.$$

Note that $\log(\varepsilon^{-1}) \leqslant S_{N(\varepsilon)+1} \leqslant \log(\varepsilon^{-1}) + R_{N(\varepsilon)}$. It follows that

$$\lim_{\varepsilon\to 0} \log(\varepsilon^{-1})/N(\varepsilon) = \mathbb{E}(R) = \sqrt{2}\pi^2.$$

The inverse of the above equation proves the lemma. □

ACKNOWLEDGEMENTS

We are grateful to Juhan Aru for pointing out a mistake in the previous version of the paper. The beginning of the project involved a number of people, including Gourab Ray, Benoit Laslier and Matan Harel. We thank them for inspiring discussions. The project would not have been possible without the numerous contributions of Aran Raoufi to whom we are very grateful. We thank Pierre Nolin for useful comments on an earlier version of this paper. We thank Wendelin Werner for reading a later version of this paper, and for insightful comments which improved the paper. Finally, we are indebted to the anonymous referees for the careful reading of the article and the valuable comments that were incorporated in the final version. The first author was supported by the NCCR SwissMap from the FNS. This project has received funding from the European Research Council (ERC) under the European Union's Horizon 2020 research and innovation program (grant agreement No. 57296).

JOURNAL INFORMATION

The *Proceedings of the London Mathematical Society* is wholly owned and managed by the London Mathematical Society, a not-for-profit Charity registered with the UK Charity Commission. All surplus income from its publishing programme is used to support mathematicians and mathematics research in the form of research grants, conference grants, prizes, initiatives for early career researchers and the promotion of mathematics.

REFERENCES

1. M. Aizenman, D. J. Barsky, and R. Fernández, *The phase transition in a general class of Ising-type models is sharp*, J. Statist. Phys. **47** (1987), no. 3-4, 343–374.
2. M. Aizenman and A. Burchard, *Hölder regularity and dimension bounds for random curves*, Duke Math. J. **99** (1999), no. 3, 419–453.
3. M. Aizenman, H. Duminil-Copin, and V. Sidoravicius, *Random currents and continuity of Ising model's spontaneous magnetization*, Comm. Math. Phys. **334** (2015), 719–742.
4. M. Aizenman, H. Duminil-Copin, V. Tassion, and S. Warzel, *Emergent planarity in two-dimensional ising models with finite-range interactions*, Invent. Math. **216** (2019), no. 3, 661–743.
5. J. Aru, T. Lupu, and A. Sepúlveda, *The first passage sets of the 2D Gaussian free field: convergence and isomorphisms*, Comm. Math. Phys. **375** (2020), no. 3, 1885–1929, DOI 10.1007/s00220-020-03718-z.
6. J. Aru and A. Sepúlveda, *Two-valued local sets of the 2D continuum Gaussian free field: connectivity, labels, and induced metrics*, Electron. J. Probab. **23** (2018), Paper No. 61, 35.
7. J. Aru, A. Sepúlveda, and W. Werner, *On bounded-type thin local sets of the two-dimensional Gaussian Free Field*, J. Inst. Math. Jussieu **18** (2019), no. 3, 591–618.
8. M. Basok and D. Chelkak, *Tau-functions a la Dubédat and probabilities of cylindrical events for double-dimers and CLE (4)*, arXiv:1809.00690, 2018.
9. C. Boutillier and B. de Tilière, *Height representation of XOR-Ising loops via bipartite dimers*, Electron. J. Probab. **19** (2014), no. 80, 33.
10. T. van de Brug, F. Camia, and M. Lis, *Random walk loop soups and conformal loop ensembles*, Probab. Theory Related Fields **166** (2016), no. 1, 553–584.
11. D. Chelkak, *Planar Ising model at criticality: state-of-the-art and perspectives*, Proceedings of the International Congress of Mathematicians (ICM 2018), 2019, pp. 2801–2828.
12. D. Chelkak, *Ising model and s-embeddings of planar graphs*, arXiv:2006.14559, 2020.
13. D. Chelkak, D. Cimasoni, and A. Kassel, *Revisiting the combinatorics of the 2D Ising model*, Ann. Inst. Henri Poincaré Comb. Phys. Interact. **4** (2017), 309–385.
14. D. Chelkak, C. Hongler, and K. Izyurov, *Conformal invariance of spin correlations in the planar Ising model*, Ann. of Math. (2) **181** (2015), no. 3, 1087–1138.
15. D. Chelkak and S. Smirnov, *Universality in the 2D Ising model and conformal invariance of fermionic observables*, Invent. Math. **189** (2012), no. 3, 515–580.
16. B. de Tilière, *Scaling limit of isoradial dimer models and the case of triangular quadri-tilings*, Ann. Inst. Henri Poincare (B) Probab. Stat.s **43** (2007), no. 6, 729–750.
17. J. Dubédat, *Exact bosonization of the Ising model*, arXiv:1112.4399, 2011.
18. J. Dubédat, *Double dimers, conformal loop ensembles and isomonodromic deformations*, J. Eur. Math. Soc. **21** (2018), no. 1, 1–54.
19. J. Dubédat, *SLE and the free field: partition functions and couplings*, J. Amer. Math. Soc. **22** (2009), no. 4, 995–1054.
20. H. Duminil-Copin, *Random currents expansion of the Ising model*, arXiv:1607:06933, 2016.
21. H. Duminil-Copin and M. Lis, *On the double random current nesting field*, Probab. Theory Related Fields **175** (2019), no. 3-4, 937–955.
22. H. Duminil-Copin, M. Lis, and W. Qian, *Conformal invariance of double random currents and XOR-Ising II: tightness and properties in the discrete*, Preprint, 2021.
23. H. Duminil-Copin, S. Goswami, and A. Raoufi, *Exponential decay of truncated correlations for the Ising model in any dimension for all but the critical temperature*, Comm. Math. Phys. **374** (2020), no. 2, 891–921.

24. H. Duminil-Copin, V. Sidoravicius, and V. Tassion, *Continuity of the phase transition for planar random-cluster and Potts models with* $1 \leqslant q \leqslant 4$, Comm. Math. Phys. **349** (2017), no. 1, 47–107.
25. H. Duminil-Copin, I. Manolescu, and V. Tassion, *Planar random-cluster model: fractal properties of the critical phase*, arXiv:2007.14707, 2020.
26. H. Duminil-Copin and V. Tassion, *A new proof of the sharpness of the phase transition for Bernoulli percolation and the Ising model*, Comm. Math. Phys. **343** (2016), no. 2, 725–745.
27. C. Fan and F. Y. Wu, *General lattice model of phase transitions*, Phys. Rev. B **2** (1970), no. 3, 723–733, DOI 10.1103/PhysRevB.2.723.
28. A. Giuliani, V. Mastropietro, and F. Toninelli, *Height fluctuations in non-integrable classical dimers*, Europhys. Lett. **109** (2015), no. 6, 60004.
29. R. B. Griffiths, C. A. Hurst, and S. Sherman, *Concavity of magnetization of an Ising ferromagnet in a positive external field*, J. Math. Phys. **11** (1970), no. 3, 790–795.
30. C. Hongler, *Conformal invariance of Ising model correlations*, Ph.D. thesis, 2010.
31. C. Hongler and S. Smirnov, *The energy density in the planar Ising model*, Acta Math. **211** (2013), no. 2, 191–225.
32. L. P. Kadanoff and H. Ceva, *Determination of an operator algebra for the two-dimensional Ising model*, Phys. Rev. B **3** (1971), no. 11, 3918.
33. P. Kasteleyn, *The statistics of dimers on a lattice. I. The number of dimer arrangements on a quadratic lattice*, Physica (1961), no. 27, 1209–1225.
34. R. Kenyon, *Conformal invariance of domino tiling*, Ann. Probab. **28** (2000), no. 2, 759–795.
35. R. Kenyon, *Dominos and the Gaussian free field*, Ann. Probab. **29** (2001), no. 3, 1128–1137.
36. R. Kenyon, *The Laplacian and Dirac operators on critical planar graphs*, Invent. Math. **150** (2002), no. 2, 409–439.
37. R. Kenyon, *Conformal invariance of loops in the double-dimer model*, Comm. Math. Phys. **326** (2014), no. 2, 477–497.
38. R. W. Kenyon, J. G. Propp, and D. B. Wilson, *Trees and matchings*, Electron. J. Combin. **7** (2000), Research Paper 25, 34. MR1756162.
39. R. W. Kenyon and S. Sheffield, *Dimers, tilings and trees*, J. Combin. Theory Ser. B **92** (2004), no. 2, 295–317. Special Issue Dedicated to Professor W.T. Tutte.
40. G. F. Lawler, O. Schramm, and W. Werner, *Conformal invariance of planar loop-erased random walks and uniform spanning trees*, Ann. Probab. **32** (2004), no. 1B, 939–995.
41. M. Lis, *On boundary correlations in planar Ashkin-Teller models*, Int. Math. Res. Not. **2022** (2022), no. 13, 9909–9940.
42. M. Lis, *Spins, percolation and height functions*, arXiv:1909.07351, 2019.
43. M. Lis, *The planar Ising model and total positivity*, J. Stat. Phys. **166** (2017), no. 1, 72–89.
44. T. Lupu, *Convergence of the two-dimensional random walk loop-soup clusters to CLE*, J. Eur. Math. Soc. **21** (2018), no. 4, 1201–1227.
45. T. Lupu and W. Werner, *A note on Ising random currents, Ising-FK, loop-soups and the Gaussian free field*, Electron. Commun. Probab. **21** (2016), 7 pp.
46. J. Miller, *Fluctuations for the Ginzburg-Landau interface model on a bounded domain*, Comm. Math. Phys. **308** (2011), no. 3, 591–639.
47. J. Miller, *Universality for SLE (4)*, arXiv:1010.1356, 2010.
48. J. Miller and S. Sheffield, *CLE(4) and the Gaussian free field*, In preparation.
49. J. Miller and S. Sheffield, *Imaginary geometry I: interacting SLEs*, Probab. Theory Related Fields **164** (2016), no. 3-4, 553–705.
50. J. Miller and S. Sheffield, *Imaginary geometry II: reversibility of* $\mathrm{SLE}_\kappa(\rho_1;\rho_2)$ *for* $\kappa \in (0,4)$, Ann. Probab. **44** (2016), no. 3, 1647–1722.
51. J. Miller and S. Sheffield, *Imaginary geometry III: reversibility of* SLE_κ *for* $\kappa \in (4,8)$, Ann. of Math. (2) **184** (2016), no. 2, 455–486.
52. J. Miller and S. Sheffield, *Imaginary geometry IV: interior rays, whole-plane reversibility, and space-filling trees*, Probab. Theory Related Fields **169** (2017), no. 3-4, 729–869.
53. J. Miller, S. Sheffield, and W. Werner, *CLE percolations*, Forum Math. Pi **5** (2017), e4, 102.
54. A. Raoufi, *Translation-invariant Gibbs states of the Ising model: general setting*, Ann. Probab. **48** (2020), no. 2, 760–777.

55. M. Russkikh, *Dominos in hedgehog domains*, Ann. Inst. Henri Poincaré D **8** (2020), no. 1, 1–33.
56. L. Schoug, A. Sepúlveda, and F. Viklund, *Dimensions of two-valued sets via imaginary chaos*, Int. Math. Res. Not. **2022** (2022), no. 5, 3219–3261, https://doi.org/10.1093/imrn/rnaa250.
57. O. Schramm, *Scaling limits of loop-erased random walks and uniform spanning trees*, Israel J. Math. **118** (2000), 221–288.
58. O. Schramm and S. Sheffield, *Contour lines of the two-dimensional discrete Gaussian free field*, Acta Math. **202** (2009), no. 1, 21–137.
59. O. Schramm and S. Sheffield, *A contour line of the continuum Gaussian free field*, Probab. Theory Related Fields **157** (2013), no. 1-2, 47–80.
60. A. Sepúlveda, *On thin local sets of the Gaussian free field*, Ann. Inst. Henri Poincaré Probab. Stat. **55** (2019), no. 3, 1797–1813.
61. O. Schramm and S. Sheffield, *Harmonic explorer and its convergence to SLE4*, Ann. Probab. **33** (2005), no. 6, 2127–2148.
62. S. Sheffield, *Exploration trees and conformal loop ensembles*, Duke Math. J. **147** (2009), no. 1, 79–129.
63. S. Sheffield and W. Werner, *Conformal loop ensembles: the Markovian characterization and the loop-soup construction*, Ann. of Math. (2) **176** (2012), no. 3, 1827–1917.
64. S. Smirnov, *Critical percolation in the plane: conformal invariance, Cardy's formula, scaling limits*, C. R. Acad. Sci. Ser. I Math. **333** (2001), no. 3, 239–244.
65. S. Smirnov, *Conformal invariance in random cluster models. I. Holomorphic fermions in the Ising model*, Ann. of Math. (2) **172** (2010), no. 2, 1435–1467.
66. H. N. V. Temperley, *Combinatorics: Being the proceedings of the conference on combinatorial mathematics held at the mathematical institute*, 1972, pp. 356–357.
67. H. Whitney, *On regular closed curves in the plane*, Compos. Math. **4** (1937), 276–284.